

การเตรียม โฟมพอลิยูรีเทนแบบแข็งเร่งปฏิกิริยาด้วยสารประกอบเชิงซ้อนคอปเปอร์-แอมีน
และแมงกานีส-แอมีน

นายวิทยา เฟื่องแจ่ม

วิทยานิพนธ์นี้เป็นส่วนหนึ่งของการศึกษาตามหลักสูตรปริญญาวิทยาศาสตรมหาบัณฑิต
สาขาวิชาปิโตรเคมีและวิทยาศาสตร์พอลิเมอร์
คณะวิทยาศาสตร์ จุฬาลงกรณ์มหาวิทยาลัย
ปีการศึกษา 2553
ลิขสิทธิ์ของจุฬาลงกรณ์มหาวิทยาลัย

PREPARATION OF RIGID POLYURETHANE FOAM CATALYZED BY
Cu-AMINE AND Mn-AMINE COMPLEXES

Mr. Wittaya Pengjam

A Thesis Submitted in Partial Fulfillment of the Requirements
for the Degree of Master of Science Program in Petrochemistry and Polymer Science
Faculty of Science
Chulalongkorn University
Academic Year 2010
Copyright of Chulalongkorn University

Thesis Title PREPARATION OF RIGID POLYURETHANE
FOAM CATALYZED BY Cu-AMINE AND
Mn-AMINE COMPLEXES
By Mr. Wittaya Pengjam
Field of Study Petrochemistry and Polymer Science
Thesis Advisor Associate Professor Nuanphun Chantarasiri, Ph. D.

Accepted by the Faculty of Science, Chulalongkorn University in
Partial Fulfillment of the Requirements for the Master's Degree

.....Dean of the Faculty of Science
(Professor Supot Hannongbua, Dr.rer.nat.)

THESIS COMMITTEE

..... Chairman
(Assistant Professor Warinthorn Chavasiri, Ph. D.)

..... Thesis Advirsor
(Associate Professor Nuanphun Chantarasiri, Ph. D.)

..... Examiner
(Associate Professor Mongkol Sukwattanasinitt, Ph. D.)

..... External Examiner
(Assistant Professor Toemsak Srikhirin, Ph. D.)

วิทยา เฟื่องแจ่ม: การเตรียมโฟมพอลิยูรีเทนแบบแข็งเร่งปฏิกิริยาด้วยสารประกอบเชิงซ้อนคอปเปอร์-แอมีน และแมงกานีส-แอมีน (PREPARATION OF RIGID POLYURETHANE FOAM CATALYZED BY Cu-AMINE AND Mn-AMINE COMPLEXES) อ. ที่ปริกษาวิทยานิพนธ์หลัก: รศ. ดร. นवलพรรณ จันทร์ศิริ, 99 หน้า.

งานวิจัยนี้ได้พัฒนาตัวเร่งปฏิกิริยาสำหรับเตรียมพอลิยูรีเทนโฟมแบบแข็ง ตัวเร่งปฏิกิริยาที่สนใจเตรียมขึ้นเป็นสารประกอบเชิงซ้อนโลหะ-แอมีน และโลหะ-แอมีน-ซาลิไซเลต โดยโลหะที่ใช้มี 2 ชนิดด้วยกันได้แก่ คอปเปอร์ และแมงกานีส หลังจากเตรียมตัวเร่งปฏิกิริยาได้แล้วจะนำตัวเร่งปฏิกิริยาที่ได้มาเตรียมพอลิยูรีเทนโฟม สำหรับเวลาของปฏิกิริยาในการเกิดโฟม สมบัติทางกายภาพ และสมบัติเชิงกลของพอลิยูรีเทน โฟมที่เร่งปฏิกิริยาด้วยสารประกอบเชิงซ้อนคอปเปอร์ และแมงกานีสจะนำมาเปรียบเทียบกับโฟมที่เตรียมด้วยตัวเร่งปฏิกิริยาทางการค้าคือ ไดเมทิลไซโคลเฮกซิลแอมีน (DMCHA) ตัวเร่งปฏิกิริยาที่เตรียมขึ้นจะนำมาศึกษาเอกลักษณ์ด้วย FTIR, UV-visible, elemental analysis และ X-ray diffraction สำหรับการหาการเปลี่ยนแปลงของหมู่ไอโซไซยานต และอัตราส่วนระหว่างพอลิไอโซไซยานูเรตต่อพอลิยูรีเทนในพอลิยูรีเทน โฟมหาจากการใช้เทคนิค ATR-IR จากผลการทดลองที่ได้พบว่าปฏิกิริยาการเกิดพอลิยูรีเทนโฟมเป็นปฏิกิริยาการคายความร้อนโดยที่อุณหภูมิของพอลิยูรีเทน โฟมที่เตรียมขึ้นจากสารประกอบเชิงซ้อนของคอปเปอร์และแมงกานีสอยู่ในช่วง 100-136 องศาเซลเซียส และความหนาแน่นของโฟมอยู่ในช่วง 39.0-50.0 kg/m³ ในระหว่างปฏิกิริยาการเกิดโฟมได้สังเกตเวลาในการเกิดปฏิกิริยาได้แก่เวลาที่สารผสมเป็นครีม เวลาที่สารผสมเป็นเจล เวลาที่ผิวหน้าของโฟมไม่เกาะติดกับวัสดุสัมผัส และเวลาที่โฟมหยุดฟู จากผลการทดลองที่ได้ พบว่าตัวเร่ง Cu(en)₂ และ Cu(trien) สามารถเร่งปฏิกิริยาปฏิกิริยาการเกิดพอลิยูรีเทนโฟมได้ดีกว่าตัวเร่งทางการค้า และนอกจากนี้ พบว่าความสามารถทนทานต่อแรงกดอัด (compressive strength) ของพอลิยูรีเทน โฟมที่เร่งปฏิกิริยาด้วย Cu(en)₂, Cu(trien) และ Cu(trien)Sal₂ มีค่าสูงกว่าโฟมที่เตรียมขึ้นด้วยตัวเร่งทางการค้า โดยค่าความสามารถทนทานต่อแรงกดอัดของโฟมเหล่านั้นที่ดัชนีไอโซไซยานต 100 มีค่าเท่ากับ 257.0, 237.7 และ 255.2 kPa ตามลำดับ ขณะที่เตรียมโฟมที่ดัชนีไอโซไซยานต 150 จะได้ค่าความสามารถทนทานต่อแรงกดอัดเท่ากับ 370.0, 338.5 และ 357.3 kPa ตามลำดับ

สาขาวิชา ปิโตรเคมีและวิทยาศาสตร์พอลิเมอร์ ลายมือชื่อนิติ.....

ปีการศึกษา.....2553..... ลายมือชื่อ อ. ที่ปริกษาวิทยานิพนธ์หลัก.....

5172450023: MAJOR PETROCHEMISTRY AND POLYMER SCIENCE

KEYWORDS: METAL COMPLEX/ RIGID POLYURETHANE FOAM/
CATALYST

WITTAYA PENGJAM: PREPARATION OF RIGID POLYURETHANE
FOAM CATALYZED BY Cu-AMINE AND Mn-AMINE COMPLEXES.
THESIS ADVISOR: ASSOC. PROF. NUANPHUN CHANTARASIRI,
Ph. D., 99 pp.

The complexes of metal-amine [$M(en)_2$ and $M(trien)$] and metal-amine-salicylate [$M(en)_2Sal_2$ and $M(trien)Sal_2$], where $M = Cu$ and Mn , were synthesized. The metal complexes were used as the catalysts in the preparation of rigid polyurethane foams. The reaction times, physical and mechanical properties of the prepared foams were investigated and compared to the foam prepared by commercial catalyst (N,N-dimethylcyclohexylamine, DMCHA). FTIR, UV-vis spectroscopy, elemental analysis and X-ray diffraction were used to characterize the catalysts. ATR-IR technique was used to determine isocyanate (NCO) conversion and polyisocyanurate:polyurethane (PIR:PUR) ratio in the polyurethane foam. The foaming reaction is an exothermic reaction. The maximum polymerization temperature is in the range of 100-136 °C. During foam preparation, the cream time, gel time, tack free time and rise time were investigated. The results showed that the apparent density of prepared foams was in the range 39.0-50.0 kg/m³. $Cu(en)_2$ and $Cu(trien)$ catalysts showed better catalytic activity than DMCHA catalyst. Furthermore, the compressive strengths of rigid polyurethane foams catalyzed by $Cu(en)_2$, $Cu(trien)$ and $Cu(trien)Sal_2$ were better than that of DMCHA. At NCO index of 100, their compressive strength values were 257.0, 237.7 and 255.2 kPa, respectively. While at NCO index of 150, their compressive strength values were 370.6, 338.5 and 357.3 kPa, respectively.

Field of Study: Petrochemistry and Polymer Science Student's Signature.....

Academic Year:.....2010..... Advisor's Signature.....

ACKNOWLEDGEMENTS

I wish to express deepest appreciation to my thesis advisor, Assoc. Prof. Dr. Nuanphun Chantarasiri for helpful suggestions, constant encouragement and guidance throughout the course of this thesis. In addition, I would like to thank to Assist. Prof. Dr. Warinthorn Chavasiri, Assoc. Prof. Dr. Mongkol Sukwattanasinitt and Assist. Prof. Dr. Toemsak Srihirin for their valuable suggestions, comments as committee members and thesis examiners.

Definitely, this thesis cannot be completed without kindness and helpful of many people. Firstly, I would like to thank South City Petrochem Co., Ltd. and The Metallurgy and Materials Science Research Institute for their chemical and SEM support, respectively. Absolutely, I am grateful to the Program of Petrochemistry and Polymer Science, Chulalongkorn University for financial support and furnishing many facilities in my research. Finally, I would like to thank I would like to thank and express my gratitude to all staffs in Sensor Research Unit especially Assoc. Prof. Dr. Sanong Ekgasit for ATR-IR support and useful suggestions.

I sincerely thank Department of Chemistry, Chulalongkorn University and Scientific and Technological Research Equipment Center, Chulalongkorn University. In addition, I would like to thank the National Center of Excellence for Petroleum, Petrochemicals and Advanced Materials, NCE-PPAM, which support this research work. I also thank members of Supramolecular Chemistry Research Unit for their encouragement and generous helps. Furthermore, I would like to express my highest gratitude to my family and my friends for their love and encouragement.

CONTENTS

	Page
ABSTRACT (IN THAI).....	iv
ABSTRACT (IN ENGLISH).....	v
ACKNOWLEDGEMENTS.....	vi
CONTENTS.....	vii
LIST OF FIGURES.....	x
LIST OF TABLES.....	xiv
LIST OF SCHEMES.....	xvi
LIST OF ABBREVIATIONS.....	xvii
CHAPTER I INTRODUCTION.....	1
CHAPTER II THEORY AND LITERATURE REVIEWS.....	5
2.1 Chemistry.....	5
2.1.1 Primary reaction of isocyanates.....	5
2.1.2 Secondary reaction of isocyanates.....	6
2.2 Raw materials.....	7
2.2.1 Isocyanates.....	7
2.2.2 Polyols.....	10
2.2.3 Catalysts.....	13
2.2.4 Surfactants.....	15
2.2.5 Blowing agents.....	17
2.2.6 Additives.....	17
2.3 Formulations.....	18
2.4 Mechanical properties.....	19
2.5 Production technologies of rigid polyurethane foam.....	22
2.6 Literature reviews.....	23
CHAPTER III EXPERIMENTAL.....	33
3.1 Materials.....	33
3.2 Measurements.....	33

	Page
3.3 Synthetic procedures.....	34
3.3.1 Synthesis of metal-amine complexes.....	34
3.3.1.1 Synthesis of copper-ethylenediamine complex (Cu(en) ₂).....	34
3.3.1.2 Synthesis of manganese-ethylenediamine complex (Mn(en) ₂).....	35
3.3.1.3 Synthesis of copper-triethylenetetramine complex (Cu(trien)).....	35
3.3.1.4 Synthesis of manganese-triethylenetetramine complex (Mn(trien)).....	36
3.3.2 Synthesis of metal-amine-salicylate complexes.....	37
3.3.2.1 Synthesis of copper-ethylenediamine-salicylate complex (Cu(en) ₂ Sal ₂).....	37
3.3.2.2 Synthesis of manganese-ethylenediamine-salicylate complex (Mn(en) ₂ Sal ₂).....	38
3.3.2.3 Synthesis of copper-triethylenetetramine-salicylate complex (Cu(trien)Sal ₂).....	39
3.3.2.4 Synthesis of manganese-triethylenetetramine- salicylate complex (Mn(trien)Sal ₂).....	40
3.3.3 Rigid polyurethane (RPUR) foam preparations.....	41
CHAPTER IV RESULTS AND DISCUSSION.....	44
4.1 Synthesis of metal-ethylenediamine and metal- triethylenetetramine complexes [(M(en) ₂ , M(trien))]......	44
4.1.1 Characterization of copper-ethylenediamine and copper- triethylenetetramine complexes.....	45
4.1.1.1 IR spectroscopy of Cu(en) ₂ and Cu(trien) complexes...	45
4.1.1.2 UV-visible spectroscopy of Cu(en) ₂ and Cu(trien) complexes.....	46
4.1.1.3 X-ray diffraction of Cu(en) ₂ complex.....	46

	Page
4.1.2 Characterization of manganese-ethylenediamine and manganese-triethylenetetramine complexes.....	47
4.1.2.1 IR spectroscopy of Mn(en) ₂ and Mn(trien) complexes.....	47
4.1.1.2 UV-visible spectroscopy of Mn(en) ₂ and Mn(trien) complexes.....	48
4.2 Synthesis of metal-ethylenediamine-salicylate and metal-triethylene tetramine-salicylate complexes [(M(en) ₂ Sal ₂ , M(trien)Sal ₂].....	49
4.2.1 Characterization of metal-ethylenediamine-salicylate and metal-triethylene tetramine-salicylate complexes.....	51
4.2.1.1 IR spectroscopy of Cu(en) ₂ Sal ₂ , Cu(trien)Sal ₂ , Mn(en) ₂ Sal ₂ and Mn(trien)Sal ₂ complexes.....	51
4.2.1.2 UV-visible spectroscopy of Cu(en) ₂ Sal ₂ , Cu(trien)Sal ₂ , Mn(en) ₂ Sal ₂ and Mn(trien)Sal ₂ complexes.....	52
4.3 Preparation of rigid polyurethane (RPUR) foams.....	53
4.3.1 Preparation of RPUR catalyzed by metal complexes.....	53
4.3.2 Reaction times and rise profiles.....	57
4.3.3 Apparent density.....	61
4.3.3.1 Effect of NCO indexes on foam density.....	62
4.3.3.2 Effect of catalyst quantity on foam density.....	63
4.3.3.3 Effect of blowing agent quantity on foam density.....	65
4.3.4 Foaming temperature.....	66
4.3.5 NCO conversion of RPUR foams.....	68
4.4 Compressive properties of RPUR foams.....	73
4.5 Thermal stability.....	76
CHAPTER V CONCLUSION.....	80
5.1 Conclusion.....	80
5.2 Suggestion for future work.....	81

LIST OF FIGURES

		Page
Figure 1.1	Diagram of foam preparation.....	3
Figure 2.1	Toluene diisocyanate isomers used for PUR foam manufacture.....	8
Figure 2.2	Molecular structure of MDI.....	8
Figure 2.3	Structure of polyether polyol based sorbitol and sucrose used in the PUR foams.....	12
Figure 2.4	Examples of aliphatic and aromatic dicarboxylic used in the production of polyester polyols.....	13
Figure 2.5	Structure of commercial catalysts used in rigid polyurethane foams manufacture.....	15
Figure 2.6	Structure of silicone surfactants used in PUR foams manufacture..	16
Figure 2.7	Compression load deflection test rig.....	20
Figure 2.8	Schematic representation of open cell deformation.....	20
Figure 2.9	Schematic representation of closed cell deformation.....	21
Figure 2.10	Typical compression stress-strain curve for rigid foams.....	21
Figure 2.11	Structure of derivative morpholines.....	30
Figure 2.12	Structures of metal complexes and metal salt complexes.....	32
Figure 3.1	RPUR foams processing.....	43
Figure 4.1	IR spectra of (a) $\text{Cu}(\text{OAc})_2$; (b) $\text{Cu}(\text{en})_2$; (c) $\text{Cu}(\text{trien})$	45
Figure 4.2	UV spectra of (a) $\text{Cu}(\text{OAc})_2$; (b) $\text{Cu}(\text{en})_2$; (c) $\text{Cu}(\text{trien})$	46
Figure 4.3	XRD diffractograms of (a) $\text{Cu}(\text{OAc})_2$; (b) $\text{Cu}(\text{en})_2$	47
Figure 4.4	IR spectra of (a) $\text{Mn}(\text{OAc})_2$; (b) $\text{Mn}(\text{en})_2$; (c) $\text{Mn}(\text{trien})$	48
Figure 4.5	UV spectra of (a) $\text{Mn}(\text{OAc})_2$; (b) $\text{Mn}(\text{en})_2$; (c) $\text{Mn}(\text{trien})$	49
Figure 4.6	IR spectra of (a) $\text{Cu}(\text{OAc})_2$; (b) $\text{Cu}(\text{en})_2\text{Sal}_2$; (c) $\text{Cu}(\text{trien})\text{Sal}_2$	51
Figure 4.7	UV spectra of (a) $\text{Cu}(\text{OAc})_2$; (b) $\text{Cu}(\text{en})_2\text{Sal}_2$; (c) $\text{Cu}(\text{trien})\text{Sal}_2$	52
Figure 4.8	UV spectra of (a) $\text{Mn}(\text{OAc})_2$; (b) $\text{Mn}(\text{en})_2\text{Sal}_2$; (c) $\text{Mn}(\text{trien})\text{Sal}_2$...	53
Figure 4.9	RPUR foams catalyzed by copper complexes at different NCO indexes (a) 100; (b) 130; (c) 150; (d) 160; (e) 180.....	57
Figure 4.10	RPUR foams catalyzed by manganese complexes at different NCO indexes (a) 80; (b) 100; (c) 130; (d) 150.....	57
Figure 4.11	Reaction times of RPUR foams catalyzed by copper complexes....	58

	Page
Figure 4.12 Reaction times of RPUR foams catalyzed by manganese complexes.....	60
Figure 4.13 Rise profiles of RPUR foams catalyzed by different metal complexes (a) DMCHA (ref.); (b) Cu(en) ₂ ; (c) Cu(trien); (d) Cu(en) ₂ Sal ₂ ; (e) Cu(trien)Sal ₂ ; (f) Mn(en) ₂ ; (f) Mn(trien); (h) Mn(en) ₂ Sal ₂ ; (i) Mn(trien)Sal ₂	60
Figure 4.14 Maximum rise rates of RPUR foams catalyzed by different metal complexes (a) DMCHA (ref.); (b) Cu(en) ₂ ; (c) Cu(trien); (d) Cu(en) ₂ Sal ₂ ; (e) Cu(trien)Sal ₂ ; (f) Mn(en) ₂ ; (f) Mn(trien); (h) Mn(en) ₂ Sal ₂ ; (i) Mn(trien)Sal ₂	61
Figure 4.15 Samples for foam density measurements.....	62
Figure 4.16 Unsuitable samples for foam density measurements.....	62
Figure 4.17 Apparent density of RPUR foam catalyzed by metal complexes (a) DMCHA (ref.); (b) Cu(en) ₂ ; (c) Cu(trien); (d) Cu(en) ₂ Sal ₂ ; (e) Cu(trien)Sal ₂ ; (f) Mn(en) ₂ ; (g) Mn(trien); (h) Mn(en) ₂ Sal ₂ ; (i) Mn(trien)Sal ₂	63
Figure 4.18 Effect of catalyst amount on RPUR foams density catalyzed by different catalysts (a) DMCHA (ref.); (b) Cu(en) ₂ ; (c) Cu(trien) at NCO index of 150.....	64
Figure 4.19 Appearance of RPUR foams catalyzed by Cu(trien) complex in various amounts at NCO index of 150.....	64
Figure 4.20 Effect of blowing agent quantities on RPUR foam density catalyzed by different catalysts (a) DMCHA (ref.); (b) Cu(en) ₂ ; (c) Cu(trien) at NCO index of 130.....	65
Figure 4.21 Appearance of RPUR foams catalyzed by Cu(trien) complex in various blowing agent amounts at NCO index of 130.....	65
Figure 4.22 Temperature profiles of RPUR foams catalyzed by different metal complexes (a) DMCHA (ref.); (b) Cu(en) ₂ ; (c) Cu(trien); (d) Cu(en) ₂ Sal ₂ ; (e) Cu(trien)Sal ₂ ; (f) Mn(en) ₂ ; (f) Mn(trien); (h) Mn(en) ₂ Sal ₂ ; (i) Mn(trien)Sal ₂	68

	Page
Figure 4.23 IR spectra of reactant and RPUR foams catalyzed by copper complexes at NCO index 130 (a) PMDI; (b) polyether polyol; (c) DMCHA (ref.); (d) Cu(en) ₂ ; (e) Cu(trien); (f) Cu(en) ₂ Sal ₂ ; (g) Cu(trien)Sal ₂	69
Figure 4.24 IR spectra of RPUR foams catalyzed by Cu(trien) at different NCO indexes (a) 100; (b) 150; (c) 200.....	69
Figure 4.25 NCO conversions of RPUR foams catalyzed by different copper complexes.....	71
Figure 4.26 PIR: PUR of RPUR foams catalyzed by different copper complexes.....	71
Figure 4.27 Parallel compression stress-strain curve of RPUR foams catalyzed by different catalysts at NCO index of 150 (a) DMCHA (ref.); (b) Cu(en) ₂ ; (c) Cu(trien); (d) Cu(en) ₂ Sal ₂ ; (e) Cu(trien)Sal ₂	74
Figure 4.28 Comparison of parallel compressive strength of RPUR foams between NCO indexes of 100 and 150.....	74
Figure 4.29 Comparison of compressive strength of RPUR foams between parallel and perpendicular direction of foam rising at NCO index of 100.....	75
Figure 4.30 Isotropic foam (a): spherical cells, equal properties in all directions; anisotropic foam (b): ellipsoid cells, properties depend on direction.....	75
Figure 4.31 SEM of RPUR foams catalyzed by Cu(en) ₂ ; (a) top view; (b) side view (70x).....	76
Figure 4.32 SEM of RPUR foams catalyzed by (a) DMCHA; (b) Cu(en) ₂ (70x).....	76
Figure 4.33 TGA thermograms of RPUR foams catalyzed by (a) DMCHA (ref.); (b) Cu(en) ₂ ; (c) Cu(trien); (d) Cu(trien)Sal ₂ at the NCO index of 150.....	77
Figure 4.34 External appearance of RPUR foams catalyzed by metal acetates, amines and salicylic acid.....	78

	Page
Figure 4.35 External appearance of RPUR foams catalyzed by different metal catalysts (a) DMCHA (ref.); (b) Cu(en) ₂ ; (c) Cu(trien); (d) Cu(en) ₂ Sal ₂ ; (e) Cu(trien)Sal ₂ ; (f) Mn(en) ₂ ; (g) Mn(trien); (h) Mn(en) ₂ Sal ₂ ; (i) Mn(trien)Sal ₂	79
Figure B1 Parallel compression stress-strain curve of RPUR foams catalyzed by different catalysts at NCO index of 100.....	94
Figure B2 Perpendicular compression stress-strain curve of RPUR foams catalyzed by different catalysts at NCO index of 100.....	94
Figure B3 Compression direction of RPUR foams (a) perpendicular direction; (b) parallel direction.....	95
Figure B4 Mass spectrum of Cu(en) ₂ complex (MALDI-TOF MS).....	95

LIST OF TABLES

		Page
Table 1.1	Foam formulations.....	4
Table 2.1	Specifications of commercial polyol including functionality values..	11
Table 2.2	Overview of frequently used catalysts in rigid polyurethane foams..	14
Table 3.1	Composition of starting materials in the preparation of metal complexes.....	41
Table 3.2	RPUR foam formulations at different NCO indexes (in part by weight unit).....	42
Table 3.3	RPUR foam formulations at different NCO indexes (in gram unit, cup test).....	42
Table 4.1	RPUR foams formulation catalyzed by metal complexes at different NCO indexes.....	54
Table 4.2	External appearance of RPUR foams catalyzed by metal-complexes at different NCO indexes.....	55
Table 4.3	Maximum core temperature of PUR foam catalyzed by metal complexes at different NCO indexes.....	66
Table 4.4	Wave number of typical PIR-PUR absorbance.....	70
Table 4.5	NCO conversions and PIR:PUR ratio of RPUR foams catalyzed copper and manganese complexes at different NCO indexes.....	72
Table 4.6	TGA data of RPUR foam catalyzed by various copper complexes catalysts at the NCO index of 150.....	77
Table 5.1	RPUR foams conclusion.....	82
Table A1	Isocyanate quantity at different NCO indexes in the above formulations.....	89
Table A2	Free NCO absorbance peak area in PMDI (MR-200) from ATR-IR.....	89
Table A3	NCO conversion of RPUR foam catalyzed by DMCHA at different NCO indexes.....	90
Table A4	NCO conversion of RPUR foam catalyzed by Cu(en) ₂ at different NCO indexes.....	91
Table A5	NCO conversion of RPUR foam catalyzed by Cu(trien) at different NCO indexes.....	91

	Page
Table A6 NCO conversion of RPUR foam catalyzed by $\text{Cu(en)}_2\text{Sal}_2$ at different NCO indexes.....	92
Table A7 NCO conversion of RPUR foam catalyzed by Cu(trien)Sal_2 at different NCO indexes.....	92
Table A8 NCO conversion of RPUR foam catalyzed by Mn(en)_2 at different NCO indexes.....	92
Table A9 NCO conversion of RPUR foam catalyzed by Mn(trien) at different NCO indexes.....	93
Table A10 NCO conversion of RPUR foam catalyzed by $\text{Mn(en)}_2\text{Sal}_2$ at different NCO indexes.....	93
Table A11 NCO conversion of RPUR foam catalyzed by Mn(trien)Sal_2 at different NCO indexes.....	93
Table B1 Formulations, reaction times, physical and mechanical properties of RPUR foams catalyzed by copper complexes.....	96
Table B2 Formulations, reaction times, physical and mechanical properties of RPUR foams catalyzed by manganese complexes.....	97
Table B3 Formulations, reaction times, physical properties of RPUR foams catalyzed by metal acetates, amines and salicylic acid.....	98

LIST OF SCHEMES

	Page
Scheme 1.1 Diagram of metal complexes synthesis.....	3
Scheme 2.1 Mechanisms of tertiary amine catalyst.....	26
Scheme 2.2 Mechanism of tin (II) salts catalyst.....	27
Scheme 2.3 Mechanism of tin (IV) salts catalyst.....	28
Scheme 2.4 Mechanism of tin-amine synergism.....	28
Scheme 3.1 Synthesis of copper-ethylenediamine complex.....	34
Scheme 3.2 Synthesis of manganese-ethylenediamine complex.....	35
Scheme 3.3 Synthesis of copper-triethylenetetramine complex.....	35
Scheme 3.4 Synthesis of manganese-triethylenetetramine complex.....	36
Scheme 3.5 Synthesis of copper-ethylenediamine-salicylate complex.....	37
Scheme 3.6 Synthesis of manganese-ethylenediamine-salicylate complex.....	38
Scheme 3.7 Synthesis of copper-triethylenetetramine-salicylate complex.....	39
Scheme 3.8 Synthesis of manganese-triethylenetetramine-salicylate complex.....	40
Scheme 4.1 Synthesis of metal-ethylenediamine and metal- triethylenetetramine complexes.....	44
Scheme 4.2 Synthesis of metal-ethylenediamine-salicylate and metal- triethylenetetramine- salicylate complexes.....	50
Scheme 4.3 Activation mechanism of metal-based catalyst on urethane formation reaction.....	59

LIST OF ABBREVIATIONS

%	percentage
ϵ	molar absorptivity
ATR-IR	Attenuated Total Reflectance-Infrared
cm	centimeter
cm^{-1}	unit of wavenumber
$^{\circ}\text{C}$	degree Celsius (centigrade)
Cu	copper element
$\text{Cu}(\text{en})_2$	copper-ethylenediamine complex
$\text{Cu}(\text{en})_2\text{Sal}_2$	copper-ethylenediamine-salicylate complex
$\text{Cu}(\text{OAc})_2$	copper acetate
$\text{Cu}(\text{trien})$	copper-triethylenetetramine complex
$\text{Cu}(\text{trien})\text{Sal}_2$	copper-triethylenetetramine-salicylate complex
DBTDL	dibutyltin dilaurate
DMCHA	N,N-dimethylcyclohexylamine
EA	Elemental Analysis
en	ethylenediamine
FTIR	Fourier Transform Infrared Spectrophotometer
g	gram
h	hour
HCCA	2-cyano-4-hydroxycinnamic acid
IDT	Initial Decomposition Temperature
KBr	potassium bromide
kg	kilogram
kV	kilovolt
M	metal
m^3	cubic meter
MDI	4,4'-methane diphenyl diisocyanate
mA	milliampere
mg	milligram
min	minute
$\text{Mn}(\text{en})_2$	manganese-ethylenediamine complex

Mn(en) ₂ Sal ₂	manganese-ethylenediamine-salicylate complex
mL	milliliter
mm	millimeter
mmol	millimole
Mn	manganese element
Mn(OAc) ₂	manganese acetate
Mn(trien)	manganese-triethylenetetramine complex
Mn(trien)Sal ₂	manganese-triethylenetetramine-salicylate complex
N	newton unit
NCO	isocyanate
OHV	hydroxyl value
pbw	part by weight
PIR	polyisocyanurate
PMDI	polymeric 4,4'-methane diphenyl diisocyanate
PUR	polyurethane
rpm	round per minute
RPUR	rigid polyurethane
RT	room temperature
s	second
Sal	salicylate
SEM	Scanning Electron Microscope
t	time
TDI	toluene diisocyanate
TGA	Thermogravimetric Analysis
T _{max}	maximum core temperature
trien	triethylenetetramine
UV	ultraviolet
XRD	X-ray diffraction

CHAPTER I

INTRODUCTION

Polymeric foams are widely used in a variety of applications for the advantages of their energy absorption characteristic, thermal properties and specific strength. Rigid polyurethane (RPUR) foams have many engineering applications in industrial product such as insulation materials, automotive parts, structural materials, packaging and refrigerators because of their extremely wide range of properties [1]. Their properties are combination of good mechanical properties, low thermal conductivity with a low density and their easy processing [2].

The rigid polyurethane foams processing can be performed by one shot or two shot methods. In one shot method, all of materials such as polyol, catalyst, surfactant, blowing agent and isocyanate are put into a mixing cup and mixed homogeneously. In two shot method, isocyanate is added to the mixture of polyol, catalyst, surfactant, and blowing agent at the second stage [3]. The foaming can be carried out with physical blowing agent, chemical blowing agent, or mixture of two. The main reactions of polyurethane foams leading to polyurethane (PUR) and polyisocyanurate (PIR) are three reactions. Firstly, the reaction between isocyanate (-NCO) and hydroxyl (-OH) groups results in urethane formations. Secondly, the reaction between isocyanate groups and blowing agent (water) releases carbon dioxide gas. Finally, the reaction of three isocyanate groups in polymer chain produces isocyanurate [4].

However, the above reactions can not be completed without catalysts for catalytic reactions. Practically, catalyst is necessary for the production of polyurethane foams because the reaction between isocyanate with hydroxyl group is slow [5]. Tertiary amines and tin compounds are used as catalysts for gelling and blowing reaction, for examples N,N-dimethylcyclohexylamine (DMCHA) and dibutyltin dilaurate (DBTDL). Although, conventional catalyst having excellent catalytic activity, but they are toxic to human beings, strong smell and expensive. Therefore, new catalysts were developed in this work.

The objectives of this work were to develop the metals complexes as catalysts for rigid polyurethane foam preparation. In this research, two groups of metal complexes were synthesized. Firstly, the complexes between metal acetate and amine,

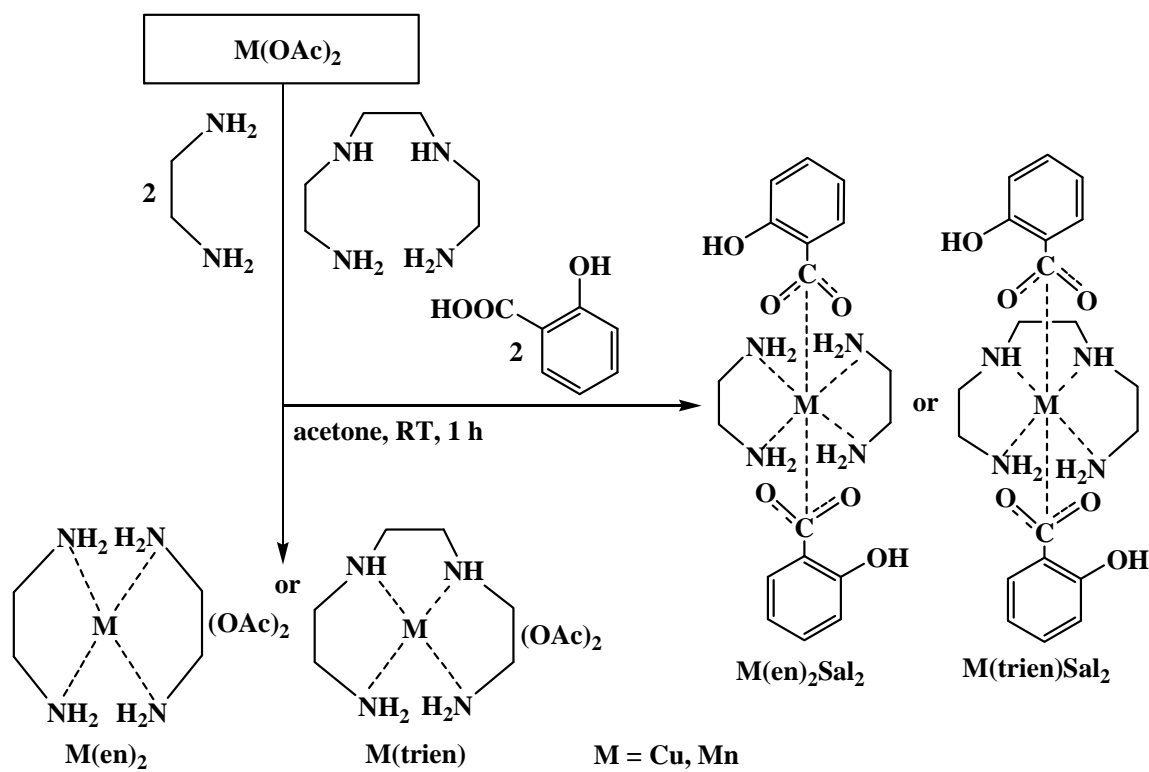
namely $M(en)_2$ and $M(trien)$. Secondly, complexes between metal acetate, amine and salicylic acid, namely $M(en)_2Sal_2$ and $M(trien)Sal_2$ (where $M = Cu$ and Mn). $M(en)_2$ and $M(trien)$ were synthesized from reaction between metal acetate with ethylenediamine (en) and triethylenetetramine (trien), respectively. $M(en)_2Sal_2$ and $M(trien)Sal_2$ were synthesized from reaction of metal acetate, salicylic acid (Sal) with ethylenediamine and triethylenetetramine, respectively.

Objectives and scope of the research

The target of this research was to prepare rigid polyurethane foams catalyzed by metal-amine complexes; $M(en)_2$, $M(trien)$ and metal-amine-salicylate complexes; $M(en)_2Sal_2$, $M(trien)Sal_2$. It was expected that the synthesized metal complexes showed good catalytic activity and the desirable physical and mechanical properties of prepared foams were presented. Moreover, the reaction times during foam preparation, the physical and mechanical properties of foams were studied by varying catalyst types, the amount of catalysts and blowing agent, and NCO indexes.

In the first step, metal complexes preparation; $M(en)_2$, $M(trien)$, $M(en)_2Sal_2$ and $M(trien)Sal_2$ were synthesized by reaction between metal acetate such as copper (II) acetate monohydrate ($Cu(OAc)_2 \cdot H_2O$), and manganese (II) acetate tetrahydrate ($Mn(OAc)_2 \cdot 4H_2O$) and aliphatic amine included ethylenediamine (en) and triethylene tetramine (trien). $M(en)_2Sal_2$ and $M(trien)Sal_2$ were added salicylic acid (Sal) into $M(en)_2$, $M(trien)$, respectively. The reaction is shown in Scheme 1.1. After that the prepared metal complexes were characterized by FTIR spectroscopy, ultraviolet-visible spectroscopy, elemental analysis, X-ray diffraction and mass spectrometry.

In the second step, rigid polyurethane foam preparations were catalyzed by prepared metal complexes prepared in the first step. Diagram of rigid polyurethane foams preparation is shown in Figure 1.1. All of the raw materials, except isocyanate (PMDI) were first premixed. Then, the isocyanate was added into the mixture and mixed by high-speed mechanical stirrer. Foam formulations are shown in Table 1.1. Various NCO indexes are employed to investigate its effect on properties of rigid polyurethane foams.



Scheme 1.1 Diagram of metal complexes synthesis

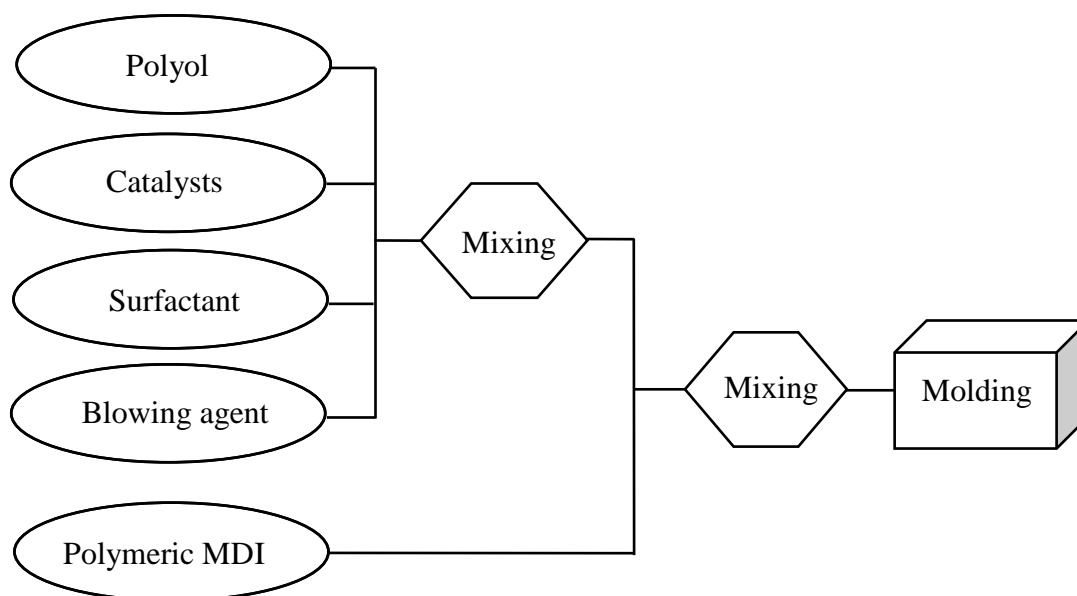


Figure 1.1 Diagram of foam preparation

Table 1.1 Foam formulations

Formulations (pbw)	NCO index				
	100	130	150	160	180
Polyol (Raypol [®] 4221)	100	100	100	100	100
Catalysts (metal complexes)	1.0	1.0	1.0	1.0	1.0
Surfactant (TEGOTAB B8460)	2.5	2.5	2.5	2.5	2.5
Blowing agent (distilled water)	3.0	3.0	3.0	3.0	3.0
Polymeric MDI (MR-200)	151	197	227	242	272

During rigid polyurethane foams preparation, reaction times included cream time, gel time, tack free time and rise time were recorded by using a stopwatch. The foaming temperatures were measured by dual thermocouple, Digicon DP-71. ATR-IR spectrometer was used to determine isocyanate conversion of prepared foams. The apparent density and compressive strength of prepared foams were measured according to ASTM D 1622-09 and ASTM D 1621-09, respectively. Morphology and cell size of rigid polyurethane foams were measured using scanning electron microscope (SEM) according to ASTM D 3576-09. Thermal properties of rigid polyurethane foams were investigated by thermogravimetric analysis (TGA).

Catalytic efficiency of the metal complexes was compared with that of N,N-dicyclohexylamine (DMCHA), which is a commercial catalyst.

CHAPTER II

THEORY AND LITERATURE REVIEWS

Polyurethane (PUR) foams were discovered by Otto Bayer and coworkers. A broad range of foam types and material properties can be synthesized by the variation of specific components in the formulations such as diisocyanate, polyols, blowing agents, surfactants, catalysts and other additives. This results in an extensive range of properties. The type of PUR foams can vary from flexible, used in applications such as cushioning, packaging and textile industry through semi-rigid, commonly found in applications in the automotive industry, and protective packaging to rigid PUR foam, mainly used in insulation and structural applications [6].

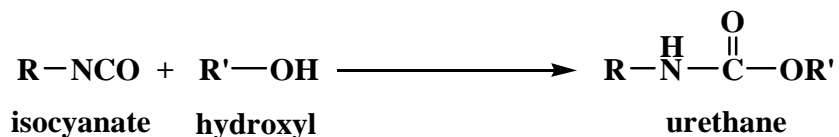
2.1 Chemistry

Polyurethane (PUR) chemistry is based on the high reactivity of the isocyanate group with any compound containing active hydrogen. Most polyurethane is formed by exothermic reaction between di- or polyfunctional isocyanates and di- or polyfunctional hydroxyl species [6]. For simplicity, the basic principle of urethane chemistry is described below using monofunctional reagents.

2.1.1 Primary reaction of isocyanates

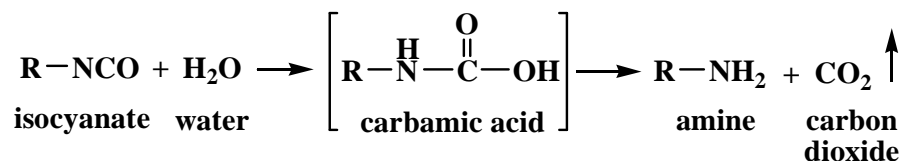
Primary isocyanate reactions produce urethane, amines, and substituted ureas, all of which still contain active hydrogen atom. In the presence of suitable catalysts at elevated temperatures, controlled secondary reactions occur which strongly influence the physical properties of the foam by introducing chain branching and crosslinking.

2.1.1.1 Reaction with hydroxyl compounds; the reaction between an isocyanate and a polyol produce a urethane.



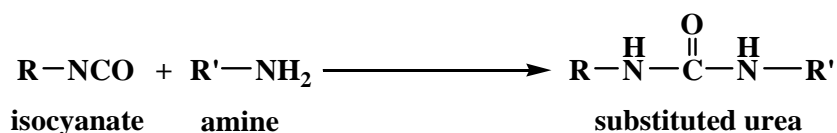
This reaction is known as the “gelling reaction”. Since it is an exothermic reaction it must be temperature controlled. The rate of polymerization is affected by the chemical structure of the isocyanate and polyol. A catalyst is used to accelerate the reaction rate.

2.1.1.2 Reaction with water; the reaction between an isocyanate and water releases carbon dioxide and an amine via a transient unstable carbamic acid.



This reaction is known as the “blowing reaction” because the CO₂ gas produced is used for blowing the foam. The reaction rate is accelerating by suitable choice of catalyst system.

2.1.1.3 Reaction with amines; the reaction of an isocyanate with an amine forms an urea linkage.

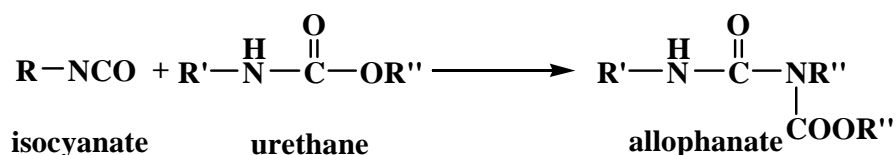


Reactions of unhindered isocyanates with primary amines occur approximately 100-1000 times faster than with primary alcohols [6]. Amines are therefore used as chain-extenders and curing agents PUR manufacture.

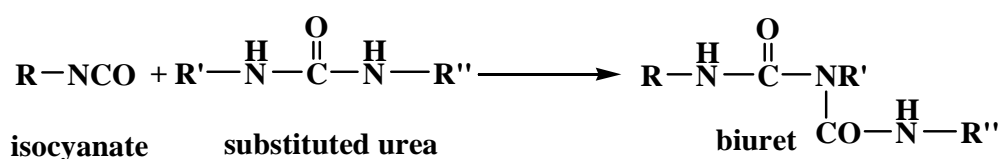
2.1.2 Secondary reaction of isocyanates

Isocyanate may react, under suitable conditions, with the active hydrogen atoms of urethane and urea linkages from the primary reactions as follows:

2.1.2.1 Reaction with urethane; isocyanate can react with the active hydrogen atoms of urethane linkages to form branched allophanates.

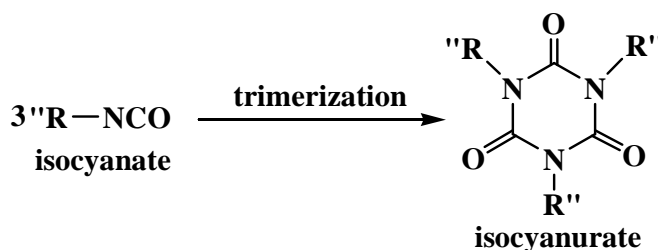


2.1.2.2 Reaction with urea; isocyanate can also react with the active hydrogen atoms of substituted ureas to form branched biuret structures.



Reaction of isocyanates with both urethanes and ureas produce crosslinking. Generally, reactions of isocyanates with urea groups are significantly faster and occur at lower temperature than that with urethane groups.

2.1.2.3 Trimer formation; isocyanate trimer can be formed on heating either aliphatic or aromatic isocyanates. The reaction is accelerated by basic catalysts such as sodium and potassium salts of carboxylic acids.



2.2 Raw materials

The properties of polyurethane foams can be modified within wide limits depending on the raw materials used. This is also true for the area of rigid foams. The density, flowability, strength, thermal stability, combustibility and other properties can be adjusted to suit the requirements of a given application. The polyols and isocyanates have a major impact on the properties of the foams [7].

2.2.1 Isocyanates

The most common isocyanate, which account for approximately 95% of isocyanate usage, are toluene diisocyanate and 4,4'-diphenylmethane diisocyanate. other isocyanate that are used are generally blends which the above two, or blends of MDI and its higher homologues.

2.2.1.1 Toluene diisocyanate (TDI) (liquid, b.p. 120°C) TDI is the most commonly available as a mixture of 80:20 and 65:35 of the 2,4 and 2,6 isomers, respectively.

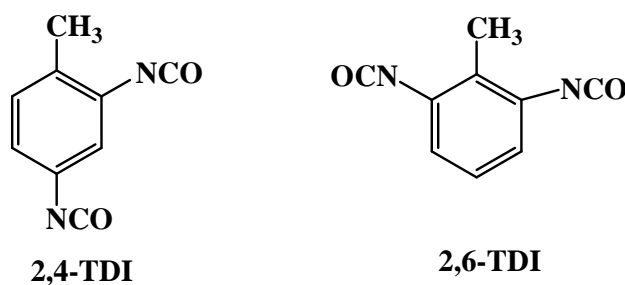


Figure 2.1 Toluene diisocyanate isomers used for PUR foam manufacture

TDI has a relatively high vapor pressure and this gives rise to the risk of airborne exposure to workers. As a consequence, it is quite a difficult material to handle on site, in transport and in the laboratory and therefore usage has been limited in favour of MDI which has a lower volatility.

2.2.1.2 4,4'-Diphenylmethane diisocyanate, or methylene diphenyl diisocyanate (MDI) (solid, m.p. 38°C, b.p. 195°C). Pure MDI is a crystalline solid at room temperature, so it must be heated slightly in order to convert it into a more manageable form, i.e. a fairly high viscosity liquid.

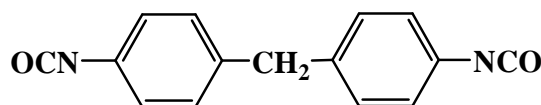
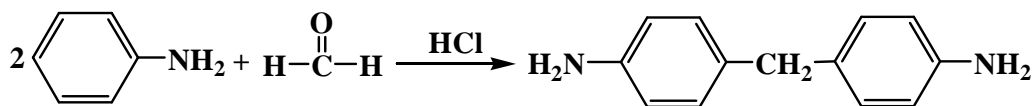


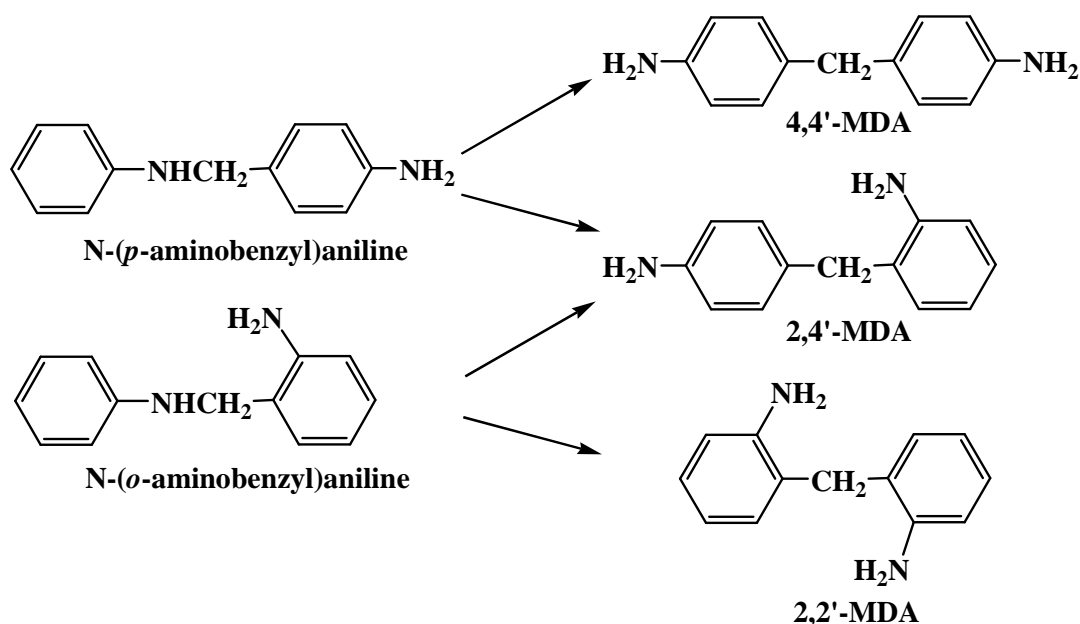
Figure 2.2 Molecular structure of MDI

Alternatively, handling of MDI can be facilitated by producing an oligomeric mixture containing approximately 55% MDI, 25% MDI trimer (functionality = 2 to 3) and 20% of polymeric MDI. This is known as polymeric MDI and is a liquid at ambient temperatures.

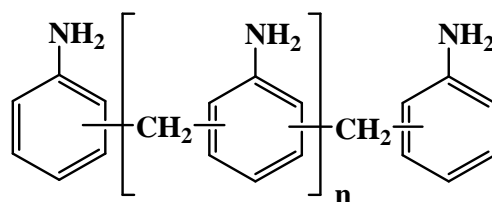
The production of MDI/PMDI is based on aniline and formaldehyde as the main raw materials. Aniline is produced from benzene. The preferred and lowest cost commercial production method is via nitration of benzene to nitrobenzene, using a mixed acid process ($\text{HNO}_3/\text{H}_2\text{SO}_4$) whereby aniline is produced from nitrobenzene via a reduction step [8]. Methylenedianiline (MDA) and a mixture of its oligomers (pMDA) subsequently results from an acid-catalyzed condensation of aniline with formaldehyde.



Three MDA isomers are predominantly produced in this reaction process: 4,4'-methylenedianiline (4,4'-MDA), 2,4'-methylenedianiline (2,4'-MDA), and 2,2'-methylene-dianiline (2,2'-MDA). The relative amounts of these products depend on the acid catalyst concentration, the aniline/formaldehyde ratio and the process temperature.

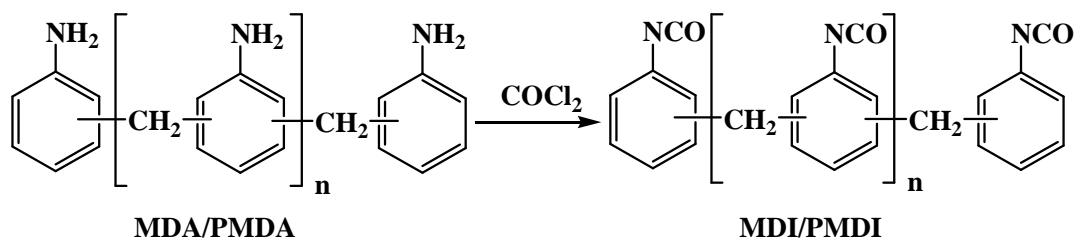


In addition to the MDA-isomers, the oligomeric mixture of PMDA is largely comprised of compounds with three ($n = 1$) to approximately six ($n = 4$) phenylamino functional groups. They are formed via further reactions of the MDA-isomers.



PMDA

PMDA is subsequently phosgenated into the corresponding PMDI in the presence of an inert solvent [8].



2.2.2 Polyols

Isocyanates react with any molecular entity possessing active hydrogen, such as hydroxylic, carboxylic, and amine groups. For rigid foams, primary and secondary hydroxyl group terminated polyether polyols are most important, followed by polyester polyols, which have the oldest application. The polyol used for the manufacture of PUR foams are usually either polyether or polyester type polyols. They are 'prepolymers' whose structure determines the final PUR foam properties with a large dependence being on their molecular weight and functionality. Generally, rigid foam polyol have molecular weight of 150-1000 g/mol, functionality 2.5-8.0 and hydroxyl value 250-1000 mgKOH/g. The rigidity of the foam can be increased by reducing the chain segment length between junction points this effectively produces more tightly crosslinked networks [6].

Specifications of commercial polyols include hydroxyl values which are used in stoichiometric formulation calculations. Examples are shown in Table 2.1.

Table 2.1 Examples of commercial polyols

Alcohol	Chemical structure	Functionality
Ethylene glycol (EG)	$\text{HO}-\text{CH}_2-\text{CH}_2-\text{OH}$	2
Glycerol	$\begin{array}{c} \text{H}_2\text{C}-\text{OH} \\ \\ \text{HC}-\text{OH} \\ \\ \text{H}_2\text{C}-\text{OH} \end{array}$	3
Trimethylol propane (TMP)	$\begin{array}{c} \text{H}_2\text{C}-\text{CH}_2-\text{OH} \\ \\ \text{HC}-\text{CH}_2-\text{OH} \\ \\ \text{H}_2\text{C}-\text{CH}_2-\text{OH} \end{array}$	3
Pentaerythritol	$\begin{array}{c} \text{H}_2\text{C}-\text{OH} \\ \\ \text{HO}-\text{CH}_2-\text{C}-\text{CH}_2-\text{OH} \\ \\ \text{H}_2\text{C}-\text{OH} \end{array}$	4
Sorbitol	$\begin{array}{ccccccc} & & \text{OH} & & \text{OH} & & \\ & & & & & & \\ \text{HO} & -\text{CH}_2 & -\text{CH} & -\text{CH} & -\text{CH}_2 & -\text{OH} & \\ & / & \backslash & / & \backslash & / & \\ & \text{OH} & & \text{OH} & & \text{OH} & \end{array}$	6
Sucrose		6

2.2.2.1 Polyether polyols

Approximately 90% of polyols used in PUR foam production are hydroxyl-terminated polyethers due to their low cost and low viscosity. Polyether-based foams have better resilience and resistance to hydrolysis than polyester-based foams. They are produced by the ring opening of alkylene oxides using a polyfunctional starter or initiator. Ethylene or propylene oxides are the most commonly used polyols. The polyols used for making rigid foams the molecular weight is approximately 500 g/mol in order to reduce the distance between crosslinks.

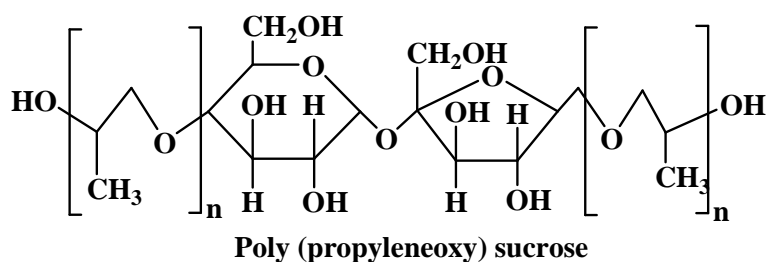
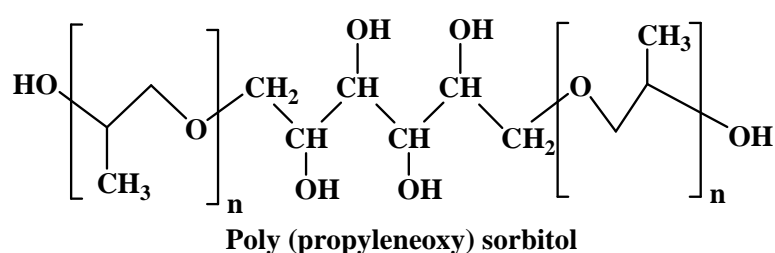


Figure 2.3 Structure of polyether polyol based sorbitol and sucrose used in the PUR foams

2.2.2.2 Polyester polyols

Compared with polyether polyols, polyester polyols tend to be more reactive, produce foams with better mechanical properties, are less susceptible to yellowing in sunlight and are less soluble in organic solvents. However, they are more expensive, more viscous and therefore more difficult to handle. Consequently, they are only used in applications that require their superior properties. Polyester polyols are made by condensation reactions between diols (and triol) and dicarboxylic acid such as adipic acid, sebacic acid and m-phthalic acid.

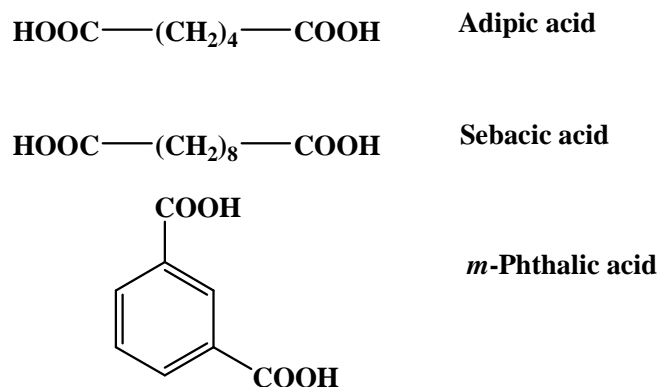


Figure 2.4 Examples of aliphatic and aromatic dicarboxylic used in the production of polyester polyols

2.2.3 Catalysts

Catalysts play a very important role in the reactions of isocyanates. Catalysts exert an influence upon the rates of competing reactions and have a major effect on the ultimate properties of the final foam. A typical catalyst system would consist of a mixture of a tertiary amine and organometallic compounds. For tin compounds, the most important one being stannous octoate. Each catalyst type is specific for a particular chemical reaction. Catalyst mixtures are generally necessary to control the balance of (a) the polymerization and (b) the gas generation reactions; both are exothermic reactions. Getting the correct balance of polymerization and foaming is of major importance in the production of closed cell foam.

- The blowing reaction of PMDI with H_2O to form CO_2 and polyurea
- The gelling reaction of PMDI with polyol to form polyurethane
- The trimerization of PMDI (as well as related reactions, such as carbodiimide and dimer formation)

In preparing formulations for specific processing and application needs, catalysts are thought to balance these reactions and synergistic effects of certain catalyst combinations are known as well. If the polymerization is complete before sufficient gas has been generated, a high density foam will result, i.e. virtually a solid product containing few gas cells. Thus blends of catalysts are required to balance the relative chemical reaction rates. The frequently used catalysts are shown in **Table 2.2** [7].

Table 2.2 Overview of frequently used catalysts in rigid polyurethane foams

Catalysts	Code	Catalytic activity
Tertiary amines		
Pentamethyldiethylene triamine	PMDETA	blowing
Triethylenediamine	TEDA	gelling
Dimethylcyclohexylamine	DMCHA	blowing/ gelling
Triethylamine	TEA	curing
Quaternary ammonium salts		
2-hydroxy propyl trimethyl ammonium (2-ethylhexoate)	TMR	gelling/ curing/ trimer formation
2-hydroxy propyl trimethyl ammonium (formiate)	TMR-2	delayed action/ trimer formation
Alkali metal carboxilates		
Potassium acetate	K Ac	gelling/ trimer formation
Potassium octoate	K Oct	gelling/ trimer formation
Sodium N-2-hydroxy, 5-nonylphenol methyl N-methyl glicinate	Curithane 52	gelling/ trimer formation
Tin complexes		
Stannous octoate	Sn Oct	gelling
Dibutyltin dilaurate	DBTDL	gelling

Catalysts for rigid polyurethane foam include a range of chemical structures, such as tertiary amines, aromatic amines, quaternary ammonium salts, alkali metal carboxylates, and organo-tin compounds. Their catalytic activity is dependent on their basicity, with steric hindrance on the active site playing a secondary role. The activity of tertiary amines is, for example, decreased in the presence of residual acidic compounds in the polyol formulation. This phenomenon is successfully exploited with so called “delayed action” catalysts which are active only after acid-blocked amine catalyst decomposes during foaming to give active amine. For example, formic acid salts are active only after decomposition of the formate at some higher temperature. Quaternary ammonium salts are widely used because of their strong gelling and trimerization action, while maintaining a relatively smooth foam rise profile. Alkali metal carboxylates are very active curing and trimerization catalysts.

Higher molecular weight carboxylates are giving smoother rise rate profiles but have to be dosed at higher amounts for a given catalytic effect.

Tin complexes are the most powerful gelling catalysts known today. Stannous octoate is hydrolytically unstable, preventing its use in aqueous formulations [7].

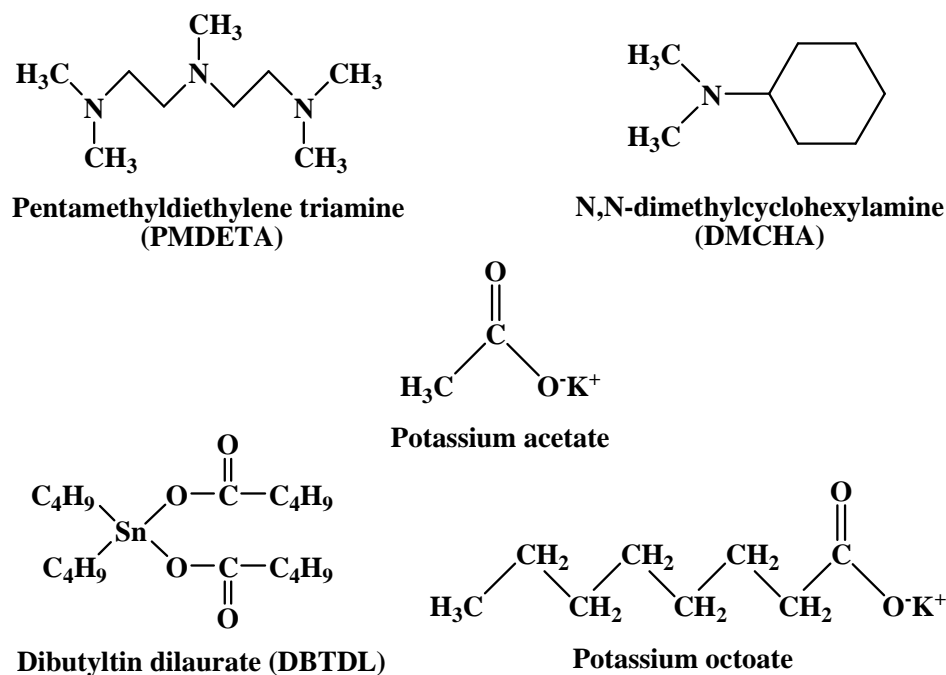


Figure 2.5 Structure of commercial catalysts used in rigid polyurethane foams manufacture

2.2.4 Surfactants

The presence of surfactants serves two purposes in polyurethane foaming. First, they stabilize the foam immediately after mixing polyol and isocyanate by lowering the surface tension of the emerging gas-liquid interface and presumably also by emulsifying the polyol-isocyanate interface. Mechanistically, this effect arises from a preferred accumulation of surfactant molecules at interfaces. A second, equally important role of surfactants is to stabilize the polymerizing liquid-gas interface during the roughly 30 to 50 fold volume increase of rising foam. Here, the mechanism is rather dynamic: the expanding foam continuously creates new surface area of high tension that needs to be stabilized by fast migration of surfactant towards the interface (the Marangoni effect).

The surfactants most commonly used in the polyurethane industry are polydimethyl siloxane-polyether copolymers. Since the late 1950s, these so called “silicone surfactants” almost completely replaced other organic, nonionic surfactants which were previously used before [8].

The surface-active character of siloxane surfactants results from high-molecular weight methyl-rich segments, attached to a flexible $-\text{O}-\text{Si}-\text{O}-\text{Si}-$ backbone, in combination with polyether chains that are grafted to the same backbone, either via $\text{Si}-\text{O}-\text{C}$ or $\text{Si}-\text{C}$ bonds. The latter type is hydrolytically stable and predominant in polyurethane foam applications. They can be represented as $\text{Me}_3\text{SiO}(\text{Me}_2\text{SiO})_x(\text{RMeSiO})_y\text{SiMe}_3$ where Me represents a methyl group:

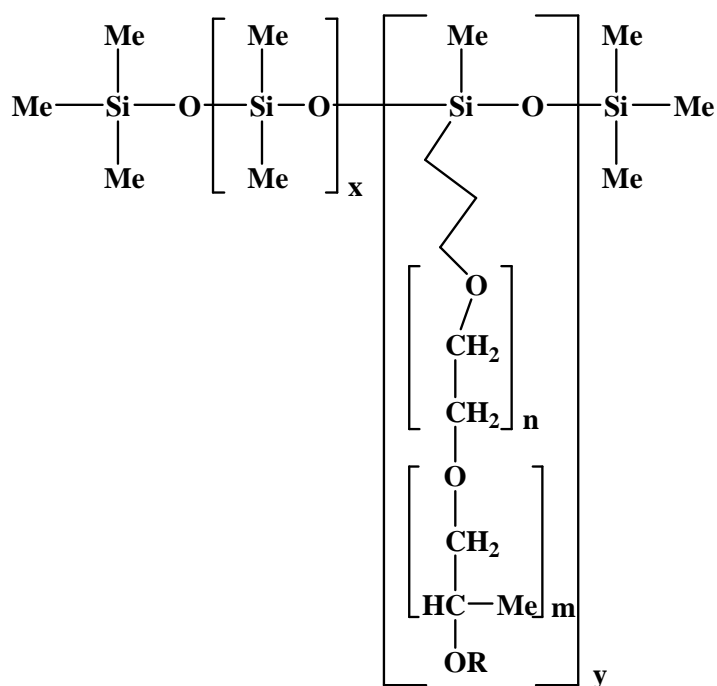


Figure 2.6 Structure of silicone surfactants used in PUR foams manufacture

Silicone surfactants are typically added in amounts of 0.4–2.0% w/w of the polyol formulation. To meet specific processing needs of different foam systems, the molecular structure may be tuned by varying the length and the composition of the polydimethylsiloxane backbone or the number, length, and composition of the pendant polyether chains [8]. Surfactants for rigid foam typically contain 10 to 50 Si-units per molecule while the average molecular weight of a polyether chain ranges from 400 to 1500 g/mol. The ethylene oxide content typically varies from about 50 to

100% and the polysiloxane/polyether ratio lies in the range of 3/1 to 10/1. The total molecular weight of the surfactant amounts to 1500 to 15000 g/mol. In general, surface activity in rigid polyol formulations increases with increasing polysiloxane molecular weight. Increasing the polyether molecular weight has a reducing effect on surface activity but is improving solubility. As a result, emulsification and thereby cell stabilization can be improved. High propylene oxide content tends to increase solubility in isocyanates, whereas high ethylene oxide content tends to increase solubility in polyols, but simultaneously reduce surface activity and flow properties.

2.2.5 Blowing agents

Water acts as a blowing agent. It produces CO₂ gas by reaction with an isocyanate. Typical water concentrations are 3-5 parts of water per 100 parts of polyester polyol and 1.8-5 parts per 100 parts of polyether polyol. The reaction of water with an isocyanate is exothermic and results in the formation of active urea sites which form crosslinks via hydrogen bonding. To reduce the high crosslink density, auxiliary blowing agents are used to produce low density foams with a softer feel than water-blown foams and to produce closed cell flexible foams.

2.2.6 Additives

2.2.6.1 Flame retardants; these are normally based on halogen or phosphorous containing compounds. The addition of small amounts (up to 2 parts hundred of polyol) of fire retardant has little or no effect on foam physical properties, but adverse effects are noticeable when higher amounts are used.

2.2.6.2 Fillers; particulate fillers tend to reduce flammability, increase compression resistance, compressive strength and weight of seat cushion. Reinforcing fibrous filler increase stiffness, heat resistance and tensile strength. Typical fillers include carbon black, clays, calcium carbonate, glass fibres and microspheres. Carbon fibres are used in high performance composites.

2.2.6.3 Coloring materials; pigments must be inert to isocyanate, stable at reaction temperatures and free of contaminants that can affect foaming.

2.2.6.4 Chain extenders/Crosslinking agents; these are low molecular weight polyols or amines. They are generally used for producing foams of

high flexibility by chain extension. Load-bearing capacity of foam is improved by augmenting the degree of crosslinking of the polymer by using polyfunctional reagents. However, because of their high reactivity, the choice of a suitable reagent, the nature of the polyol and the catalyst system and their respective concentrations are critical.

2.3 Formulations [5, 6]

The amount of isocyanate needed to react with polyol and other reactive components can be calculated to obtain chemically stoichiometric equivalents. This theoretical amount may be adjusted up or down dependent on the PUR system, properties required, ambient conditions and scale of production. The adjusted amount of isocyanate used is referred to as the “isocyanate index”,

$$\text{Isocyanate index} = \frac{\text{actual amount of isocyanate}}{\text{theoretical amount of isocyanate}} \times 100$$

The conventional way of calculating the ratio of the components required for PUR manufacture is to calculate the the number of part by weight of the isocyanate needed to react with 100 parts by weight of polyol and use proportionate amount of additives. The analytical data require for the calculation are the isocyanate value of the isocyanate and hydroxyl value, residual acid value and water content of the polyol and other reactive additives.

Isocyanate value (or isocyanate content) is the weight percentage of reactive -NCO groups:

$$\begin{aligned} \text{Isocyanate value} = \% \text{ NCO group} &= \frac{42 \times \text{functionality}}{\text{molar mass}} \times 100 \\ &= \frac{4200}{\text{equivalent weight}} \end{aligned}$$

Hydroxyl value (hydroxyl number; OHV) is expressed in mgKOH/g polyol. This may be defined as the weight of KOH in milligrams that will neutralize the acetyl group produced by acetylation of 1 g of polyol.

$$\begin{aligned}\text{Hydroxyl value} &= \frac{56.1 \times \text{functionality}}{\text{molar mass}} \times 1000 \\ &= \frac{56.1}{\text{equivalent weight}} \times 1000\end{aligned}$$

Acid value is also expressed as mgKOH/g of polyol and numerically equal to OHV in isocyanate useage.

Water content; water reacts with two -NCO groups and the equivalent weight of water is thus:

$$\text{Equivalent weight} = \frac{\text{molar mass}}{\text{functionality}} = \frac{18}{2}$$

Isocyanate conversion (α), isocyanate conversion can be calculated by FTIR method [9], defined as the ratio between isocyanate peak area at time t and isocyanate peak area at time 0:

$$\text{Isocyanate conversion (\%)} = \left[1 - \frac{\text{NCO}^f}{\text{NCO}^i} \right] \times 100$$

where;

NCO^f = the area of isocyanate absorbance peak area at time t (final isocyanate)

NCO^i = the area of isocyanate absorbance peak area at time 0 (initial isocyanate)

2.4 Mechanical properties

The mechanical properties of rigid foams differ markedly from those of flexible foams. The tests used to characterize both types of foam therefore differ, as do their application areas.

Compression load deflection is used to determine the compressive stress-strain behavior, i.e. it is a measure of the load-bearing properties of the material. The test method is somewhat similar to that developed for noncellular plastics. Test on rigid and flexible foams can be determined according to ASTM D 1621-04. A universal

testing machine fitted with a compression rig (cage) consisting of two parallel flat plates (Figure 2.7) is used for the tests.

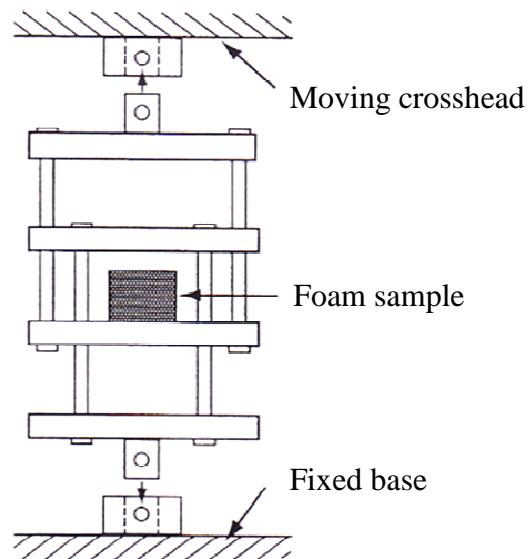


Figure 2.7 Compression load deflection test rig [6]

Compressive properties are perhaps the most important mechanical properties for cellular polymers. Compressive energy absorption characteristics and deformation characteristics of foam depend mainly on density, type of base polymer and the predominance of either open or closed cells. In simple terms, open cell foam (invariably flexible) relies on cell walls bending and buckling, which is essentially a reversible process (Figure 2.8)

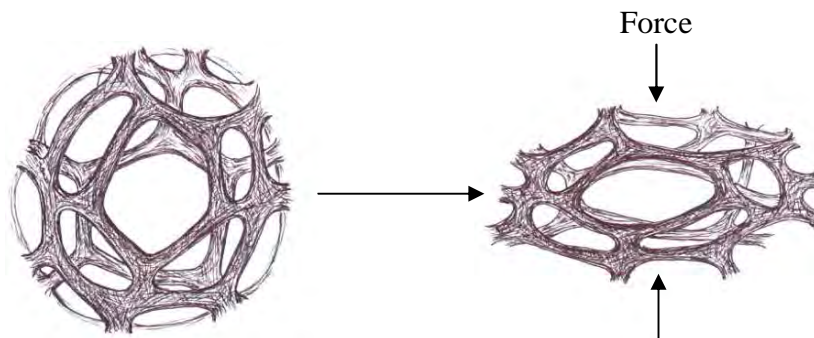


Figure 2.8 Schematic representation of open cell deformation [6]

In addition, as the cell become more compacted during compression, the escape of air through and out of the foam will become increasingly more difficult. The entrapped air will therefore offer some resistance to foam deformation during the

final stages of compression. On the other hand, air flow is not a consideration with closed cell foams. In this case (Figure 2.9) deformation involves cell wall bending/buckling (reversible), gas compression, cell wall stretching/yielding (non-reversible). Severe compression causes cell rupture.

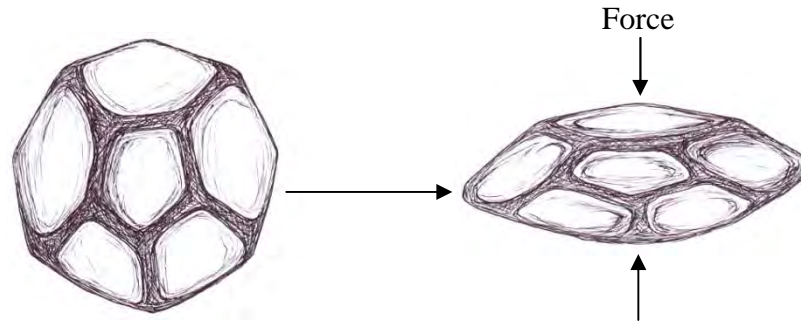


Figure 2.9 Schematic representation of closed cell deformation [6]

Closed cell rigid foams (e.g. PS and PUR foams) exhibit from very limited to no yielding behavior. Consequently, gas compression and matrix strength play important roles during the mechanical deformation of rigid foams. In addition, cell rupture often occurs during the energy absorption process. The energy absorption characteristics of foam can be represented in term of compression stress-strain curves. Figure 2.10 show typical compression stress-strain curve of rigid cellular polymers.

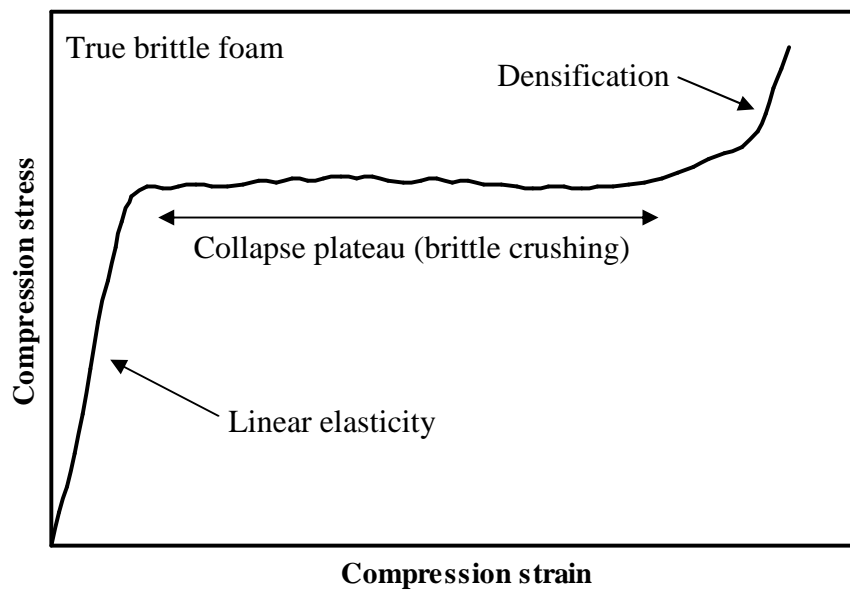


Figure 2.10 Typical compression stress-strain curve for rigid foams

For rigid foams, elements of true brittle crushing are superimposed on the elastic/plastic response. The erratic nature of the collapse plateau corresponds to intermittent rupturing of individual cells. Due to cell rupture in rigid foams, resilience is dramatically affected. Foams can generally withstand only single impacts, for example the liners used inside riding or cycle helmets.

The compressive strength of rigid cellular polymers is usually reported at some definite deformation (5 or 10%). The modulus is then extrapolated to 0% deformation unless otherwise stated. Structural variables that affect the compressive strength and modulus of this foam are, in order of decreasing importance, plastic phase composition, density, cell structure, and gas composition.

2.5 Production technologies of rigid polyurethane foam

Rigid polyurethane foams can be produced by different methods, as shown below [10].

2.5.1 Slabstock production: slabstock rigid polyurethane foams are produced continuously by using horizontal-conveyor-type machine. In contrast, discontinuous production is carried out by using a box. The box-foaming method is not efficient, but it is suitable for small-scale production of various foams with low investment cost. Slabstock foam and box-foaming foams are used for the production of insulation boards, pipe coverings and many other insulation materials.

2.5.2 Foam-in-place: The foam-in-place (or pour-in-place) method is used for the production of refrigerators, deep freezers, sandwich panels and similar applications. This process is also used for field applications, such as indoor and outdoor tank insulation, LPG tank insulation, heavy oil tank insulation, chemical tank car insulation and pipe covering insulation.

2.5.3 Molding: This method is used for producing molded foam products such as pipe covering, window frames, chair shells and picture frames.

2.5.4 Lamination: This method is used for producing laminated panels having flexible facing materials, such as aluminum foil, kraft paper and asphalt paper. The panels produced are used as insulation board for roofs and walls. Rigid facing

materials such as gypsum board can also be used for semi-continuous production of building materials.

2.5.5 Spraying: Two component rigid foam systems can be sprayed onto any surface at a temperature of about 10°C and higher. Examples of spray insulation applications are outdoor tanks, such as heavy oil storage tanks, wall surfaces in cold-storage warehouses and provisions of ships.

2.6 Literature reviews

Rigid polyurethane foams are widely made from polymeric MDI and polyol, especially polyether polyol is used in polyurethane foam production because it is low cost and ease of handling (low viscosity). The manufacture of low density rigid polyurethane foam does, of course, require the use of a blowing agent to create the foam structure. Most rigid foam, however, is made using physical blowing with volatile liquid chlorofluoromethane, CFM-11. The CFM gas has a much low thermal conductivity than air and, because it is retained within the closed cell structure [10]. Although, rigid polyurethane foam blow from CFM gas has a much lower thermal conductivity than foams containing air or other gases, but CFM gas is toxic to human and to be phase out. Accordingly, water-blown system is necessary to replace this physical blowing agent.

Nowadays, the requirement for the development of all water-blown polyurethane foam system is getting higher, because the environmentally friendly blowing agent is carbon dioxide, which is obtained in the reaction between polyisocyanurate and water, but the dimensional stability of the foams of this type is not sufficient [11]. All water-blown polyisocyanurate (PIR) foams system having excellent fire resistance properties. However, all water-brown PIR foams have several problems. They have poor dimensional stability, poor surface friability, as well as poor long-term storage stability of polyol system. Studies of water-blown PIR foam preparation were conducted by Naruse and coworkers [12]. It has been shown that, using phthalic acid-based aromatic ester polyol in mixture with Mannich condensate-based polyether polyol, it is possible to prepare PIR foams for metal-faced continuous sandwich panel. The PIR foams prepared thereby, in terms of the main criteria, are competitive with PIR foams, in which HCFC 141b was as a blowing agent. Water-

blown PIR foam preparation from vegetable oil polyol is facing some problems, and the main reasons are as follows: vegetable oil polyol are very hydrophilic products and do not form homogeneous system even with small quantities of water, and the collapse is observed in their foaming process. The optimal physical and mechanical properties of water-blown PIR foams are achieved at the isocyanate index values 150-200.

Silicone surfactant is the one of component in polyurethane foam formulation that has effect for PUR foam. Surfactants are initial additives used in PUR foam formulations. They assist in mixing incompatible components of the formulation, controlling cell size, open cell content, and uniformity through reduced surface tension. Grimminger and coworkers [13] studied of silicone surfactants for pentane blown rigid foam. They discussed that the influence of different silicone surfactants on the emulsification and stabilization of pentane in polyol premixes, reaction mixture and during foam formation and the influence of silicone surfactants on physical and mechanical properties of foams. Effects of silicone surfactant in rigid polyurethane foams are reported by Lim and coworkers [14]. They found that cream time, gel time and tack free time increased with the content of surfactant increasing due to the increased stability of reaction mixture and rising bubbles.

Nowadays, the improvement of the fire behavior and thermal stability of polyurethane thermal insulators foams is the aim of numerous works. Influence of different flame retardants on fire behavior of modified PIR/PUR polymeric foams are reported by Modesti and coworkers [15]. Flame retardants, melamine cyanurate and ammonium polyphosphate are used in this work. They found that the fire behavior of flame retardant foams is better than that of unfilled foams and they also found that the fire behavior of PUR-PIR foams can be significantly improved by use of expendable graphite (EG). A number of work concerning and modifying PUR and PIR foams based on polyether polyol. Lorenzenti and coworkers [16] studied thermally stable hybrid foams based on cyclophosphazenes and polyurethanes. They found that the introduction of increasing amount of cyclotriphosphazene in foams lead to a significant improvement of thermal stability and fire behavior.

In polyurethane foam industry, catalyst is one component has played significant role in catalytic system. Catalyst is necessary for the production of

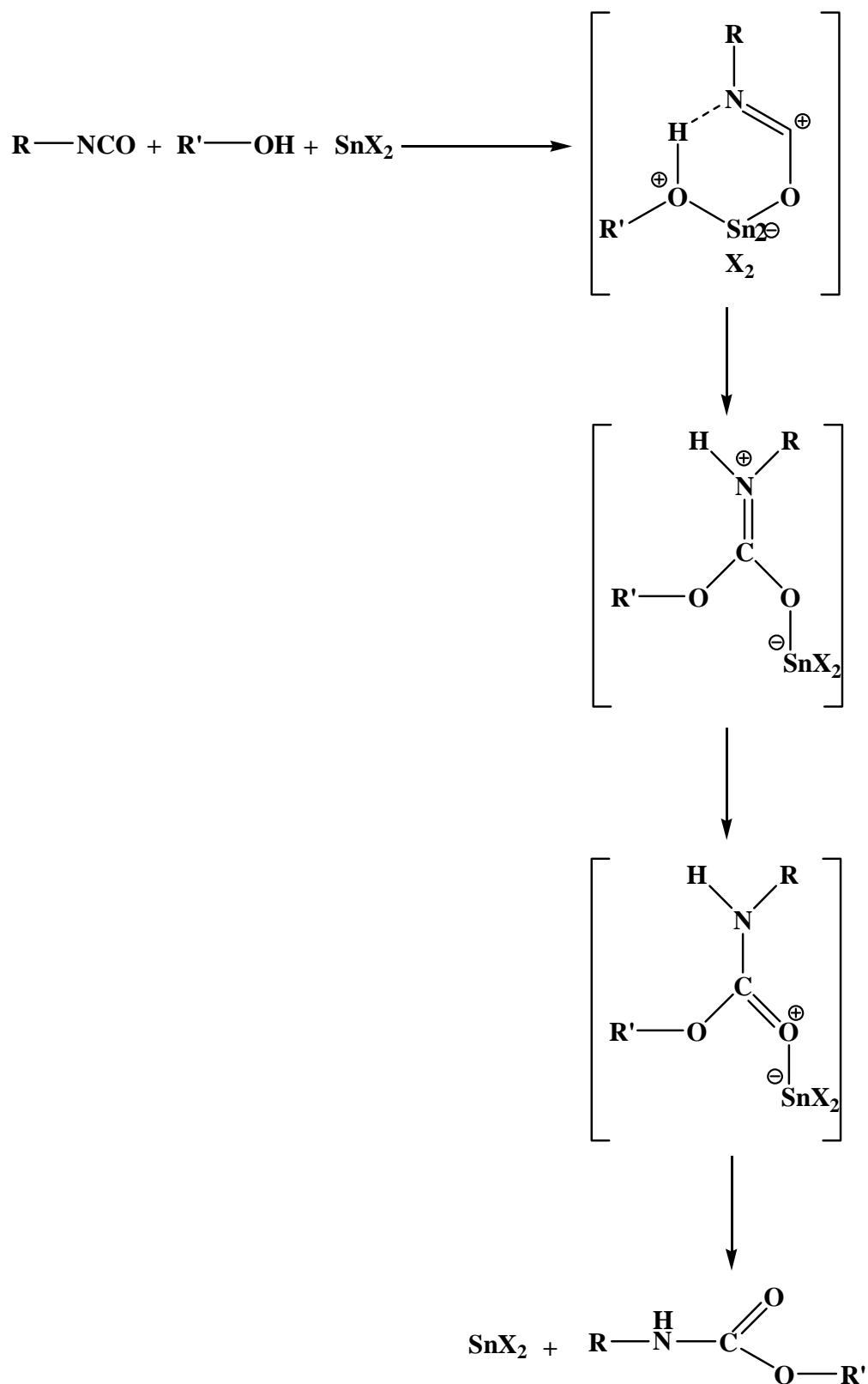
polyurethane foam. Because the reaction between isocyanate with hydroxyl group is slow. Tertiary amines and tin compounds [17-19] are widely used as catalysts for gelling and blowing reactions such as dibutyltin dilaurate (DBTDL) and dimethylcyclohexylamine (DMCHA). There are many works concerning the development of catalyst for polyurethane (PUR) and polyisocyanurate (PIR) foams preparation as follows:

Maris and coworkers [19] studies polyurethane catalysis by tertiary amines. They found that tertiary amines play an important role. The mechanism of tertiary amine catalysts are shown in Scheme 2.1. In general, the tertiary amine coordinate to the positive electron charged carbon of the NCO group or hydrogen of the OH group and forms a transition state to activate urethane formation reaction. It is said that a tertiary amine can be tuned by maximizing its ability to form a hydrogen bond with alcohol, thereby activating the O–H bond so it can attach to the isocyanate more easily. In this work a deeper insight into the molecular catalyst structure–polymer properties relationship will be given. They discussed the selection of catalyst is based on its activity as well as performance on physical foam properties. Depending on the molecular structure of the catalyst, the activity will be different. This activity relates to the catalysis of the gel and blow reaction but also the allophanate, biuret, and trimerization reactions. Via a model system, each of these reactions is studied to understand the reaction mechanism in a better way.

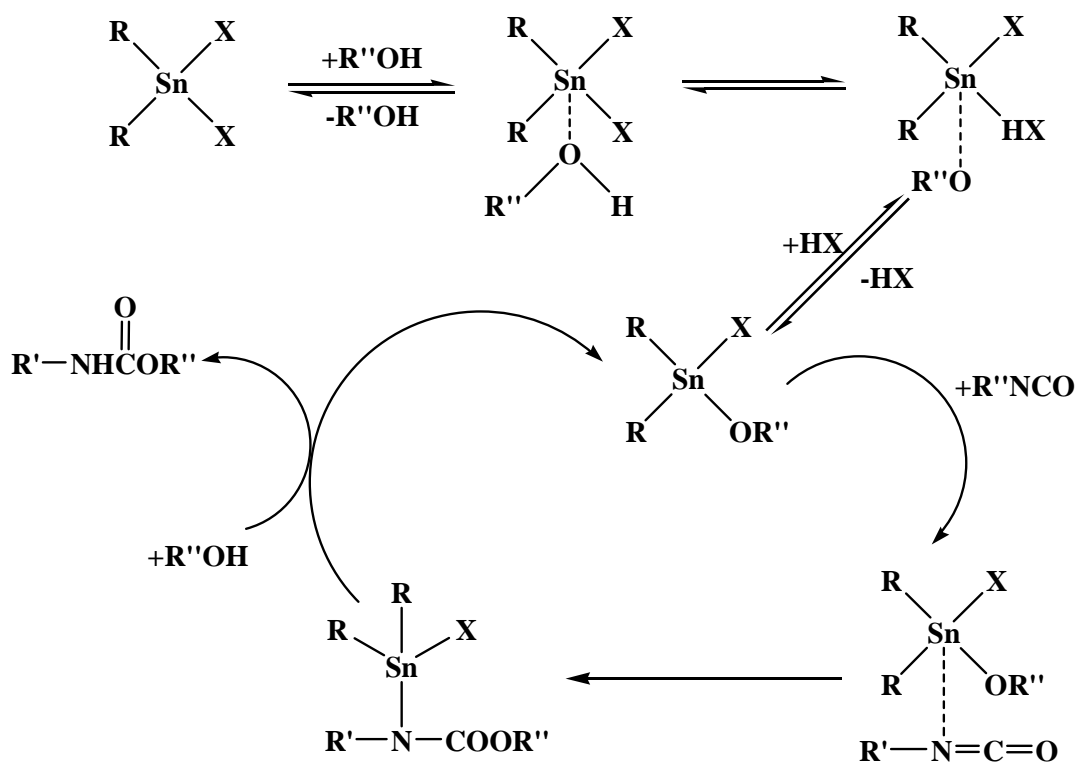
Organotin catalysts [20]

The tin (II) salts the following mechanism has been proposed (Scheme 2.2). The isocyanate, polyol and tin catalyst form a ternary complex, which then gives the urethane product. Two routes, not shown, to the complex have been proposed. In the first one the tin first adds to the polyol then the isocyanate. In the second one the tin adds to the oxygen of the isocyanate the reacts with the polyol.

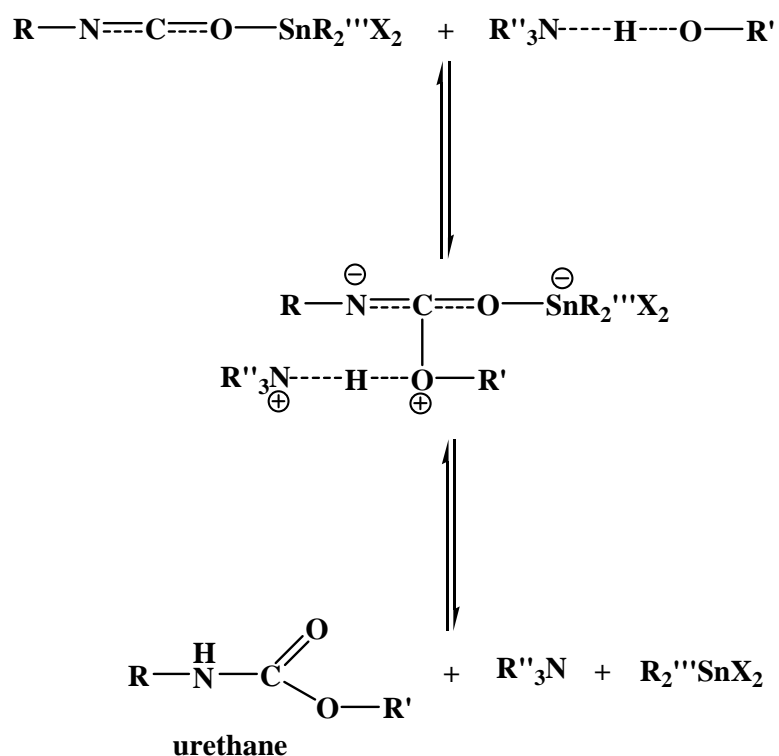
The proposed mechanisms for tin (IV) catalysts, dialkyltin dicarbonates and dialkyltin dialkylthiolates, is the reaction of the tin with a polyol forming a tin alkoxide, which can then react with the isocyanate to form a complex (Scheme 2.3). Transfer of the alkoxide anion onto the coordinated isocyanate affords an N-stannylurethane, which then undergoes alcoholysis to produce the urethane group and the original tin alkoxide.



Scheme 2.2 Mechanism of tin (II) salts catalyst



Scheme 2.3 Mechanism of tin (IV) salts catalyst



Scheme 2.4 Mechanism of tin-amine synergism

Okuzono and coworkers [21] studied new polyisocyanurate catalysts which exhibit high activity at low temperature. The combination of other tertiary amine catalysts could improve the flowability; however, the flammability of the foam would be a hazard because the isocyanurate reaction has not fully progressed. For the improvement of the above-mentioned problems, Tosoh Corp. has developed several new quaternary ammonium salt compounds, such as Toyocat-TR20. TR20, however, should be used in conjunction with an alkali metal co-catalyst. Presently, Tosoh has succeeded in developing another new catalyst having even higher catalytic activity at low temperature, which can replace the use of the alkali metal catalyst. The new catalyst provides the low temperature dependency in the isocyanurate reaction activity compared to the traditional isocyanurate catalysts. The new catalyst provides the following advantages:

1. The catalytic activity is high.
2. The isocyanurate reaction activity at low temperature is high.
3. The initial foaming reaction is improved, thereby the rise profile is now smooth.

In this report, new quaternary ammonium salts will be introduced with comparison data using the FT-IR analytical methods, as well as the evaluation in panel and sprayed foams.

Molero and coworkers [22] studied activities of octoate salts as novel catalysts for the transesterification of flexible polyurethane foams with diethylene glycol. They found that the entire family of commercial metal octoates shows a certain ability catalyzing that process. The octoates have showed different catalytic activities according to their hardness and coordination ability. The activity of alkaline and alkaline-earth metal octoates is basically related with their hardness as cation that determines their potential for the formation of a metal alkoxylate. In the case of transition metals the mechanism involves several steps, including the formation of a metal alkoxylate, coordination-insertion of the alkoxide into the urethane group and transfer from recovered polyol to glycol. Furthermore, lithium and stannous octoates showed a remarkable catalytic activity.

Strachota and coworkers [23] studied comparison of environmentally friendly, selective polyurethane catalysts. Selected commercially available amines, including N-substituted morpholines, were evaluated as single catalyst and as catalyst mixtures for polyurethane foam preparation. The motivation was the search for economically and environmentally attractive replacements of “classical” catalyst like diazabicyclooctane, dibutyltindilaurate and N,N-bis(2-dimethylaminoethyl)methylamine. Especially interesting was replacing dibutyltindilaurate, and also the possibility of using reactive catalyst derivatives that would be incorporated into polyurethane, thus reducing the content of volatile organic compounds in the polymer. They found the functionalized morpholine (MEO) showed a poor gelling activity even in comparison to other morpholines. Its reduced mobility due to the desired incorporation into the polyurethane, as well as H-bridging is the probable reasons. Higher amounts of MEO in combination with an analogously OH-functionalized good gelation catalyst should lead to better results. The structures of derivative morpholines as catalysts are shown in Figure 2.11.

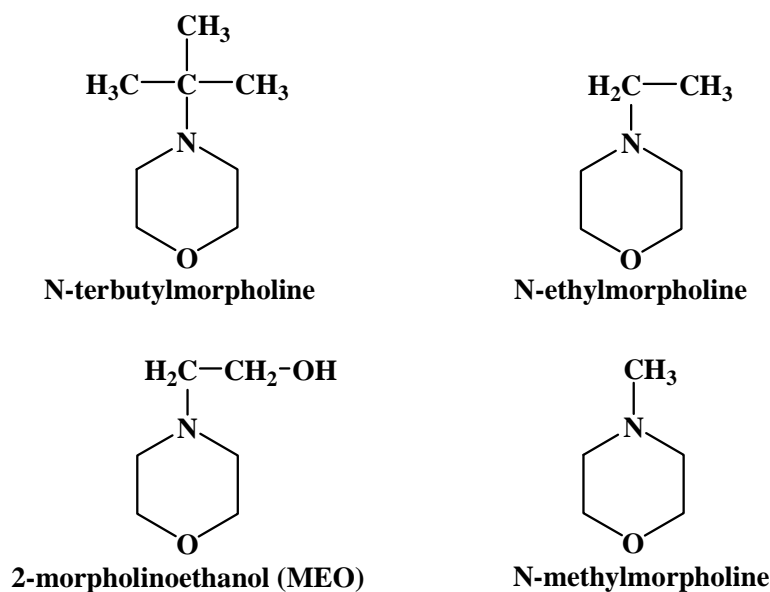


Figure 2.11 Structure of derivative morpholines

Carroy and coworkers [24] studied novel latent catalysts for 2K-PUR systems. The replacement of the most versatile metal catalyst in polyurethane crosslinking catalysis, namely dibutyltindilaurate (DBTDL), is still a big challenge, but a necessity in view of its bad toxicological profile. As none of the existing numerous metal compounds have proven to be a completely satisfactory alternative, they decided to

focus our development on a latent system, targeting both a fast curing time of the coating while maintaining a long pot-life of the formulation. They have successfully developed a smart way of meeting the two opposite requirements through the development of photo-latent metal catalysts, including non-tin based compounds, for curing 2-component polyurethane coatings.

Inoue and coworkers [25] studied amine-metal complexes as an efficient catalyst for polyurethane syntheses. Since the reaction of aliphatic isocyanates on preparations of polyurethane are very slow compared with aromatic isocyanates. Therefore, tertiary amines and tin compounds having excellent catalytic activity are used mainly as catalysts for polyurethane formation. In particular, dibutyl tin dilaurate (DBTDL) has been used. However, tin is toxic to human beings. Accordingly, a new catalyst or catalytic system is necessary to replace this catalyst. In this research they prepared the complexes of $M(\text{acac})_n$ [$M = \text{Mn}, \text{Fe}, \text{Co}, \text{Ni}$ and Cu] and tertiary amines are used as new catalysts for the reaction between hexamethylene diisocyanate (HDI) and polyols. They found that $\text{Mn}(\text{acac})_n$ -TEDA complex shows better catalytic activity than other $M(\text{acac})_n$ complexes and shows nearly catalytic activity with DBTDL catalyst.

Kurnoskin [26, 27] synthesized metaliferous epoxy chelate polymers (MECPs) by hardening of the diglycidyl ether of bisphenol A (DGEBA) with chelates of metal (Mn^{4+} , Fe^{3+} , Ni^{2+} , Cu^{2+} , Zn^{2+} and Cd^{2+}) and aliphatic amines (ethylenediamine, diethylenetriamine, triethylenetetramine and cycloethylated diethylenetriamine). The reactivity of the complexes in reactions with DGEBA and its dependence on the structures of the chelates have been investigated. MECPs have been found to possess increased strength and heat resistance. The structures of the chelates as hardeners are shown in Figure 2.12.

The research of Inoue and coworkers indicated that the metal complexes between transition metal and amine can be catalyzed urethane formation. Therefore, we are interested to develop some metal complexes in Kurnoskin's work to use as catalysts replaced commercial catalysts for rigid polyurethane foam preparation.

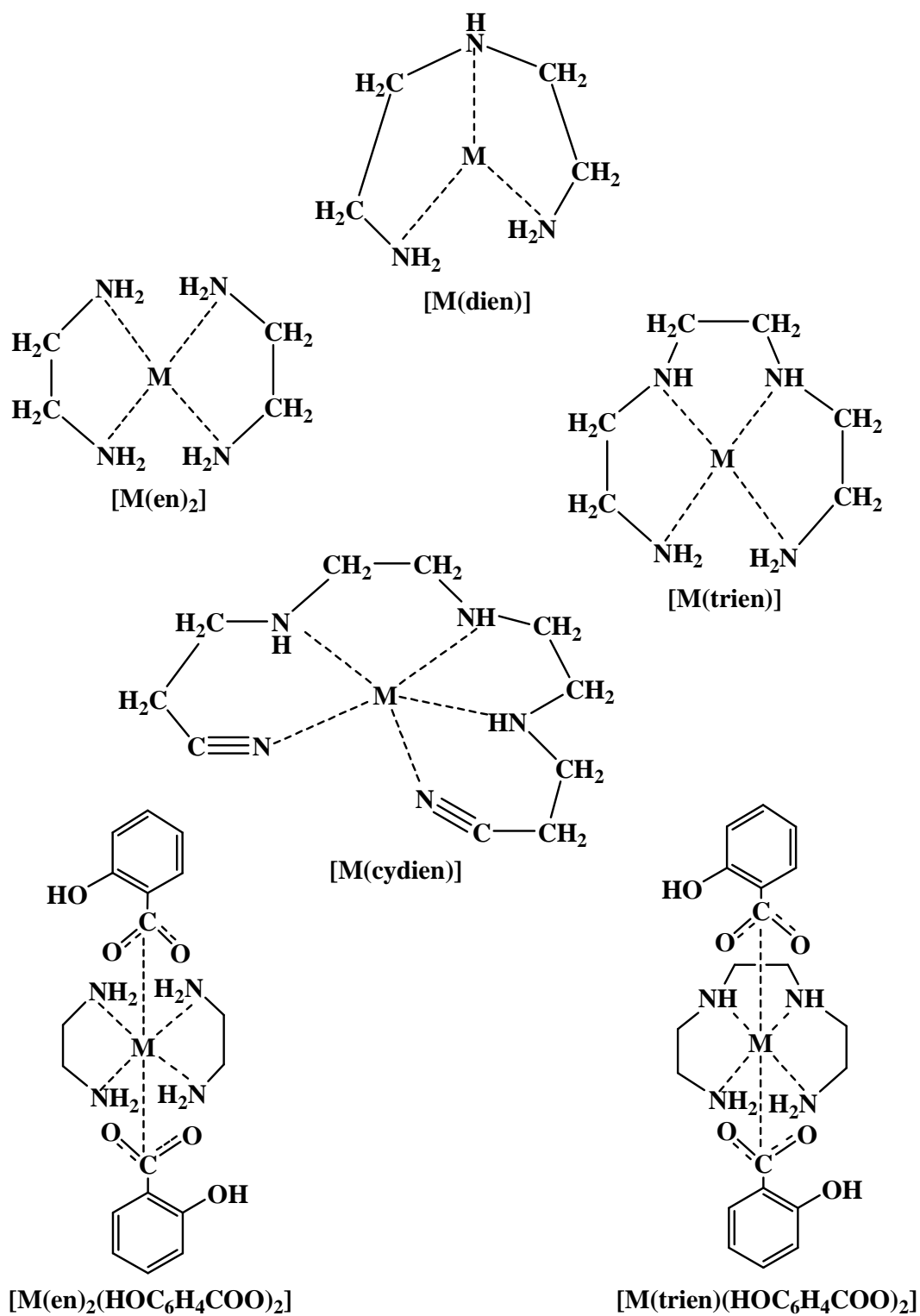


Figure 2.12 Structures of metal complexes and metal salt complexes

CHAPTER III

EXPERIMENTAL

3.1 Materials

Copper (II) acetate monohydrate ($\text{Cu}(\text{OAc})_2 \cdot \text{H}_2\text{O}$), manganese (II) acetate tetrahydrate ($\text{Mn}(\text{OAc})_2 \cdot 4\text{H}_2\text{O}$), ethylenediamine (en), triethylenetetramine (trien) and salicylic acid (Sal) were obtained from Fluka and Aldrich. Polymeric MDI (4,4'-methane diphenyl diisocyanate; PMDI, MR-200): %NCO = 31.0 (%wt.), average functionality = 2.7 and polyol (Raypol[®] 4221, sucrose-based polyether polyol), hydroxyl value (OHV) = 440 mgKOH/g, functionality = 4.3 were supplied by South City Petrochem CO., LTD. Polysiloxane (TEGOSTAB B8460, Goldschmidt) were obtained from South City Petrochem CO., LTD. was used as a surfactant. Distilled water was used as a chemical blowing agent. Metal complexes were prepared and used as catalysts. N,N-dimethylcyclohexylamine (DMCHA) (South City Petrochem CO., LTD.) was used as a commercial reference catalyst.

3.2 Measurements

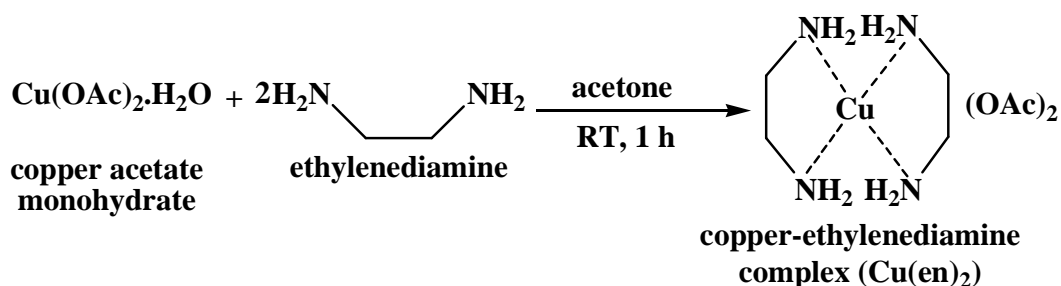
IR spectra of the samples were recorded on a Nicolet Impact 410 FT-IR spectrometer using potassium bromide (KBr) disk method and on Perkin-Elmer ATR-IR spectrometer at room temperature. The samples were scanned over a range of 500-4000 cm^{-1} at a resolution of 4 cm^{-1} and a number of scan was 64. The measurement was controlled by Omnic software. UV-vis spectra were recorded on ultraviolet and visible spectrophotometer at room temperature. The samples were scan over range 200-800 nm and speed was medium. MALDI-TOF mass spectra were obtained on a Bruker Bifex mass spectrometer using 2-cyano-4-hydroxycinnamic acid (HCCA) as a matrix. Elemental analysis was carried out using a Perkin-Elmer EP 2400 analyzer. X-ray diffractometer (XRD) used in study was Bruker model D8 Discover with nickel filtered $\text{CuK}\alpha$ radiation (40 kV, 40 mA) at an angle of 2θ range from 10-40°. The foaming reaction times, cream time, gel time tack free time and rise time were investigated by using a stopwatch. The foaming temperatures were recorded by dual thermocouple, Digicon DP-71. The apparent density of foams was measured according to ASTM D 1622-09, the size of specimen was 3.0 x 3.0 x 3.0 cm dimension and the average values of three samples were reported. The compression testing of foams in parallel and perpendicular to the foam rise direction were

performed using universal testing machine (Lloyd/LRX) according to ASTM D 1621-09, the specimen size was 3.0 x 3.0 x 3.0 cm dimension, the rate of crosshead movement was fixed at 2.54 mm/min and the preload cell used was 0.100 N. Thermogravimetric analysis (TGA) was examined using a Netzsch STA 409C thermogravimetric analyzer. All samples were heated from 25 °C to 600 °C at heating rate of 20 °C/min under N₂ gas. The result of thermal stability was report in percentage weight residue of foams. Initial decomposition temperature (IDT) was taken at the temperature where 5 wt% loss of foam occurred. The morphology and cell size of foams were studied using scanning electron microscope (SEM) Hitachi/S-4800. The samples were gold coated before scanning in order to provide an electrically conductive surface. The accelerating voltage was 20 kV in order to a void degradation of the sample.

3.3 Synthetic procedures

3.3.1 Synthesis of metal-amine complexes

3.3.1.1 Synthesis of copper-ethylenediamine complex (Cu(en)₂)



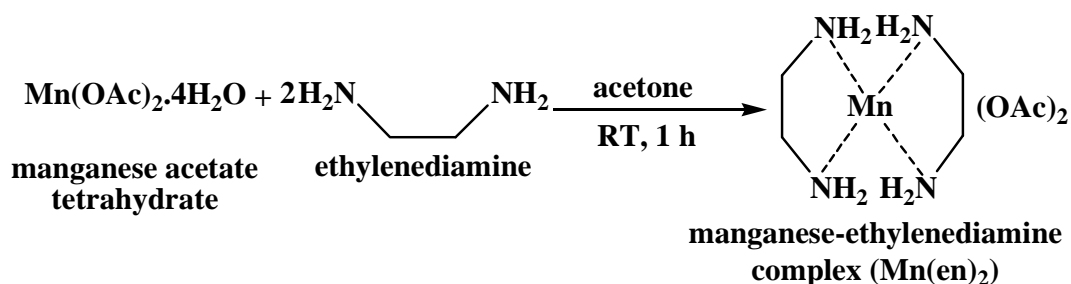
Scheme 3.1 Synthesis of copper-ethylenediamine complex

The preparation of Cu(en)₂ was performed according to the method reported in the literature [26] as follows: a solution of copper (II) acetate monohydrate (0.624 g, 3.12 mmol) was stirred in acetone (25 mL) at room temperature. A solution of ethylenediamine (0.42 ml, 6.28 mmol) in acetone (10 ml) was added dropwise to copper acetate solution over a period of 10 minutes and stirred at room temperature for 1 hour. Cu(en)₂ precipitated from blue solution and was subsequently isolated by filtration and was dried under vacuum to remove solvent. The yield of Cu(en)₂ was obtained as a purple powder. (0.62 g, 62%): IR (KBr, cm⁻¹); 3318, 3269, 3139 (N-H), 2986, 2953, 2884 (C-H), 1545 (asymmetric C=O, acetate), 1396 (symmetric C=O,

acetate), 1326 (C-N), 1039 (C-O). UV; $\lambda_{\max}(\text{MeOH}) = 230 \text{ nm}$, molar absorptivity (ϵ) = 4,790. Anal. Calcd. For $\text{CuC}_8\text{O}_4\text{H}_{22}\text{N}_4\cdot\text{H}_2\text{O}$: C 30.04; H 7.56; N 17.52; found C 29.79; H 7.81; N 17.48. AAS. Calcd. For $\text{CuC}_8\text{O}_4\text{H}_{22}\text{N}_4$: Cu 21.05; found Cu 21.94.

3.3.1.2 Synthesis of manganese-ethylenediamine complex

($\text{Mn}(\text{en})_2$)

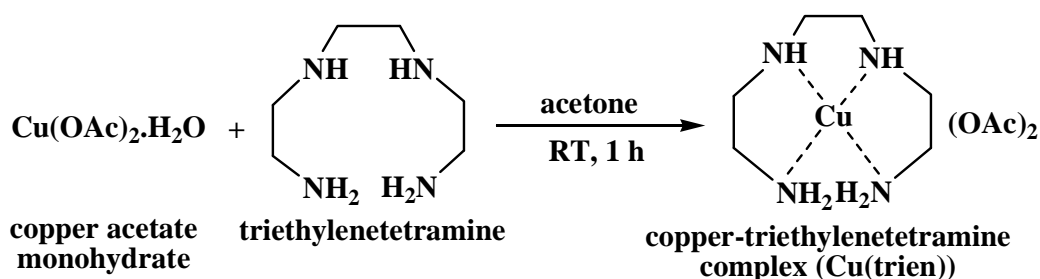


Scheme 3.2 Synthesis of manganese-ethylenediamine complex

The experiment of $\text{Mn}(\text{en})_2$ was carried out according to the procedure described in experiment 3.3.1.1 employing manganese (II) acetate tetrahydrate (0.671 g, 2.74 mmol) instead of copper (II) acetate monohydrate. A solution of ethylenediamine (0.37 ml, 5.47 mmol) in acetone (10 mL) was added dropwise to manganese acetate solution. $\text{Mn}(\text{en})_2$ precipitated from brown solution but could not be isolated by filtration because it was unstable in the air. $\text{Mn}(\text{en})_2$ was isolated by evaporation and was dried under vacuum to remove solvent. $\text{Mn}(\text{en})_2$ was obtained as a brown viscous liquid. (0.98 g, 98%): IR (KBr, cm^{-1}): 3281 (N-H), 2966 (C-H), 1557 (asymmetric C=O, acetate), 1408 (symmetric C=O, acetate), 1337 (C-N), 1013 (C-O). UV; $\lambda_{\max}(\text{MeOH}) = 229 \text{ nm}$, molar absorptivity (ϵ) = 1,220.

3.3.1.3 Synthesis of copper-triethylenetetramine complex

($\text{Cu}(\text{trien})$)

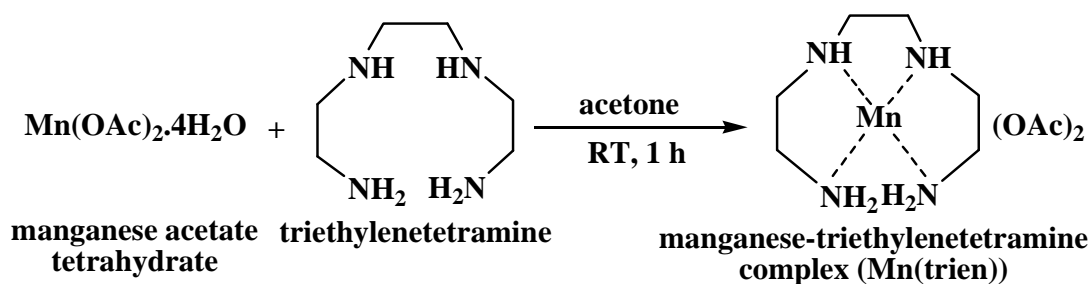


Scheme 3.3 Synthesis of copper-triethylenetetramine complex

The preparation of Cu(trien) was performed according to the method reported in the literature [26] as follows: a solution of copper (II) acetate monohydrate (0.577 g, 2.89 mmol) was stirred in acetone (25 mL) at room temperature. A solution of triethylenetetramine (0.43 ml, 2.89 mmol) in acetone (10 ml) was added dropwise to copper acetate solution over a period of 10 minutes and stirred at room temperature for 1 hour. After the reaction mixture was stirred at room temperature for 1 hour, the solution was evaporated and was dried under vacuum. Cu(trien) was obtained as a blue viscous liquid. (0.99 g, 99%): IR (KBr, cm^{-1}); 3249 (N-H), 2954, 2887 (C-H), 1556 (asymmetric C=O, acetate), 1401 (symmetric C=O, acetate), 1339 (C-N), 1019 (C-O). UV; $\lambda_{\text{max}}(\text{MeOH}) = 258 \text{ nm}$, molar absorptivity (ϵ) = 3,480.

3.3.1.4 Synthesis of manganese-triethylenetetramine complex

(Mn(trien))



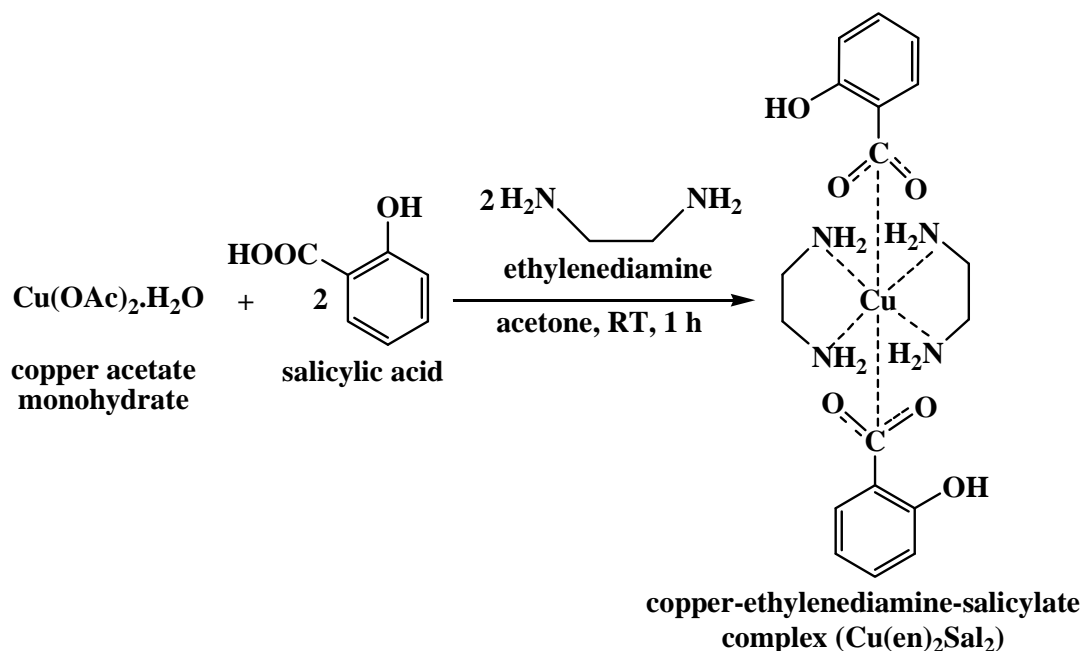
Scheme 3.4 Synthesis of manganese-triethylenetetramine complex

The preparation of Mn(trien) was performed according to the procedure described in experiment 3.3.1.3 employing manganese (II) acetate tetrahydrate (0.630 g, 2.57 mmol) was stirred in acetone and using triethylenetetramine (0.38 mL, 2.53 mmol) instead of ethylenediamine. The brown viscous liquid of Mn(trien) was obtained by evaporation and dried under vacuum. (0.95 g, 95%): IR (KBr, cm^{-1}); 3264 (N-H), 2930, 2874 (C-H), 1558 (asymmetric C=O, acetate), 1402 (symmetric C=O, acetate), 1338 (C-N), 1011 (C-O). UV; $\lambda_{\text{max}}(\text{MeOH}) = 232 \text{ nm}$, molar absorptivity (ϵ) = 980.

3.3.2 Synthesis of metal-amine-salicylate complexes

3.3.2.1 Synthesis of copper-ethylenediamine-salicylate complex

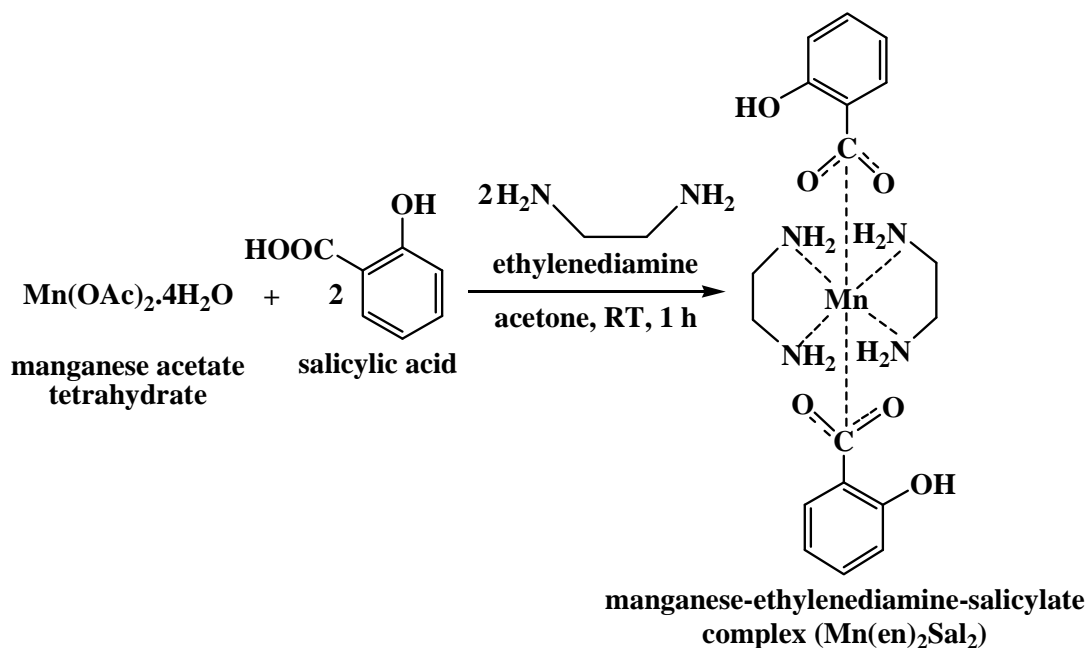
(Cu(en)₂Sal₂)



Scheme 3.5 Synthesis of copper-ethylenediamine-salicylate complex

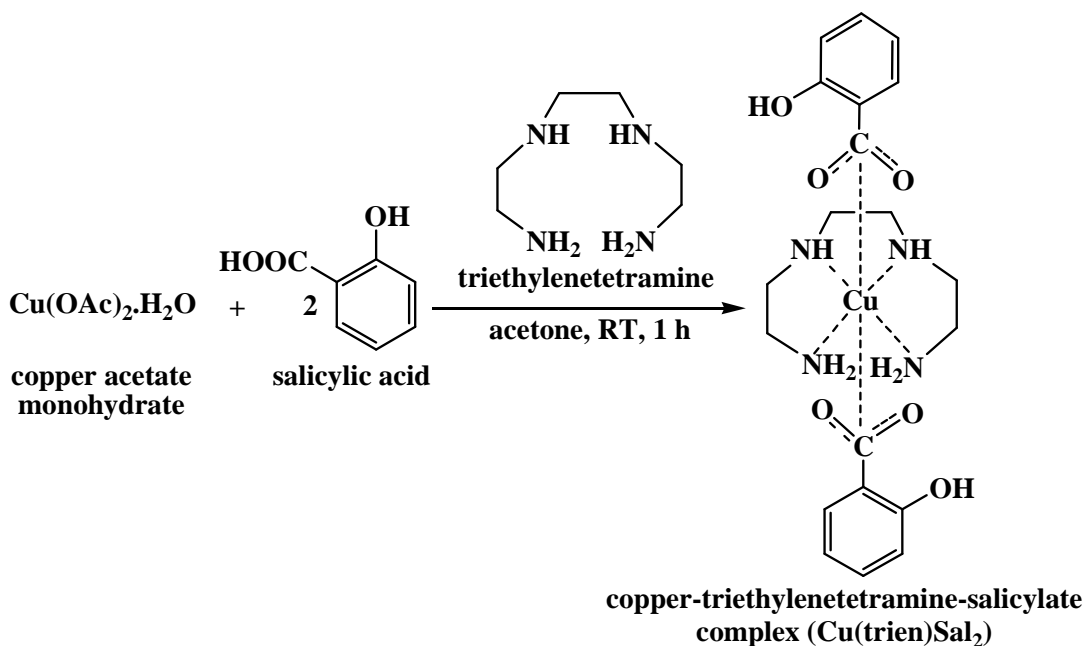
The preparation of Cu(en)₂Sal₂ was carried out according to the method reported in the literature [26]. The mixture of copper (II) acetate monohydrate (0.335 g, 1.78 mmol) and salicylic acid (0.463 g, 3.35 mmol) was stirred in acetone (25 mL) at room temperature for 30 minutes. A solution of ethylenediamine (0.23 mL, 3.36 mmol) in acetone (10 mL) was added dropwise to mixture over a period of 10 minutes. The reaction was stirred at room temperature for 1 hour. Cu(en)₂Sal₂ was subsequently isolated from solution by evaporation and was dried under vacuum to remove residue solvent. Cu(en)₂Sal₂ was obtained as a purple viscous liquid (0.99 g, 99%): IR (KBr, cm⁻¹); 3250 (N-H), 2875 (C-H), 1708 (C=O, 1590 (Ar-H), 1485 (asymmetric C=O, salicylate), 1455 (symmetric C=O, salicylate), 1384 (C-N), 1250, 1030 (C-O), 858, 760 (Ar-H). UV; λ_{max}(MeOH) = 300 nm, molar absorptivity (ε) = 5,300.

3.3.2.2 Synthesis of manganese-ethylenediamine-salicylate complex

 $(\text{Mn}(\text{en})_2\text{Sal}_2)$ **Scheme 3.6** Synthesis of manganese-ethylenediamine-salicylate complex

The experiment was performed according to the procedure described in experiment 3.3.2.1 employing manganese (II) acetate tetrahydrate (0.382 g, 1.56 mmol), salicylic acid (0.431 g, 3.12 mmol) and ethylenediamine (0.21 mL, 3.11 mmol). The brown viscous liquid of $\text{Mn}(\text{en})_2\text{Sal}_2$ was evaporated and dried under vacuum (0.94 g, 94%): IR (KBr, cm^{-1}): 3254 (NH), 2870 (CH), 1709 (C=O, salicylate), 1600 (Ar-H), 1485 (asymmetric C=O, acetate), 1459 (symmetric C=O, acetate), 1385 (CN), 1252, 1222, 1030 (CO), 860, 761 (Ar-H). UV; $\lambda_{\text{max}}(\text{MeOH}) = 295 \text{ nm}$, molar absorptivity (ϵ) = 3,000.

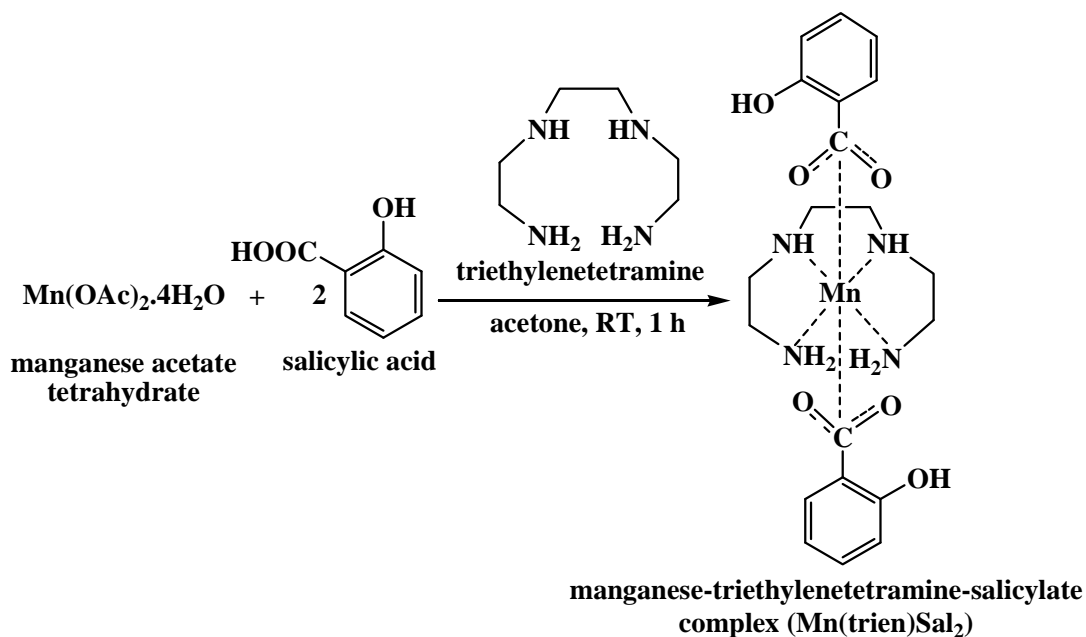
3.3.2.3 Synthesis of copper-triethylenetetramine-salicylate complex (Cu(trien)Sal₂)



Scheme 3.7 Synthesis of copper-triethylenetetramine-salicylate complex

The preparation of Cu(trien)Sal₂ was performed according to the method reported in the literature [26]. The mixture of copper (II) acetate monohydrate (0.321 g, 1.61 mmol) and salicylic acid (0.444 g, 3.21 mmol) was stirred in acetone (25 mL) at room temperature for 30 minutes. A solution of triethylenetetramine (0.24 mL, 1.61 mmol) in acetone (10 mL) was added dropwise to mixture over a period of 10 minutes. The reaction was stirred at room temperature for 1 hour. Cu(trien)Sal₂ was subsequently isolated from solution by evaporation and was dried under vacuum to remove residue solvent. Cu(trien)Sal₂ was obtained as a blue viscous liquid (0.99 g, 99%): IR (KBr, cm⁻¹); 3256, 3156 (N-H), 2942, 2875 (C-H), 1590 (Ar-H), 1484 (asymmetric C=O, salicylate), 1455 (symmetric C=O, salicylate), 1384 (C-N), 1251, 1222, 1029 (C-O), 859, 760 (Ar-H). UV; λ_{max} (MeOH) = 294 nm, molar absorptivity (ϵ) = 16,300.

3.3.2.4 Synthesis of manganese-triethylenetetramine-salicylate complex (Mn(trien)Sal₂)



Scheme 3.8 Synthesis of manganese-triethylenetetramine-salicylate complex

The experiment was performed according to the procedure described in experiment 3.3.2.3 employing manganese (II) acetate tetrahydrate (0.367 g, 1.50 mmol), salicylic acid (0.414 g, 3.00 mmol) and triethylenetetramine (0.22 mL, 1.50 mmol). The brown viscous liquid of $\text{Mn}(\text{trien})\text{Sal}_2$ was evaporated and dried under vacuum (0.96 g, 96%): IR (KBr, cm^{-1}); 3252 (N-H), 2870 (C-H), 1600 (Ar-H), 1484 (asymmetric C=O, salicylate), 1458 (symmetric C=O, salicylate), 1385 (C-N), 1253, 1223, 1030 (C-O), 858, 762 (Ar-H). UV; $\lambda_{\text{max}}(\text{MeOH}) = 300 \text{ nm}$, molar absorptivity (ϵ) = 5,600.

Compositions of starting materials in the preparation of all metal complexes are shown in Table 3.1.

Table 3.1 Composition of starting materials in the preparation of metal complexes

Metal complexes	Wt. of M(OAc) ₂ (g)	Weight of composition			Yield (%)	Appearance
		en (mL)	trien (mL)	Salicylic acid (g)		
Cu(en) ₂	0.624	0.42	-	-	62	Purple powder
Mn(en) ₂	0.671	0.37	-	-	98	Brown viscous liquid
Cu(trien)	0.577	-	0.43	-	99	Blue viscous liquid
Mn(trien)	0.630	-	0.38	-	95	Brown viscous liquid
Cu(en) ₂ Sal ₂	0.335	0.23	-	0.463	99	Purple viscous liquid
Mn(en) ₂ Sal ₂	0.382	0.21	-	0.431	94	Brown viscous liquid
Cu(trien)Sal ₂	0.321	-	0.24	0.444	99	Blue viscous liquid
Mn(trien)Sal ₂	0.367	-	0.22	0.414	96	Brown viscous liquid

en = ethylenediamine, trien = triethylenetetramine

3.3.3 Rigid polyurethane (RPUR) foam preparations

The rigid polyurethane foams preparation procedure catalyzed by M(en)₂, M(trien), M(en)₂Sal₂ and M(trien)Sal₂ (M = Cu and Mn) is shown in Figure 3.1. The foams were prepared by mechanical mixing technique in two steps of the mixing. In the first mixing step, polyol, catalysts (metal complexes or DMCHA), surfactant and blowing agent were mixed. In the second mixing step, the isocyanate was added to the mixed polyol from first mixing then the mixture were mixed in homogeneous mixture by mechanical stirrer at 2000 rpm for 20 seconds. During the reaction, cream time, gel time, tack free time and rise time were measured [16-18]. After that, the foams were kept at room temperature for 48 hours and then carrying out physical and mechanical characterization. The foam formulations are reported in Tables 3.2 and 3.3. Polyurethane foams with different NCO indexes were prepared by using different catalysts.

Table 3.2 RPUR foam formulations at different NCO indexes (in part by weight unit)

Formulations (pbw)	NCO index							
	80	100	130	150	160	180	200	250
Polyol (Raypol [®] 4221)	100	100	100	100	100	100	100	100
Catalysts (metal complexes)	1.0	1.0	1.0	1.0	1.0	1.0	1.0	1.0
Surfactant (TEGOTAB B8460)	2.5	2.5	2.5	2.5	2.5	2.5	2.5	2.5
Blowing agent (H ₂ O)	3.0	3.0	3.0	3.0	3.0	3.0	3.0	3.0
Polymeric MDI (MR-200)	121	151	197	227	242	272	303	378

Table 3.3 RPUR foam formulations at different NCO indexes (in gram unit, cup test)

Formulations (g)	NCO index							
	80	100	130	150	160	180	200	250
Polyol (Raypol [®] 4221)	10.0	10.0	10.0	10.0	10.0	10.0	10.0	10.0
Catalysts (metal complexes)	0.10	0.10	0.10	0.10	0.10	0.10	0.10	0.10
Surfactant (TEGOTAB B8460)	0.25	0.25	0.25	0.25	0.25	0.25	0.25	0.25
Blowing agent (H ₂ O)	0.30	0.30	0.30	0.30	0.30	0.30	0.30	0.30
Polymeric MDI (MR-200)	12.1	15.1	19.7	22.7	24.2	27.2	30.3	37.8

Since the rigid polyurethane foams obtained from different catalysts have similar IR spectra, therefore, only the IR data PUR foams obtained from Cu(en)₂ catalyst is shown as follows:

RPUR foam catalyzed by Cu(en)₂: IR (IR-ATR, cm⁻¹); 3318 (N-H), 2933, 2874 (C-H), 2277 (free NCO), 1709 (C=O), 1595 (Ar-H), 1515 (N-H), 1412 (C-N isocyanurate), 1309 (C-H), 1220, 1077 (C-O urethane), 814, 766 (C-H aromatic ring).

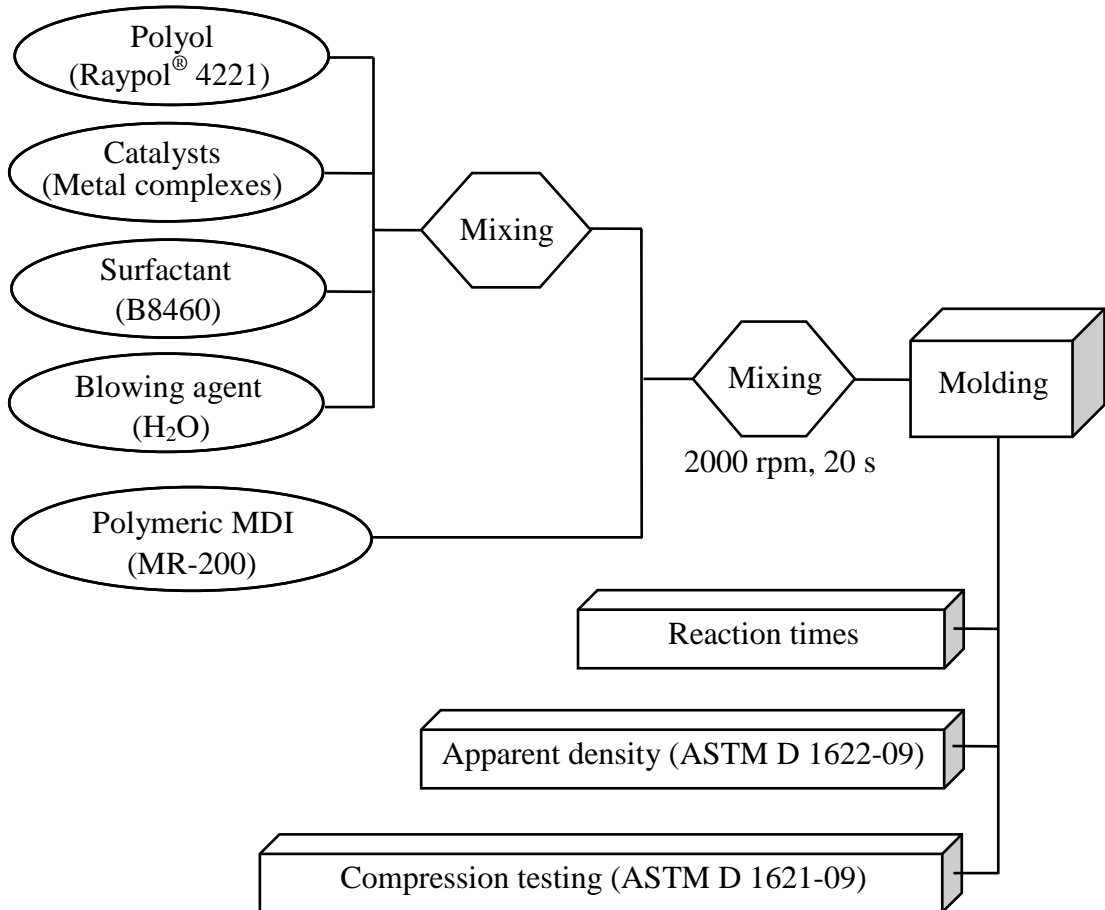


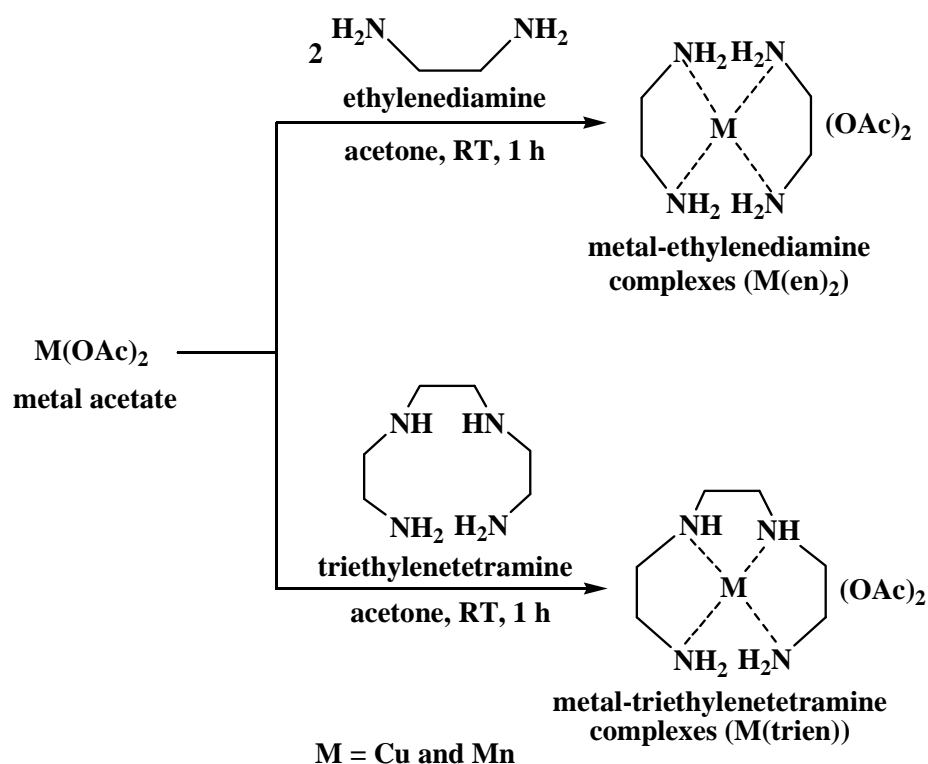
Figure 3.1 RPUR foams processing

CHAPTER IV

RESULTS AND DISCUSSION

4.1 Synthesis of metal-ethylenediamine and metal-triethylenetetramine complexes $[(M(en)_2, M(trien))]$

Metal-ethylenediamine and metal-triethylenetetramine complexes were synthesized following the synthetic route described in the literature [26, 27]. The reaction between metal (II) acetate and aliphatic amine (ethylenediamine (en), triethylenetetramine (trien)) in acetone gave metal complexes $[(M(en)_2, M(trien))]$; $M = Cu$ and Mn] as shown in Scheme 4.1.



Scheme 4.1 Synthesis of metal-ethylenediamine and metal-triethylenetetramine complexes

$Cu(en)_2$, $Mn(en)_2$, $Cu(trien)$ and $Mn(trien)$ complexes were obtained as purple solid, brown, blue and brown viscous liquid, respectively.

4.1.1 Characterization of copper-ethylenediamine and copper-triethylene tetramine complexes

4.1.1.1 IR spectroscopy of Cu(en)₂ and Cu(trien) complexes

IR spectra of Cu(en)₂ and Cu(trien) are shown in Figure 4.1. They exhibited absorption band at 3142-3269 cm⁻¹ (N-H stretching), 2884-2973 cm⁻¹ (C-H stretching), 1545-1556 cm⁻¹ (C=O asymmetric stretching), 1396-1401 cm⁻¹ (C=O symmetric stretching), 1328-1340 cm⁻¹ (C-N stretching) and 1011-1044 cm⁻¹ (C-O stretching). The C=O stretching of carbonyl group in Cu(en)₂ and Cu(trien) appeared as absorption band at 1545 and 1556 cm⁻¹ (asymmetric C=O), and 1396 and 1401 cm⁻¹ (symmetric C=O), respectively, which were different from the typical Cu(OAc)₂ normally appears as absorption band around at 1596 cm⁻¹ (asymmetric C=O) and 1443 cm⁻¹ (symmetric C=O) [28]. The absorption bands of Cu(en)₂ and Cu(trien) exhibited C-O stretching at 1039 and 1044 cm⁻¹, respectively which shifted from typical absorption band of Cu(OAc)₂ at 1033 cm⁻¹. It was found that the IR peak of Cu(en)₂ and Cu(trien) complexes shifted from those of Cu(OAc)₂ to lower energy because of the influence of amine coordination, which suggested that the complexes were formed.

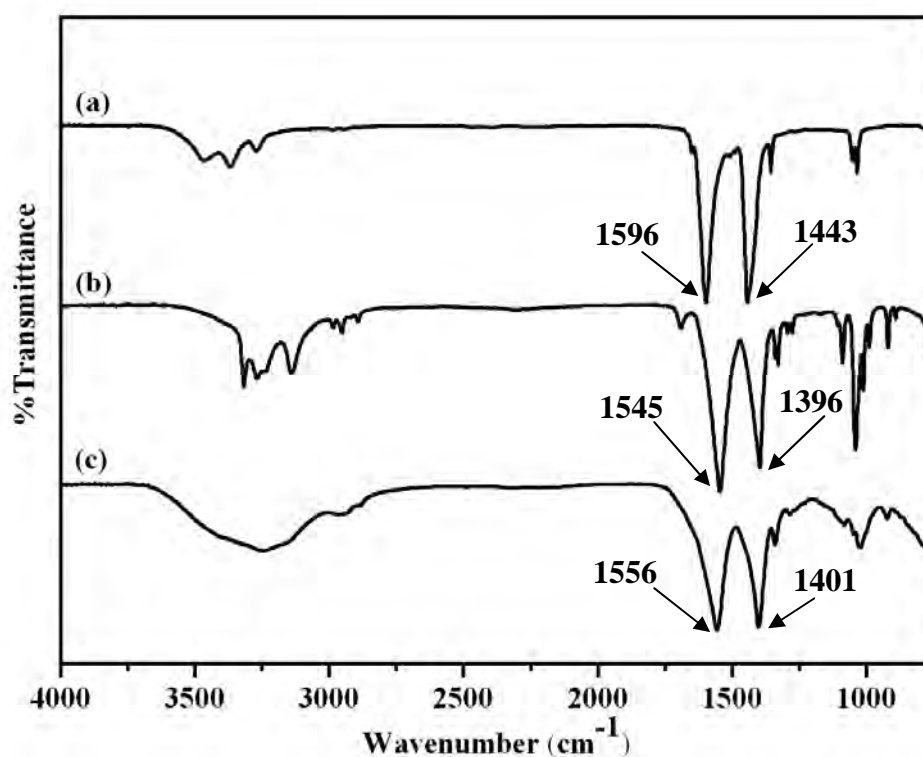


Figure 4.1 IR spectra of (a) Cu(OAc)₂; (b) Cu(en)₂; (c) Cu(trien)

4.1.1.2 UV-visible spectroscopy of Cu(en)_2 and Cu(trien) complexes

UV-visible spectra of Cu(en)_2 and Cu(trien) complexes are shown in Figure 4.2. The maximum wavelength of Cu(en)_2 and Cu(trien) complexes appeared at 230 and 258 nm, respectively. Evidently, the maximum wavelength of Cu(en)_2 and Cu(trien) complexes shifted from typical maximum wavelength of Cu(OAc)_2 at 243 nm which confirmed the complexes formation.

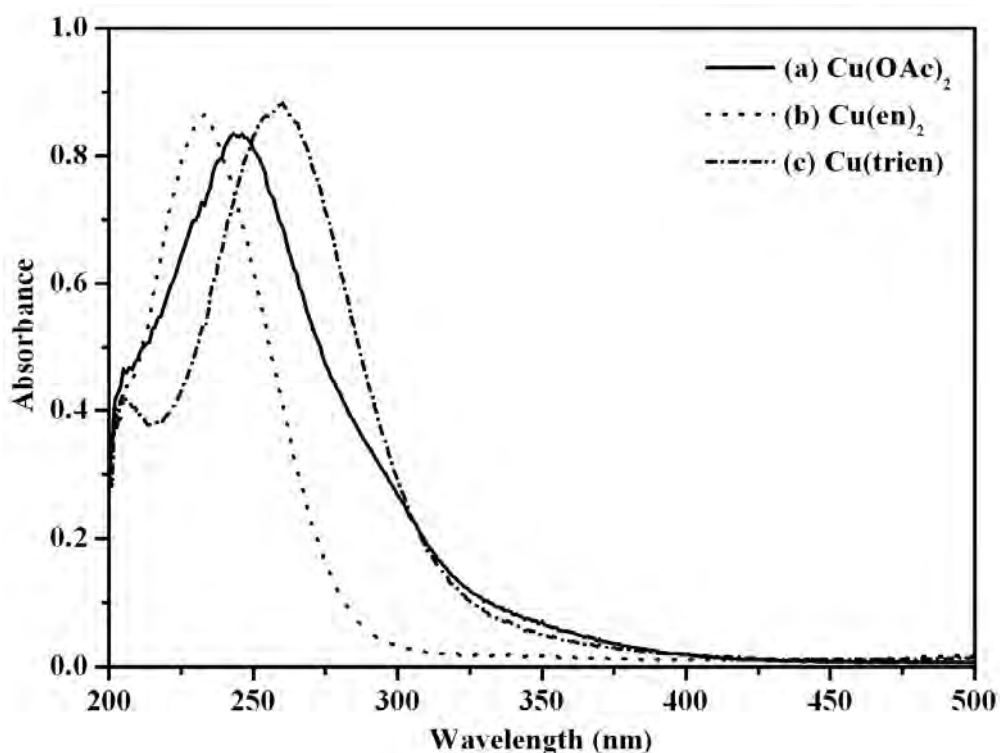


Figure 4.2 UV spectra of (a) Cu(OAc)_2 ; (b) Cu(en)_2 ; (c) Cu(trien)

4.1.1.3 X-ray diffraction of Cu(en)_2 complex

XRD diffractograms of Cu(OAc)_2 and Cu(en)_2 complexes are shown in Figure 4.3. The XRD pattern of Cu(en)_2 is significantly different from that of Cu(OAc)_2 confirming that the Cu(en)_2 complex was formed.

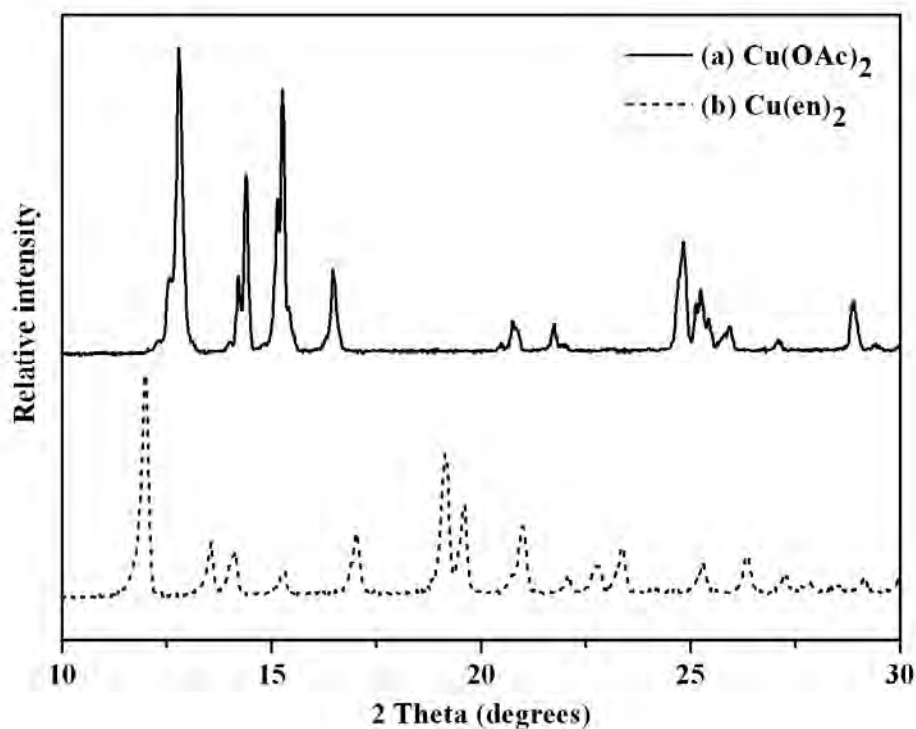


Figure 4.3 XRD diffractograms of (a) $\text{Cu}(\text{OAc})_2$; (b) $\text{Cu}(\text{en})_2$

4.1.2 Characterization of manganese-ethylenediamine and manganese-triethylenetetramine complexes

4.1.2.1 IR spectroscopy of $\text{Mn}(\text{en})_2$ and $\text{Mn}(\text{trien})$ complexes

$\text{Mn}(\text{en})_2$ and $\text{Mn}(\text{trien})$ spectra (Figure 4.4) exhibited absorption band at 3142-3281 cm^{-1} (N-H stretching), 2874-2966 cm^{-1} (C-H stretching), 1547-1559 cm^{-1} (C=O asymmetric stretching), 1402-1408 cm^{-1} (C=O symmetric stretching), 1335-1338 cm^{-1} (C-N stretching), and 1012-1040 cm^{-1} (C-O stretching). The C=O stretching in $\text{Mn}(\text{en})_2$ and $\text{Mn}(\text{trien})$ appeared absorption band at 1557 and 1559 cm^{-1} (asymmetric C=O), and 1408 and 1402 cm^{-1} (symmetric C=O), respectively, which were different from the typical $\text{Mn}(\text{OAc})_2$ normally appears as absorption band around at 1553 cm^{-1} (asymmetric C=O) and 1415 cm^{-1} (symmetric C=O). The absorption bands of $\text{Mn}(\text{en})_2$ and $\text{Mn}(\text{trien})$ exhibited of C-O stretching at 1037 and 1038 cm^{-1} , respectively which shifted from typical absorption band of $\text{Mn}(\text{OAc})_2$ at 1027 cm^{-1} . It was found that the IR peak of $\text{Mn}(\text{en})_2$ and $\text{Mn}(\text{trien})$ complexes slightly shifted from those of $\text{Mn}(\text{OAc})_2$, which indicated that the complexes were formed.

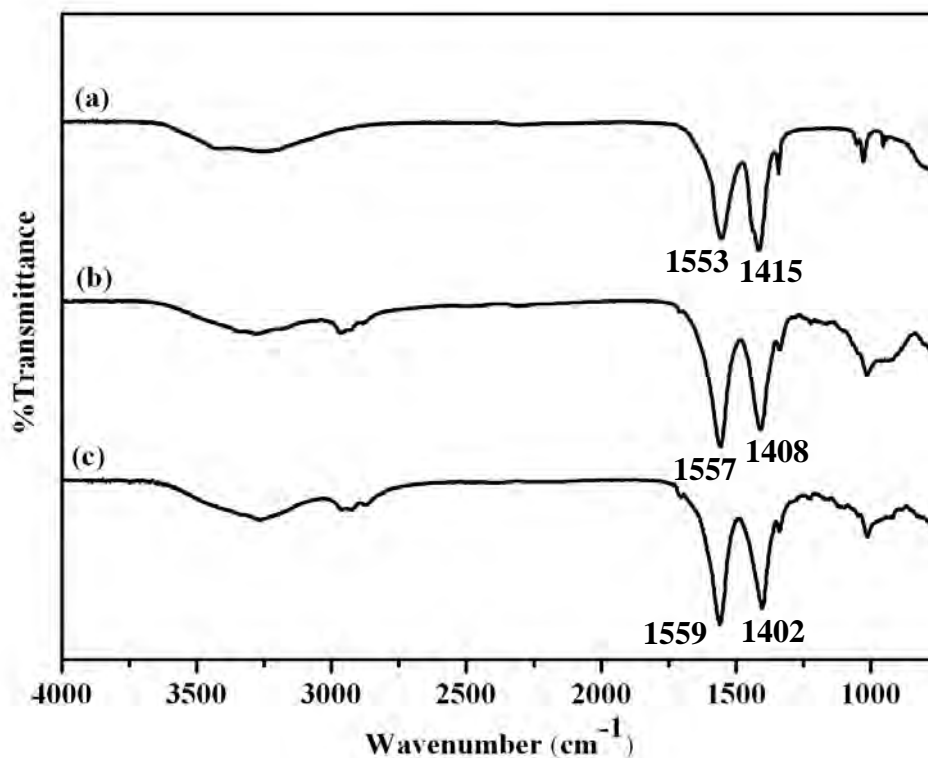


Figure 4.4 IR spectra of (a) Mn(OAc)₂; (b) Mn(en)₂; (c) Mn(trien)

4.1.1.2 UV-visible spectroscopy of Mn(en)₂ and Mn(trien) complexes

UV-visible spectra of Mn(en)₂ and Mn(trien) complexes are shown in Figure 4.5. The maximum wavelength of Mn(en)₂ and Mn(trien) complexes appeared at 229 and 232 nm, respectively. They were different from the maximum wavelength of Mn(OAc)₂, which appeared at 264 nm. Suggesting the complex formation indicated that the complexes were obtained.

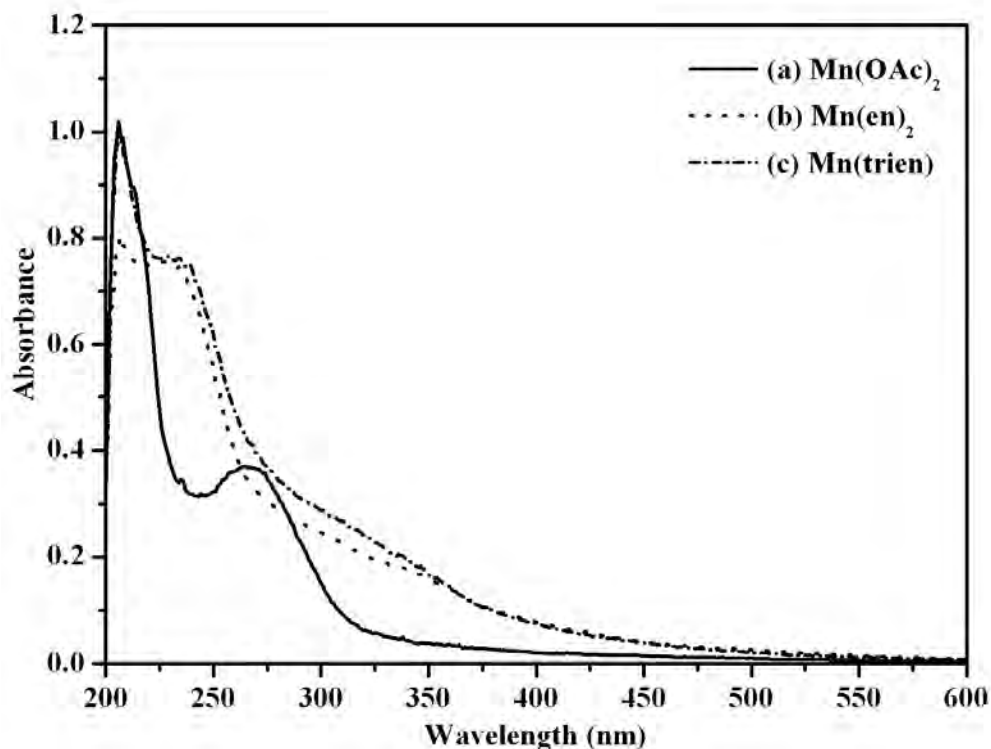
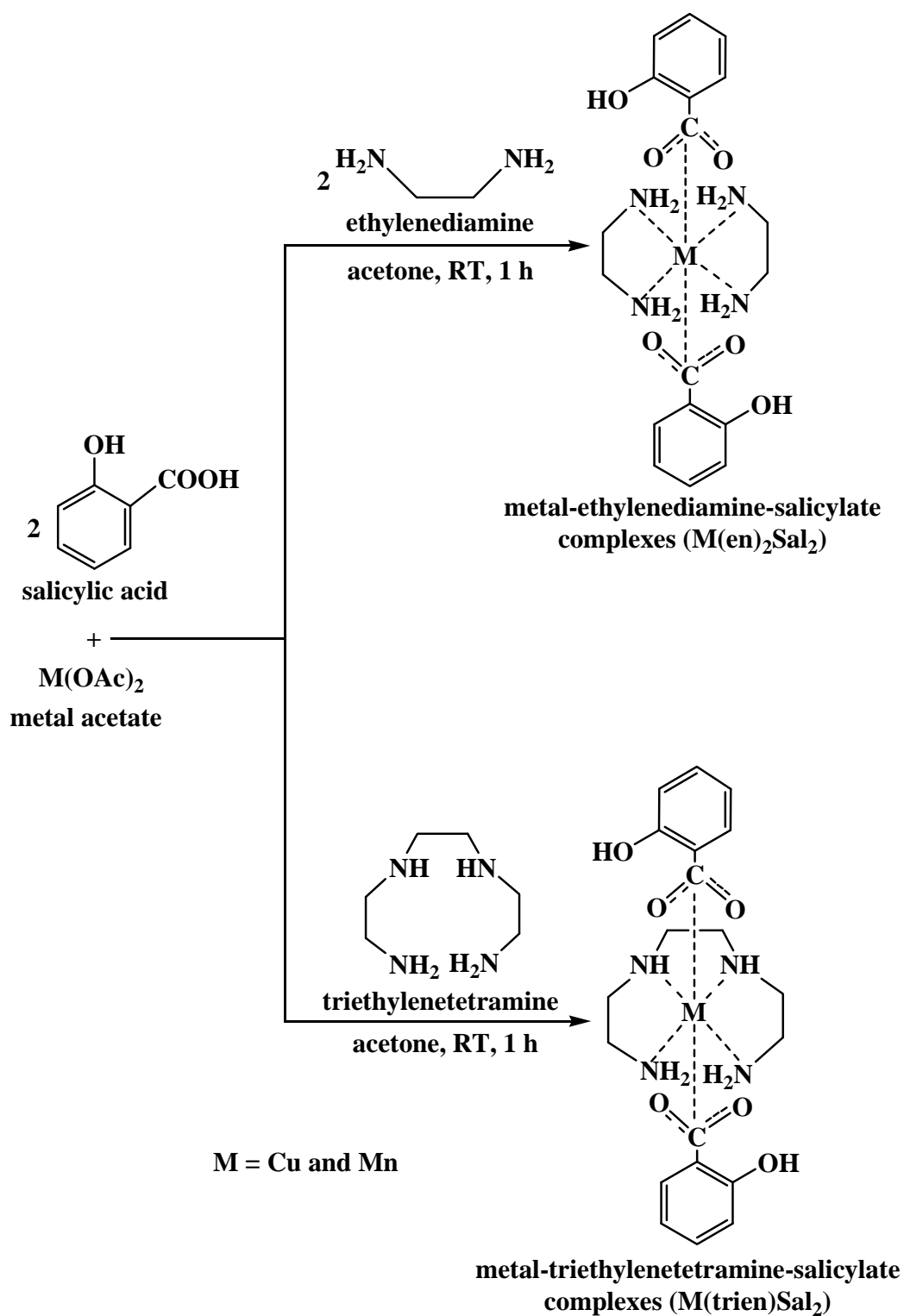


Figure 4.5 UV spectra of (a) $\text{Mn}(\text{OAc})_2$; (b) $\text{Mn}(\text{en})_2$; (c) $\text{Mn}(\text{trien})$

4.2 Synthesis of metal-ethylenediamine-salicylate and metal-triethylenetetramine-salicylate complexes [$\text{M}(\text{en})_2\text{Sal}_2$, $\text{M}(\text{trien})\text{Sal}_2$]

Metal-ethylenediamine-salicylate and metal-triethylenetetramine-salicylate complexes were prepared according to the method in the literature [26, 27]. The reaction between metal (II) acetate and salicylic acid in acetone gave green solution. Subsequently, the solution of aliphatic amine (ethylenediamine (en) or triethylenetetramine (trien)) were then added to obtain metal complexes [$\text{M}(\text{en})_2\text{Sal}_2$, $\text{M}(\text{trien})\text{Sal}_2$; $\text{M} = \text{Cu}$ and Mn] as shown in Scheme 4.2.

$\text{Cu}(\text{en})_2\text{Sal}_2$, $\text{Mn}(\text{en})_2\text{Sal}_2$, $\text{Cu}(\text{trien})\text{Sal}_2$ and $\text{Mn}(\text{trien})\text{Sal}_2$ complexes were obtained as violet, brown, blue and brown viscous liquid, respectively.



Scheme 4.2 Synthesis of metal-ethylenediamine-salicylate and metal-triethylene tetramine- salicylate complexes

4.2.1 Characterization of metal-ethylenediamine-salicylate and metal-triethylene tetramine-salicylate complexes

4.2.1.1 IR spectroscopy of $\text{Cu(en)}_2\text{Sal}_2$, $\text{Cu(trien)}\text{Sal}_2$, $\text{Mn(en)}_2\text{Sal}_2$ and $\text{Mn(trien)}\text{Sal}_2$ complexes

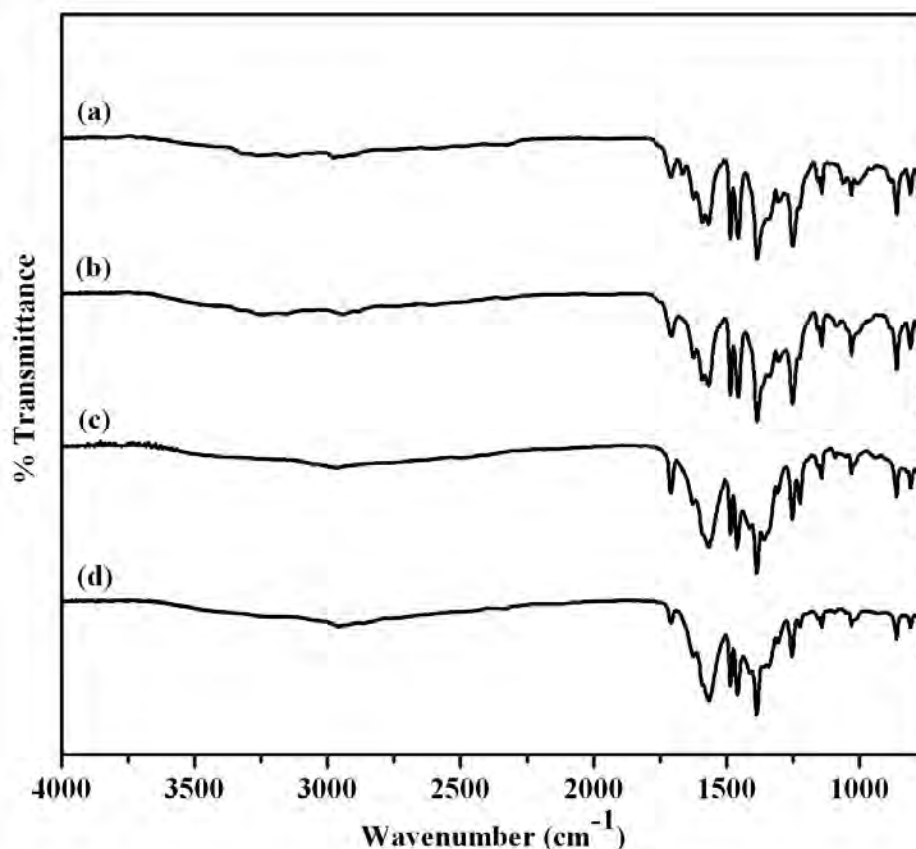


Figure 4.6 IR spectra of (a) $\text{Cu(en)}_2\text{Sal}_2$; (b) $\text{Cu(trien)}\text{Sal}_2$; (c) $\text{Mn(en)}_2\text{Sal}_2$; (d) $\text{Mn(trien)}\text{Sal}_2$

IR spectra of $\text{Cu(en)}_2\text{Sal}_2$, $\text{Cu(trien)}\text{Sal}_2$, $\text{Mn(en)}_2\text{Sal}_2$ and $\text{Mn(trien)}\text{Sal}_2$ are shown in Figure 4.6. The important characteristic absorption bands were observed at $3269\text{-}3250\text{ cm}^{-1}$ (N-H stretching), $2880\text{-}2974\text{ cm}^{-1}$ (C-H stretching), $1588\text{-}1595\text{ cm}^{-1}$ (Ar-H stretching), $1562\text{-}1567\text{ cm}^{-1}$ (C=O asymmetric stretching in salicylate), $1455\text{-}1460\text{ cm}^{-1}$ (C=O symmetric stretching in salicylate), $1455\text{-}1484\text{ cm}^{-1}$ (C-H bending), 1384 cm^{-1} (C-N stretching), $1029\text{-}1250\text{ cm}^{-1}$ (C-O stretching), and $760\text{-}860\text{ cm}^{-1}$ (C-H bending in aromatic ring). It was found that $\text{Cu(en)}_2\text{Sal}_2$, $\text{Cu(trien)}\text{Sal}_2$, $\text{Mn(en)}_2\text{Sal}_2$ and $\text{Mn(trien)}\text{Sal}_2$ complexes showed similar IR spectra. This might be because the complex structures were similar with only different of aliphatic amine ligand from ethylenediamine to triethylenetetramine.

4.2.1.2 UV-visible spectroscopy of $\text{Cu}(\text{en})_2\text{Sal}_2$, $\text{Cu}(\text{trien})\text{Sal}_2$, $\text{Mn}(\text{en})_2\text{Sal}_2$ and $\text{Mn}(\text{trien})\text{Sal}_2$ complexes

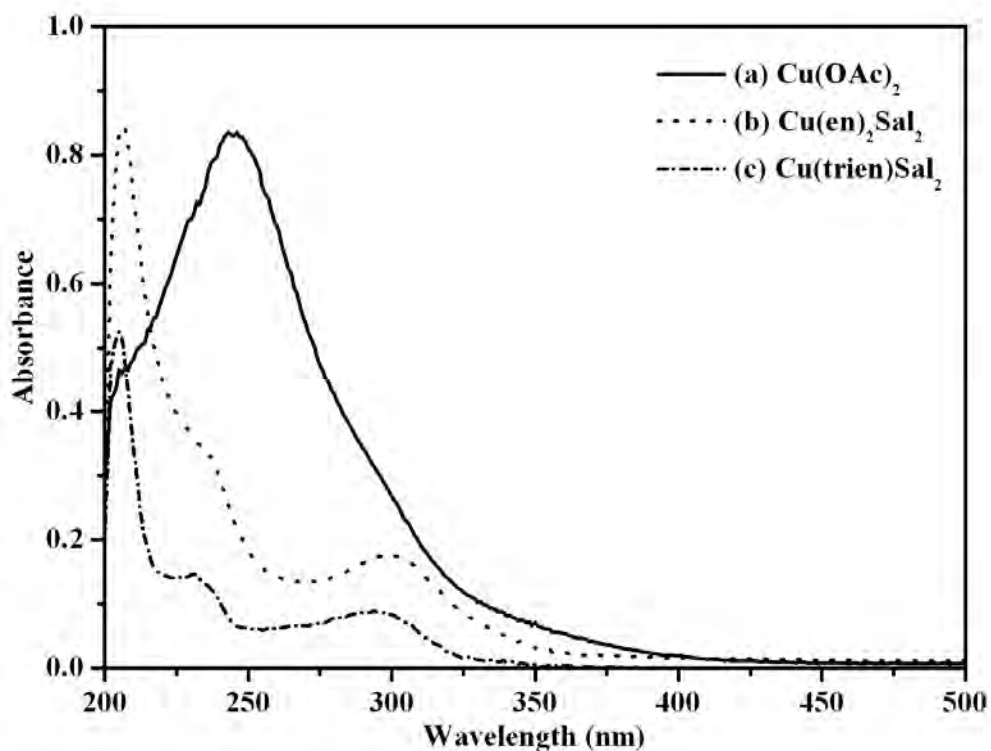


Figure 4.7 UV spectra of (a) $\text{Cu}(\text{OAc})_2$; (b) $\text{Cu}(\text{en})_2\text{Sal}_2$; (c) $\text{Cu}(\text{trien})\text{Sal}_2$

UV-visible spectra of $\text{Cu}(\text{en})_2\text{Sal}_2$ and $\text{Cu}(\text{trien})\text{Sal}_2$ complexes are shown in Figure 4.7. The maximum wavelength of $\text{Cu}(\text{en})_2\text{Sal}_2$ and $\text{Cu}(\text{trien})\text{Sal}_2$ complexes appeared at 300 and 294 nm, respectively. They were different from the maximum wavelength of $\text{Cu}(\text{OAc})_2$, which appeared at 243 nm. It was found that the maximum wavelength of $\text{Cu}(\text{en})_2\text{Sal}_2$ and $\text{Cu}(\text{trien})\text{Sal}_2$ complexes shifted from typical maximum wavelength of $\text{Cu}(\text{OAc})_2$, which indicated that the complexes were obtained. The maximum wavelength of ethylenediamine, triethylnetetramine, salicylic acid and cut off solvent (MeOH) appeared at 205, 206, 234 and 206-210 nm, respectively.

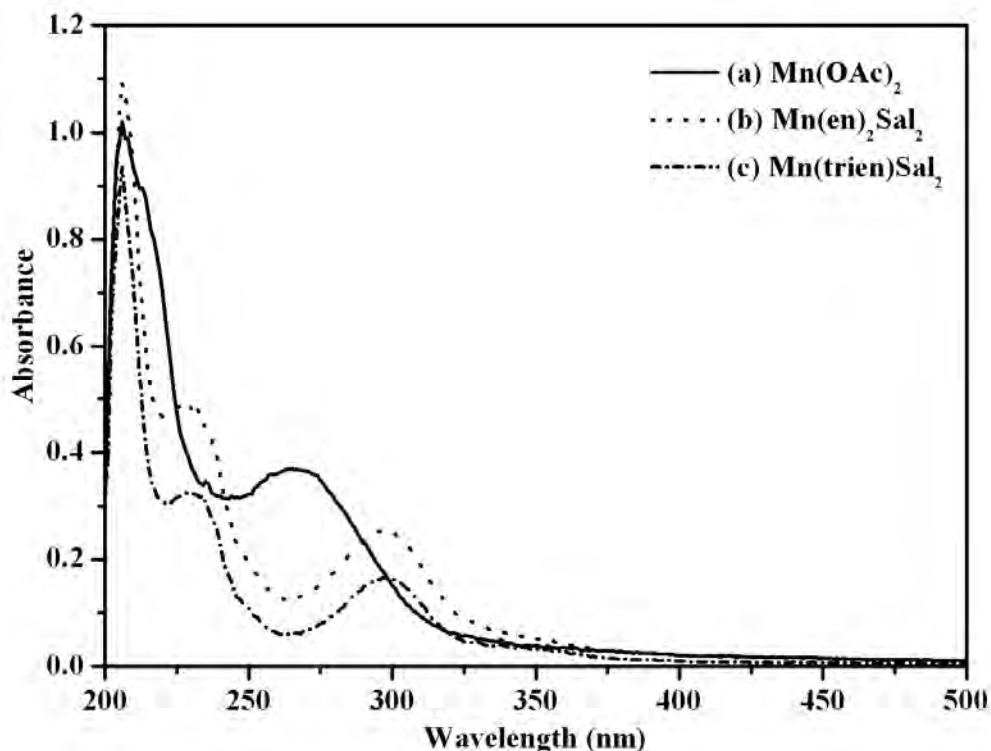


Figure 4.8 UV spectra of (a) Mn(OAc)₂; (b) Mn(en)₂Sal₂; (c) Mn(trien)Sal₂

UV-visible spectra of Mn(en)₂Sal₂ and Mn(trien)Sal₂ complexes are shown in Figure 4.8. The maximum wavelength of Mn(en)₂Sal₂ and Mn(trien)Sal₂ complexes appeared at 295 and 300 nm, respectively. They were different from the maximum wavelength of Mn(OAc)₂, which appeared at 264 nm. It was found that the maximum wavelength of Mn(en)₂Sal₂ and Mn(trien)Sal₂ complexes shifted from typical maximum wavelength of Mn(OAc)₂, which indicated that the complexes were obtained.

4.3 Preparation of rigid polyurethane (RPUR) foams

4.3.1 Preparation of RPUR catalyzed by metal complexes

The rigid polyurethane foams catalyzed by M(en)₂, M(trien), M(en)₂Sal₂ and M(trien)Sal₂ (M = Cu and Mn) were prepared by mechanical mixing technique in two steps of the mixing. In the first step, polyol, catalysts (metal complexes or DMCHA), surfactant and blowing agent were mixed in 700 mL paper cup. In the second step, the isocyanate was added to the mixed polyol from first mixing, then the mixture were mixed to obtained homogeneous mixture by mechanical stirrer at 2000 rpm for 20

seconds. During the reaction, cream time, gel time, tack free time and rise time were measured. After that, the foams were kept at room temperature for 48 hours before carrying out physical and mechanical characterization. In this work, the amount of polyol, catalyst, surfactant (B8460), and blowing agent (water) were fixed. The polymeric MDI was varied according to NCO indexes of 100, 150, 200, 250, and 300 and RPUR foams were prepared by using different catalysts at the same 1.0 pbw. The foam formulation and the external appearances of foams are shown in Tables 4.1 and 4.2, respectively.

Table 4.1 RPUR foam formulations catalyzed by metal complexes at different NCO indexes

Formulations (pbw)	NCO index				
	100	150	200	250	300
Raypol [®] 4221	100	100	100	100	100
DMCHA (commercial catalyst)	1.0	1.0	1.0	1.0	1.0
Copper complexes					
Cu(en) ₂	1.0	1.0	1.0	1.0	1.0
Cu(trien)	1.0	1.0	1.0	1.0	1.0
Cu(en) ₂ Sal ₂	1.0	1.0	1.0	1.0	1.0
Cu(trien)Sal ₂	1.0	1.0	1.0	1.0	1.0
Manganese complexes					
Mn(en) ₂	1.0	1.0	1.0	1.0	-
Mn(trien)	1.0	1.0	1.0	1.0	-
Mn(en) ₂ Sal ₂	1.0	1.0	1.0	1.0	-
Mn(trien)Sal ₂	1.0	1.0	1.0	1.0	-
Surfactant (B8460)	2.5	2.5	2.5	2.5	2.5
Water (blowing agent)	3.0	3.0	3.0	3.0	3.0
PMDI (MR-200)	151	227	303	378	454

Table 4.2 External appearance of RPUR foams catalyzed by metal-complexes at different NCO indexes

Catalyst types	NCO indexes	External appearance
DMCHA	100	Good foam with dimension stability
	150	Good foam with high dimension stability
	200	Good foam with slightly brittle
	250	Brittle foam
	300	Very brittle foam
Cu(en) ₂	100	Good foam with dimension stability
	150	Good foam with high dimension stability
	200	Good foam with slightly brittle
	250	Brittle foam
	300	Very brittle foam
Cu(trien)	100	Good foam with dimension stability
	150	Good foam with high dimension stability
	200	Good foam with slightly brittle
	250	Brittle foam
	300	Very brittle foam
Cu(en) ₂ Sal ₂	100	Good foam with dimension stability
	150	Good foam with high dimension stability
	200	Good foam with slightly brittle
	250	Brittle foam
	300	Very brittle foam
Cu(trien)Sal ₂	100	Good foam with dimension stability
	150	Good foam with high dimension stability
	200	Good foam with slightly brittle
	250	Brittle foam
	300	Very brittle foam
Mn(en) ₂	100	Good foam with dimension stability
	150	Good foam with dimension stability
	200	Brittle foam
	250	Very brittle foam

Table 4.2 External appearance of RPUR foams catalyzed by metal-complexes at different NCO indexes (continued)

Catalyst types	NCO indexes	External appearance
Mn(trien)	100	Good foam with low dimension stability
	150	Good foam with dimension stability
	200	Brittle foam
	250	Very brittle foam
Mn(en) ₂ Sal ₂	100	Good foam with dimension stability
	150	Good foam with dimension stability
	200	Brittle foam
	250	Very brittle foam
Mn(trien)Sal ₂	100	Good foam with low dimension stability
	150	Good foam with dimension stability
	200	Brittle foam
	250	Very brittle foam

From the above results of foam preparation, RPUR foams catalyzed by copper complexes gave good foams in the range of 100-200 NCO indexes. RPUR foams catalyzed by manganese complexes gave good foams in the range of 100-150 NCO indexes. When foams were prepared with higher NCO indexes, the foams were so brittle that they were not suitable for foam applications. For RPUR foams catalyzed by copper and manganese complexes, the NCO indexes of 100, 130, 150, 160, and 180 and 80, 100, 130, and 150, respectively, were studied. All RPUR foams catalyzed by copper complexes (Figure 4.9) were good foams and could be cut to measure the apparent density. For the foams prepared from manganese complexes, good foams were obtained but the foams formation occurred with lower blowing reaction than those prepared from copper complexes (Figure 4.10).

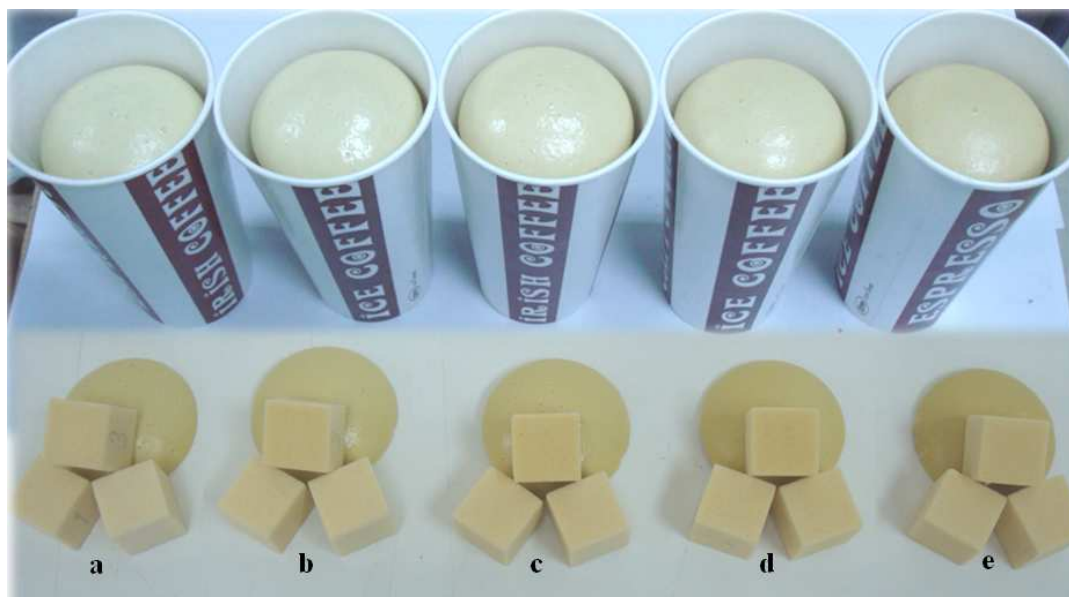


Figure 4.9 RPUR foams catalyzed by copper complexes at different NCO indexes (a) 100; (b) 130; (c) 150; (d) 160; (e) 180

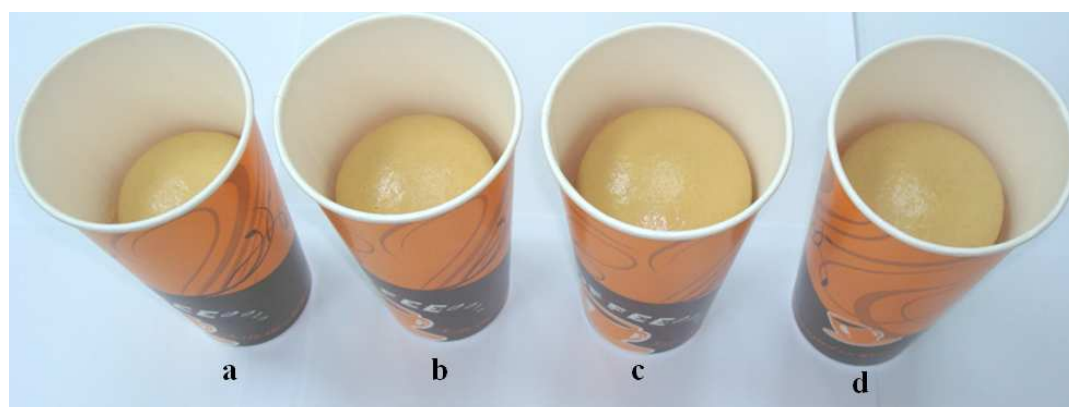


Figure 4.10 RPUR foams catalyzed by manganese complexes at different NCO indexes (a) 80; (b) 100; (c) 130; (d) 150

4.3.2 Reaction times and rise profiles

The reaction time of RPUR foams catalyzed by copper and manganese complexes are shown in Figures 4.11 and 4.12, respectively. The reaction times measured were cream time (which is the time of the foam start to rise or blowing reaction), gel time (which is the time of foam mixture begin to gel or gelling reaction), tack free time (which is the time of the foam could not tack with other materials or crosslinking reaction) and rise time (which is the time of the foam stop rising). The reaction time of RPUR foams catalyzed by copper complexes showed

that Cu(en)_2 and Cu(trien) showed better catalytic activity than the commercial reference catalyst (DMCHA, dimethylcyclohexylamine), especially tack free time, which Cu(en)_2 and Cu(trien) showed shorter time than DMCHA of about 2.0-2.5 and 0.5-1.0 folds, respectively.

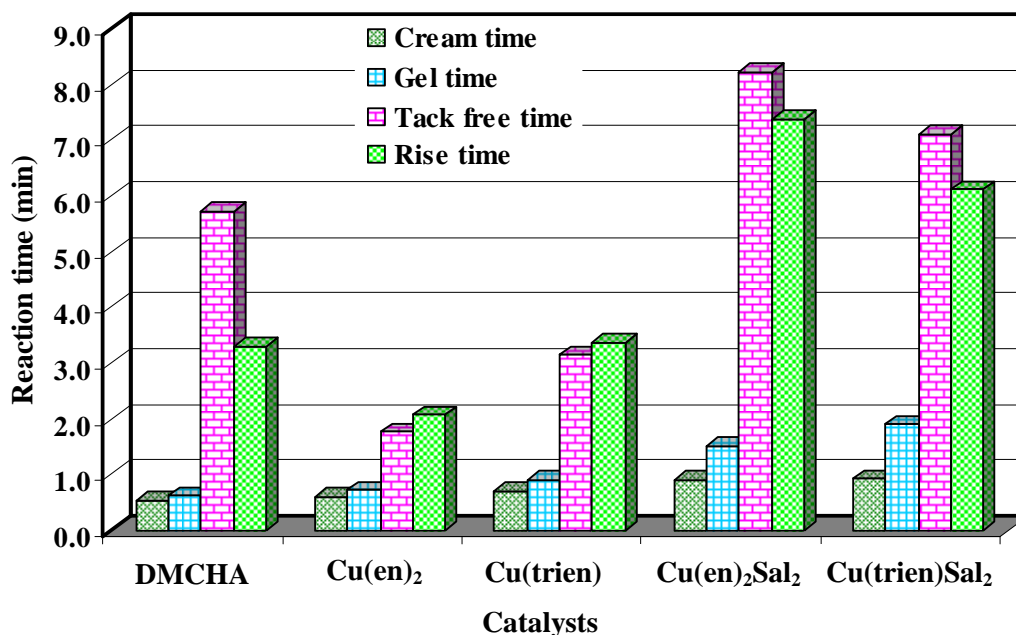
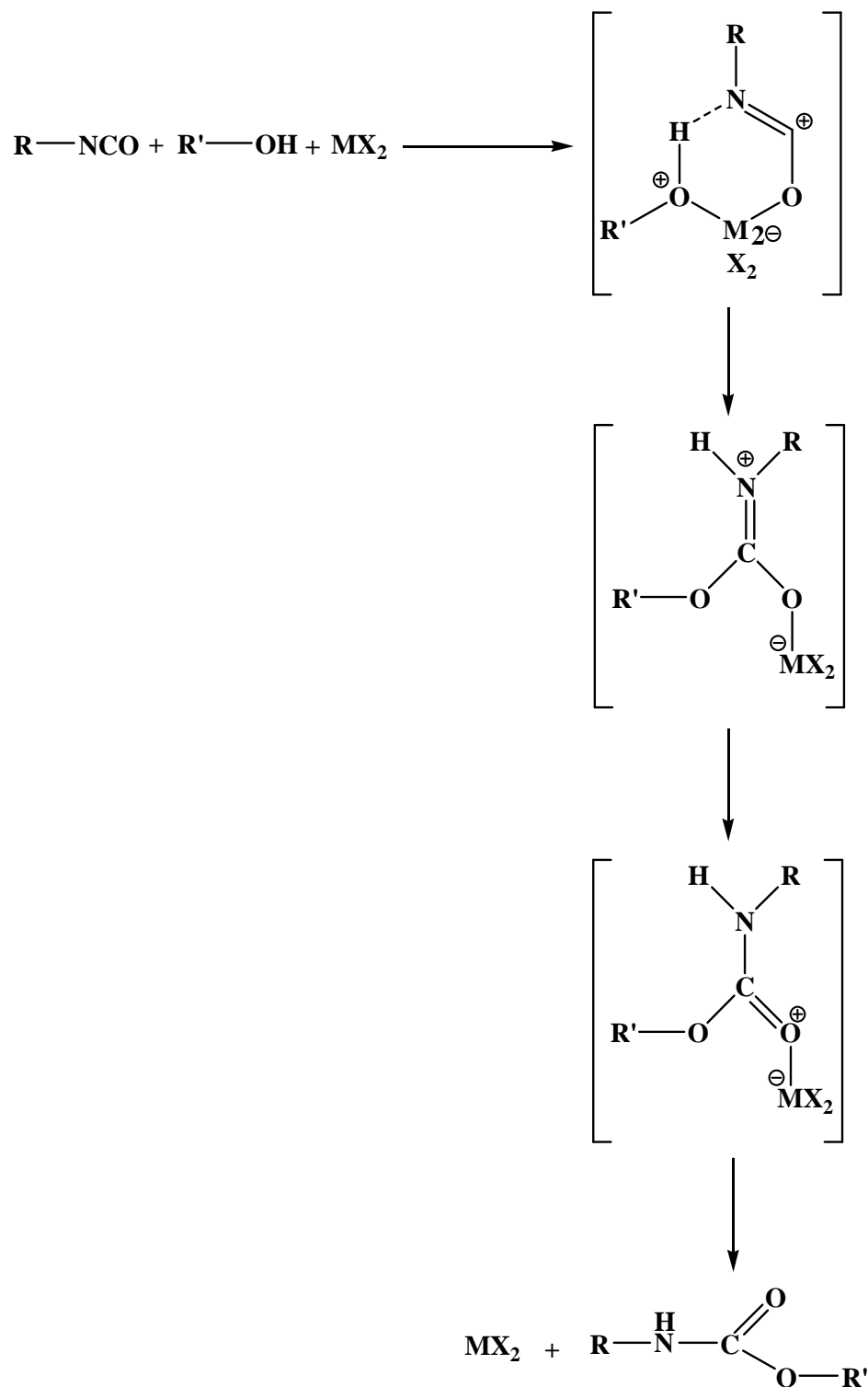


Figure 4.11 Reaction times of RPUR foams catalyzed by copper complexes

Although some copper complexes had lower catalytic activity than DMCHA catalyst, but some complexes also showed good catalytic activity. The copper complexes could catalyze RPUR foam polymerization since the copper complexes (metal-based catalyst) acted as a Lewis acid, primarily coordinated to the oxygen atom of the NCO group and activated the electrophilic nature of the carbon [19] and amine interacting with the proton of hydroxyl group in polyol, which then reacts with the isocyanate (Schemes 2.1 and 2.4).

For the reaction times of RPUR foam catalyzed by manganese complexes (Figure 4.12), it was found that all manganese complexes showed lower catalytic activity than DMCHA catalyst. Furthermore, rise profile of RPUR foams was investigated as shown in Figure 4.13. It was found that the RPUR foams prepared from Cu(en)_2 and Cu(trien) catalysts showed the similar reaction profiles those of DMCHA catalysts which were a short time to initiate the reaction and exhibited a very quick rise curve in the latter stage. The other complex catalysts showed longer

initial time (which were cream time and gel time) than that of foam prepared from DMCHA. DMCHA is a tertiary amine-based catalyst and therefore had strong catalytic activity towards urethane formation (Scheme 2.1).



Scheme 4.3 Activation mechanism of metal-based catalyst on urethane formation reaction

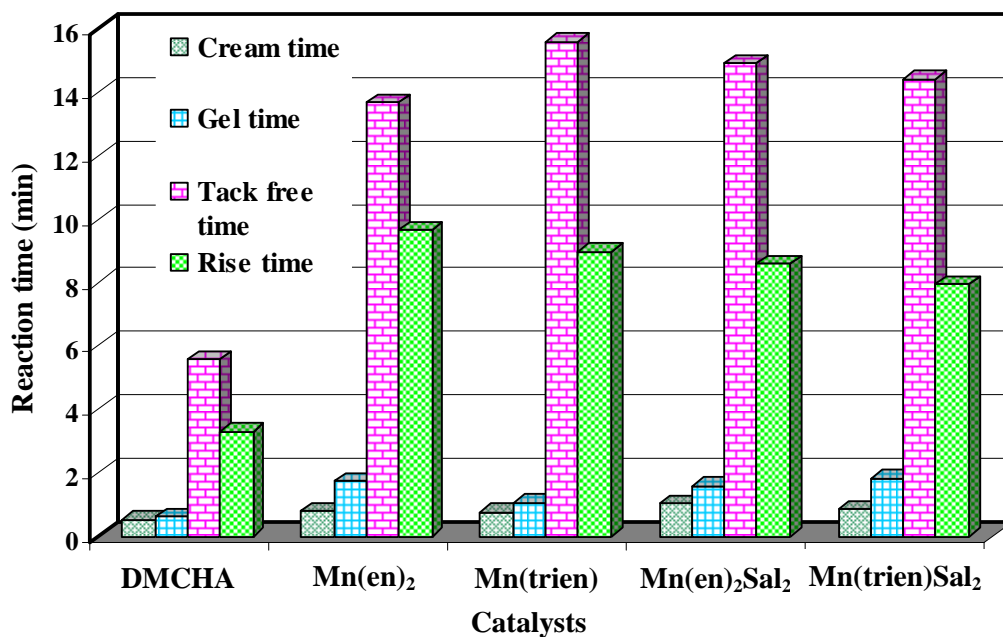


Figure 4.12 Reaction times of RPUR foams catalyzed by manganese complexes

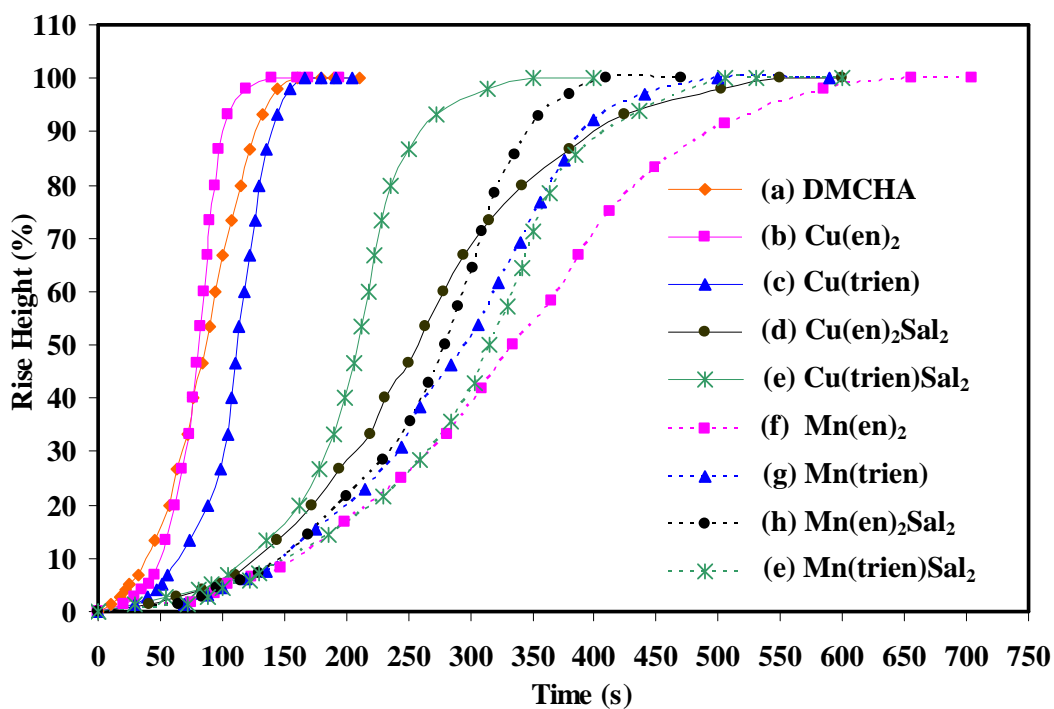


Figure 4.13 Rise profiles of RPUR foams catalyzed by different metal complexes (a) DMCHA (ref.); (b) Cu(en)₂; (c) Cu(trien); (d) Cu(en)₂Sal₂; (e) Cu(trien)Sal₂; (f) Mn(en)₂; (f) Mn(trien); (h) Mn(en)₂Sal₂; (i) Mn(trien)Sal₂.

The maximum rise rates were calculated by differential at secondary stage of rise profile (which is maximum slope) as shown in Figure 4.14. It was demonstrated that the RPUR foams catalyzed by Cu(en)_2 and Cu(trien) showed higher maximum rise rate than that DMCHA and these two catalysts showed higher maximum rise rate than foams prepared from other metal complex catalysts. The results from the reaction time and maximum rise rate indicated that the RPUR foams catalyzed by Cu(en)_2 and Cu(trien) showed better catalytic activity than DMCHA.

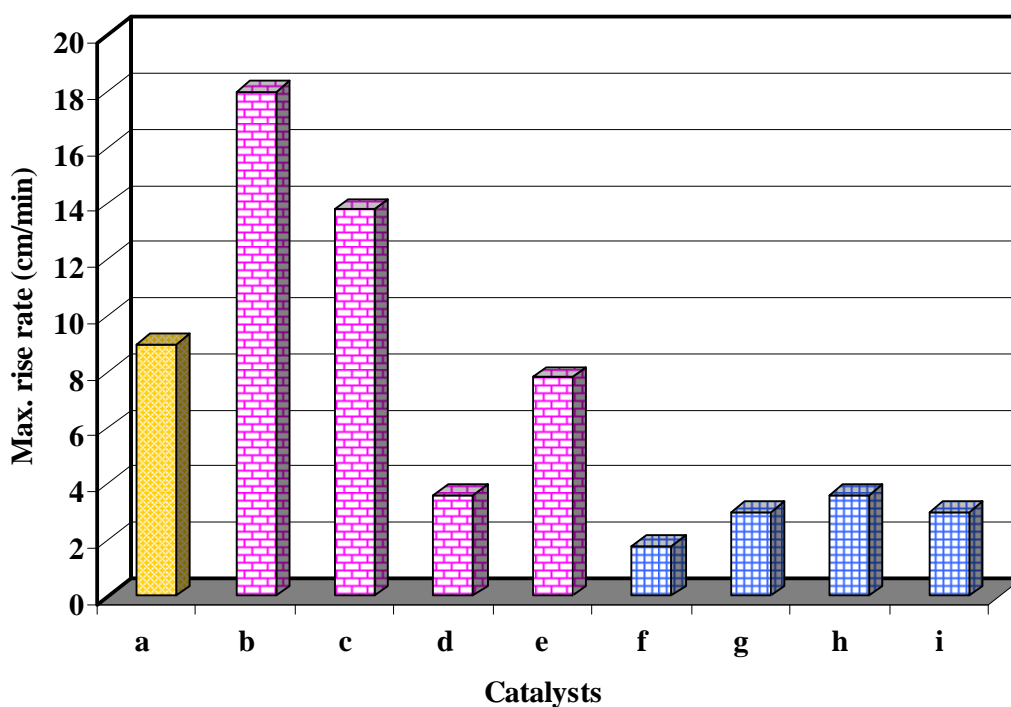


Figure 4.14 Maximum rise rates of RPUR foams catalyzed by different metal complexes (a) DMCHA (ref.); (b) Cu(en)_2 ; (c) Cu(trien) ; (d) $\text{Cu(en)}_2\text{Sal}_2$; (e) Cu(trien)Sal_2 ; (f) Mn(en)_2 ; (g) Mn(trien) ; (h) $\text{Mn(en)}_2\text{Sal}_2$; (i) Mn(trien)Sal_2 .

4.3.3 Apparent density

The apparent density of RPUR foams were measured according to ASTM D 1622. After foam preparation, RPUR foams were kept in room temperature for 48 hours, and then the foams were cut into cubic shape with 3.0 cm x 3.0 cm x 3.0 cm dimensions before apparent density of foams were measured as shown in Figure 4.15.

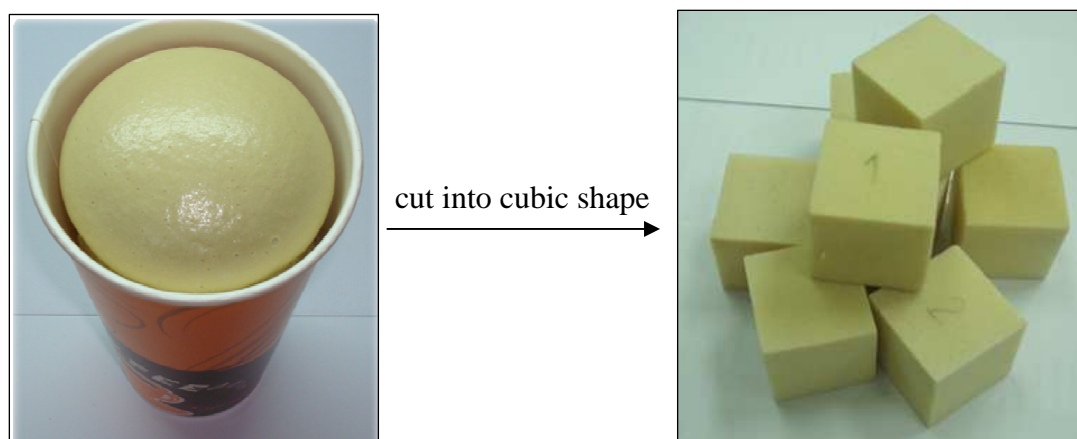


Figure 4.15 Samples for foam density measurements

4.3.3.1 Effect of NCO indexes on foam density

The apparent density of RPUR foams catalyzed by metal complexes at different NCO indexes is shown in Figure 4.17. It was found that the apparent density of RPUR foams increased with increasing the content of NCO indexes because the excess of isocyanate in PUR system could undergo further polymerization to give crosslinked structure [5]. RPUR foams prepared from copper complexes had suitable density when prepared at the NCO index of 100-180 while the foams prepared from manganese complexes at the NCO index of 100-150 had appropriate density. If RPUR foams were prepared over those NCO indexes, the obtained foam were brittle and therefore the density could not be measured (Figure 4.16).

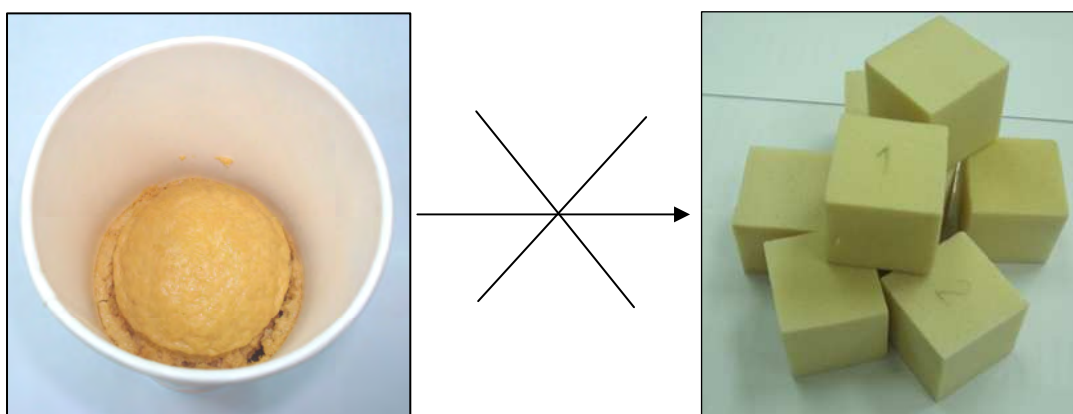


Figure 4.16 Unsuitable samples for foam density measurements

In comparison between the density of foams prepared from metal complexes and DMCHA, it was found that the foams prepared from copper complexes showed apparent density similar to those prepared from DMCHA, especially NCO indexes of 100-130. RPUR foams catalyzed by Mn(en)_2 and Mn(trien) showed higher than those catalyzed by DMCHA. Density of RPUR foams catalyzed by copper complexes at NCO indexes 100-150 was in range of 40-50 kg/m^3 , which was the desirable density for foam applications [10, 20].

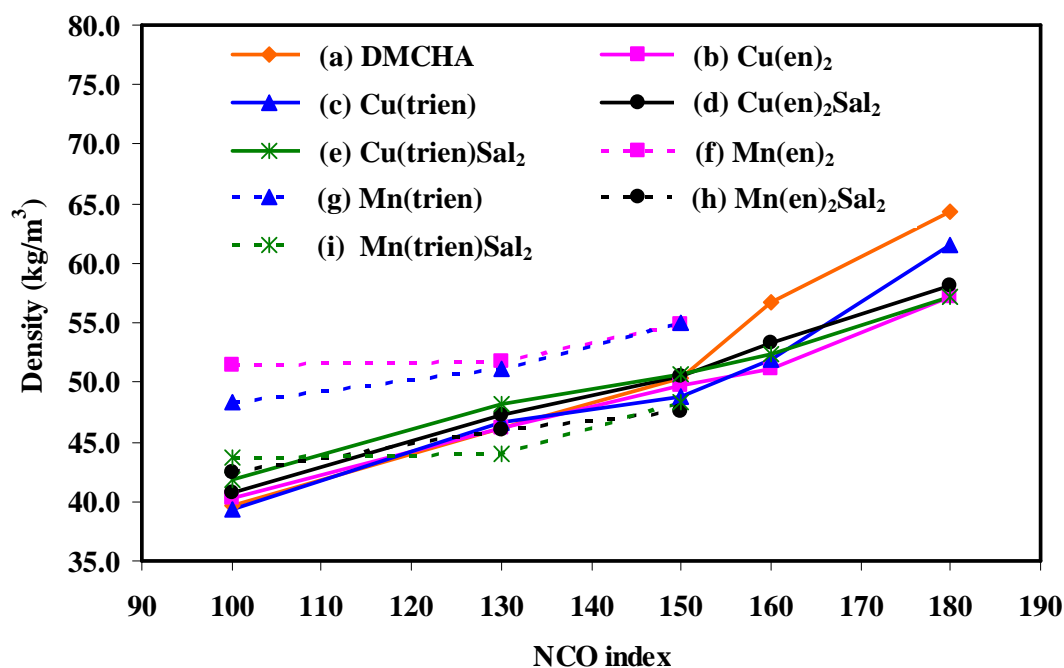


Figure 4.17 Apparent density of RPUR foams catalyzed by metal complexes (a) DMCHA (ref.); (b) Cu(en)_2 ; (c) Cu(trien) ; (d) $\text{Cu(en)}_2\text{Sal}_2$; (e) Cu(trien)Sal_2 ; (f) Mn(en)_2 ; (g) Mn(trien) ; (h) $\text{Mn(en)}_2\text{Sal}_2$; (i) Mn(trien)Sal_2 at different NCO indexes

4.3.3.2 Effect of catalyst quantity on foam density

The effect of catalyst quantity on RPUR foam density catalyzed by DMCHA, Cu(en)_2 and Cu(trien) is shown in Figure 4.18. It was found that the foam density decreased with increasing the content of catalyst in foam formulation since more blowing reactions could occur when increasing amount of catalyst. This is indicated from the foam appearance as shown in Figure 4.19. It was observed that the foam prepared at catalyst quantity of 0.25 part by weight (pbw) showed lower blowing

reaction than those prepared from 0.50, 1.0 and 2.0 pbw of catalyst. Although high catalyst quantities resulted in good blowing reaction, however, the gel time and tack free time were too short and therefore caused difficult practice in foam process. This resulted in brittle foam which is undesirable foam for applications.

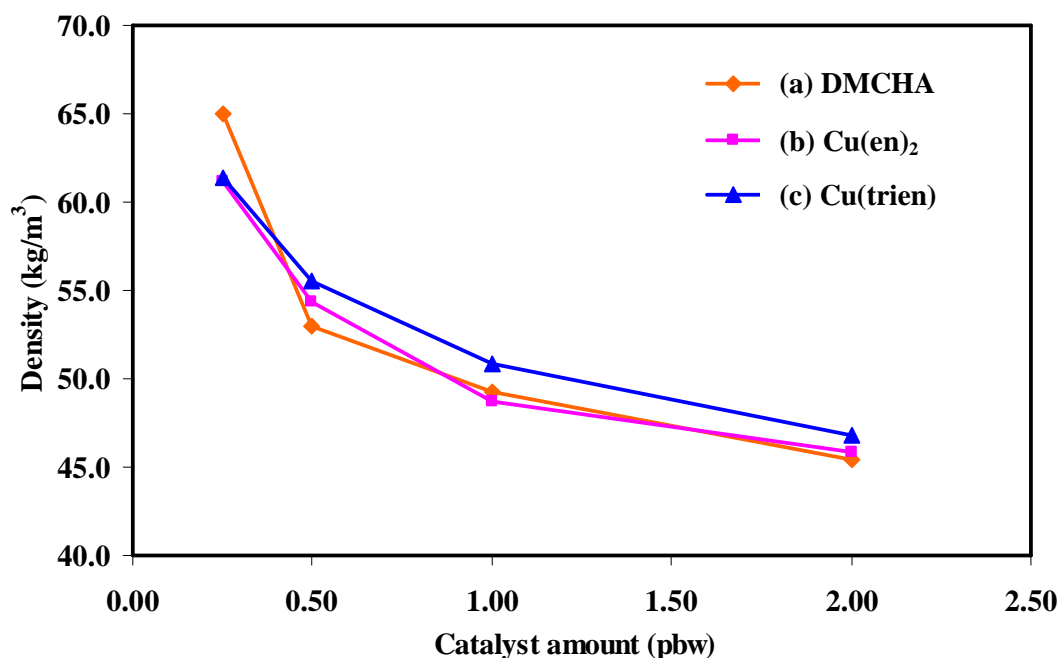


Figure 4.18 Effect of catalyst amount on RPUR foams density catalyzed by different catalysts (a) DMCHA (ref.); (b) Cu(en)₂; (c) Cu(trien) at NCO index of 150

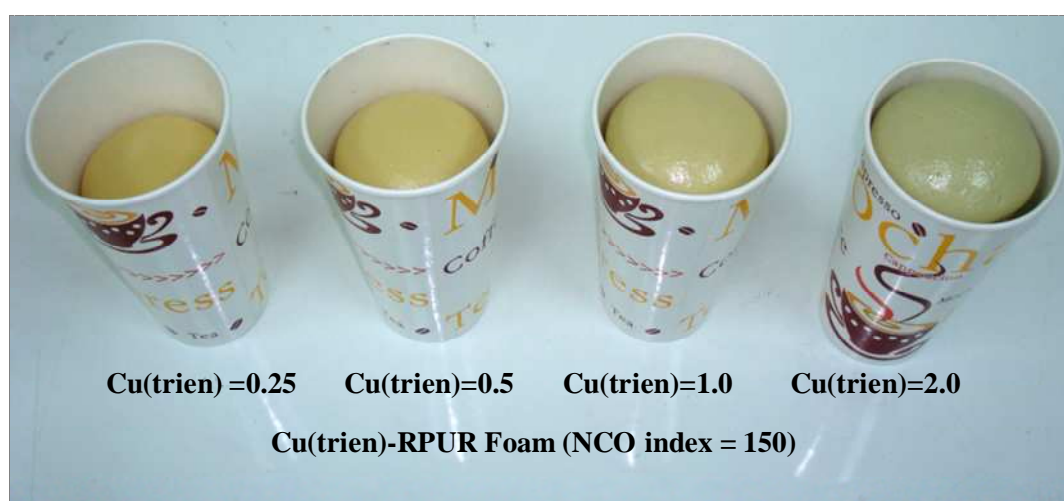


Figure 4.19 Appearance of RPUR foams catalyzed by Cu(trien) complex in various amounts at NCO index of 150

4.3.3.3 Effect of blowing agent quantity on foam density

The effect of the content of blowing agent on RPUR foams density is shown in Figure 4.20. It was found that the apparent density of RPUR foams decreased with increasing of blowing agent content. Since blowing agent (water) could react with isocyanate group to generate CO_2 gas (Figure 4.21), therefore the blowing agent of 4.0 pbw released more CO_2 than that of 3.0 pbw. Therefore, the foams prepared at blowing agent of 3.0 pbw showed higher apparent density than those prepared from 4.0 pbw.

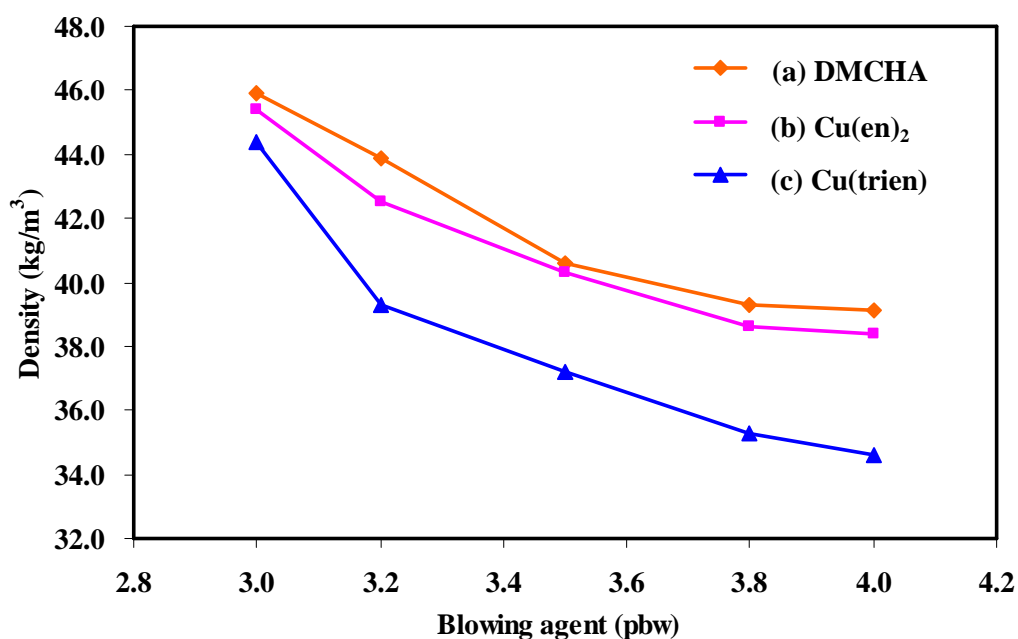


Figure 4.20 Effect of blowing agent quantities on RPUR foam density catalyzed by different catalysts (a) DMCHA (ref.); (b) $\text{Cu}(\text{en})_2$; (c) $\text{Cu}(\text{trien})$ at NCO index of 130

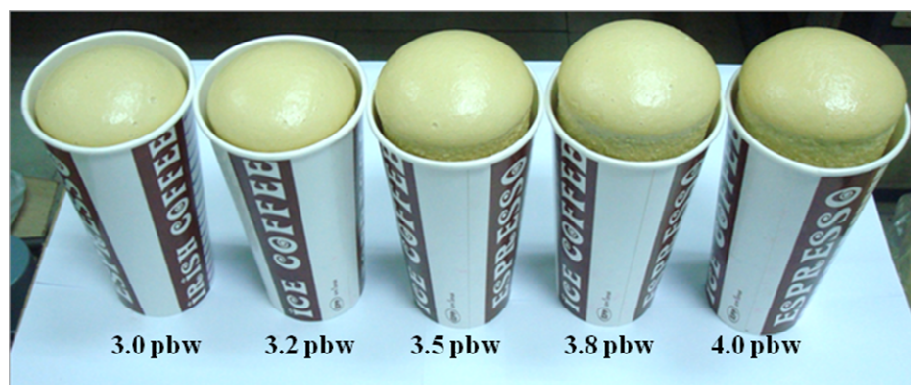


Figure 4.21 Appearance of RPUR foams catalyzed by $\text{Cu}(\text{trien})$ complex in various blowing agent amounts at NCO index of 130

4.3.4 Foaming temperature

The maximum core temperature of RPUR foams catalyzed by various catalysts at different NCO indexes is shown in Table 4.3. It was found that the polymerization reaction is exothermic reaction. The maximum core temperature of foams from copper complexes and manganese complexes was in the range of 100-136 °C and 100-122 °C, respectively. It was found that RPUR foams catalyzed by copper complexes showed higher core temperature than those prepared from manganese complexes. The RPUR foams catalyzed by metal complexes and DMCHA at NCO index of 130 showed highest core temperature than those prepared at other NCO indexes.

Table 4.3 Maximum core temperature of PUR foam catalyzed by metal complexes at different NCO indexes

Catalysts	NCO indexes	Maximum core temperature (°C)	Starting time s (min) at T _{max}
DMCHA	100	109	270 (4:30)
	130	121	330 (5:30)
	150	108	300 (5:00)
	180	87	345 (5:45)
	200	78	255 (4:15)
Cu(en) ₂	100	125	345 (5:45)
	130	136	345 (5:45)
	150	128	345 (5:45)
	180	106	360 (6:00)
	200	98	375 (6:15)
Cu(trien)	100	123	285 (4:45)
	130	132	360 (6:00)
	150	114	315 (5:15)
	180	109	330 (5:30)
	200	105	375 (6:15)
Cu(en) ₂ Sal ₂	100	126	480 (8:00)
	130	131	525 (8:45)
	150	126	525 (8:45)
	180	106	525 (8:45)
	200	101	465 (7:45)

Table 4.3 Maximum core temperature of PUR foam catalyzed by metal complexes at different NCO indexes (continued)

Catalysts	NCO indexes	Maximum core temperature (°C)	Starting time s(min) at T _{max}
Cu(trien)Sal ₂	100	118	375 (6:15)
	130	134	450 (7:30)
	150	131	525 (8:45)
	180	106	495 (8:15)
	200	98	525 (8:45)
Mn(en) ₂	80	110	375 (6:15)
	100	119	450 (7:30)
	130	122	525 (8:45)
	150	119	495 (8:15)
Mn(trien)	80	112	375 (6:15)
	100	111	450 (7:30)
	130	115	525 (8:45)
	150	103	495 (8:15)
Mn(en) ₂ Sal ₂	80	110	375 (6:15)
	100	115	450 (7:30)
	130	122	525 (8:45)
	150	121	495 (8:15)
Mn(trien)Sal ₂	80	108	375 (6:15)
	100	104	450 (7:30)
	130	113	525 (8:45)
	150	100	495 (8:15)

The temperature profiles of RPUR foam prepared from different catalysts at NCO index of 130 were investigated as shown in Figure 4.22. It was found that the profiles of foams prepared from Cu(en)₂ and Cu(trien) catalysts were the same as that prepared with DMCHA. The foams prepared from those showed higher maximum core temperature than those prepared from DMCHA and also Cu(en)₂Sal₂ and Cu(trien)Sal₂ were higher similar. The RPUR foams prepared from Cu(en)₂, Cu(trien) and DMCHA catalyst showed shorter time of initial profile than other catalysts which were they showed lower cream and gel times than other catalysts.

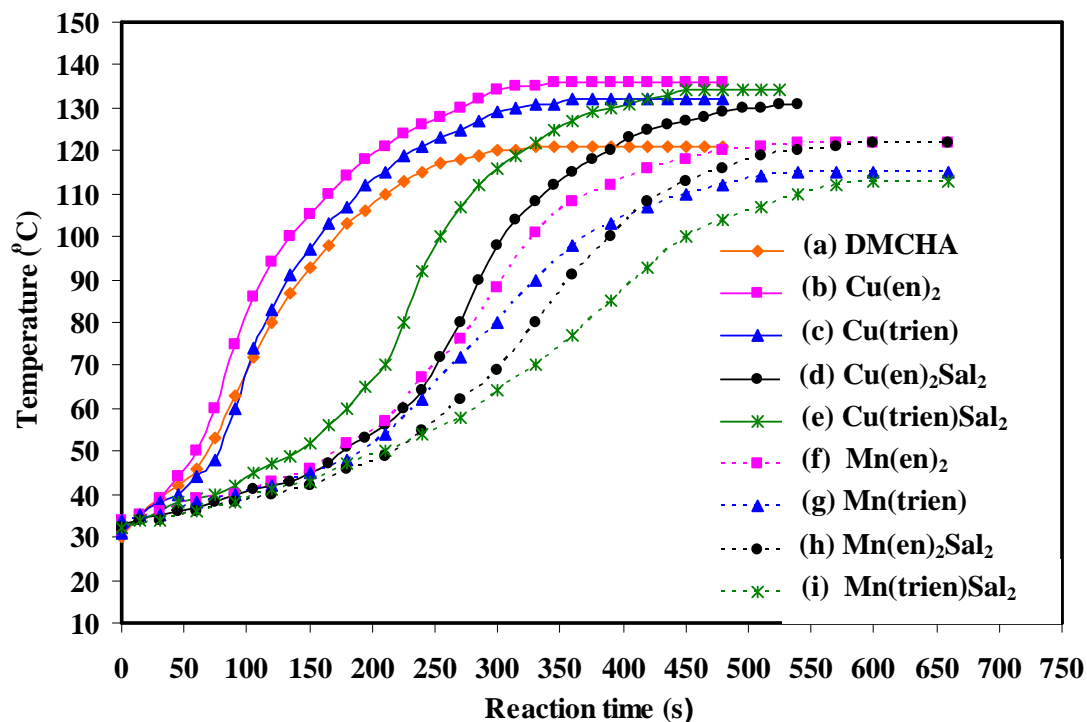


Figure 4.22 Temperature profiles of RPUR foams catalyzed by different metal complexes (a) DMCHA (ref.); (b) $\text{Cu}(\text{en})_2$; (c) $\text{Cu}(\text{trien})$; (d) $\text{Cu}(\text{en})_2\text{Sal}_2$; (e) $\text{Cu}(\text{trien})\text{Sal}_2$; (f) $\text{Mn}(\text{en})_2$; (f) $\text{Mn}(\text{trien})$; (h) $\text{Mn}(\text{en})_2\text{Sal}_2$; (i) $\text{Mn}(\text{trien})\text{Sal}_2$

4.3.5 NCO conversion of RPUR foams

FTIR spectroscopy was employed to investigate the polymerization of RPUR foam system. IR spectra of polymeric MDI, polyether polyol and RPUR foams prepared from copper complexes are shown in Figure 4.23. It was found that the absorption band of isocyanate could be observed at 2277 cm^{-1} . Therefore, the NCO conversion was determined from FTIR spectra. When higher NCO index was used in the foam formulation, high intensity of free NCO absorption band could be observed in RPUR foam as shown in Figure 4.24.

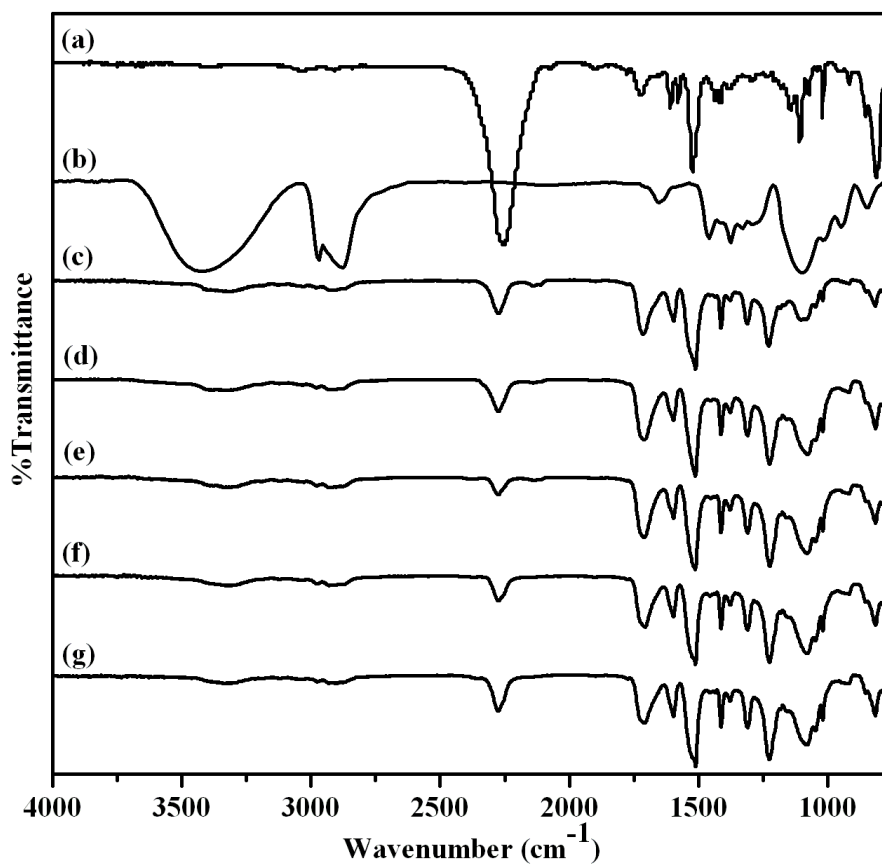


Figure 4.23 IR spectra of starting materials and RPUR foams catalyzed by copper complexes (a) PMDI; (b) polyether polyol; (c) DMCHA (ref.); (d) $\text{Cu}(\text{en})_2$; (e) $\text{Cu}(\text{trien})$; (f) $\text{Cu}(\text{en})_2\text{Sal}_2$; (g) $\text{Cu}(\text{trien})\text{Sal}_2$

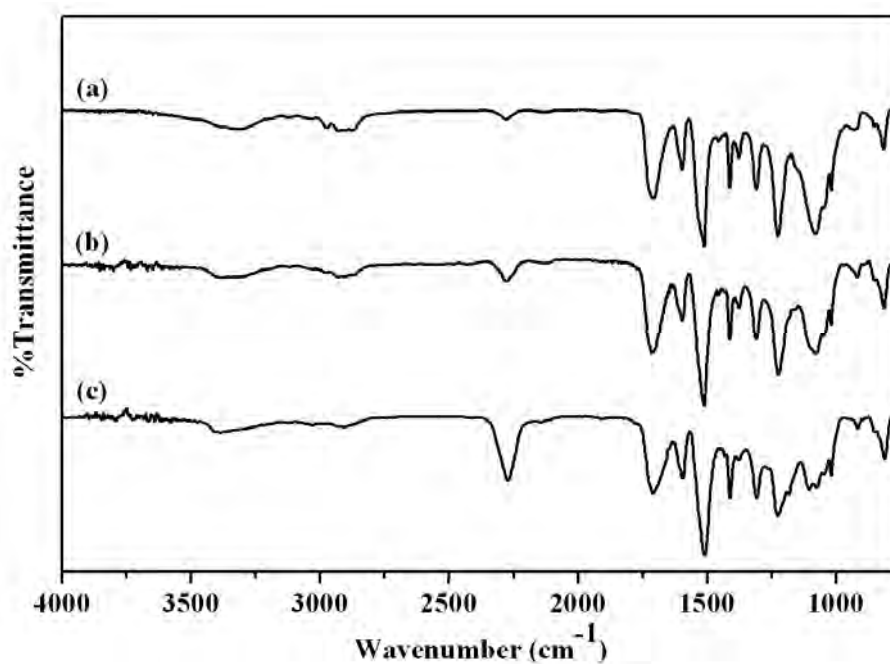


Figure 4.24 IR spectra of RPUR foams catalyzed by $\text{Cu}(\text{trien})$ at different NCO indexes (a) 100; (b) 150; (c) 200

The NCO conversion defined as the ratio between isocyanate peak area at time t and isocyanate peak area at time 0 as shown in following equation [29-34]:

$$\text{Isocyanate conversion (\%)} = \left[1 - \frac{\text{NCO}^f}{\text{NCO}^i} \right] \times 100$$

where;

NCO^f is the area of isocyanate absorbance peak area at time t (spectra (c), (d), (e), (f) and (g) in Figure 4.23)

NCO^i is the area of isocyanate absorbance peak area at initial time 0 (spectrum (a) in Figure 4.23)

Quantity of free NCO in RPUR foams were normalized by aromatic ring absorption band at 1595 cm^{-1} .

Polyisocyanurate:polyurethane (PIR:PUR) ratio was calculated from the peak area of isocyanurate and urethane at 1415 and 1220 cm^{-1} , respectively (Table 4.4).

Table 4.4 Wavenumber of the functional groups used in calculation [9]

Functional groups	Wave number (cm^{-1})	Chemical structure
Isocyanate	2277	$\text{N}=\text{C}=\text{O}$
Phenyl	1595	Ar-H
Isocyanurate	1415	PIR
Urethane	1220	-C-O-

The results of NCO conversion of RPUR foams catalyzed by copper complexes at NCO indexes 100, 150 and 200 are shown in Figure 4.25. It was found that NCO conversion decreased with increasing of the content of NCO indexes. The access isocyanate could not undergo trimerization to give isocyanurate group since copper complex catalysts were not specific toward of isocyanurate formation. Although, the NCO conversion decreased with increasing content of NCO index, the conversion was 95-99%. The ratio of polyisocyanurate:polyurethane (PIR:PUR) in RPUR foams prepared from copper complex catalysts is shown in Figure 4.26. From these results, PIR:PUR of all RPUR foam slightly increased with increasing the content of NCO index. Therefore, this result indicated that copper complexes were not good catalyst for polyisocyanurate formation. RPUR foam catalyzed by manganese complexes showed NCO conversion and PIR:PUR ratio like to RPUR foams prepared

from copper complexes. It could be concluded that both copper and manganese complexes were good catalysts for polyurethane formation and blowing reaction but were unsuitable catalyst for trimerization reaction. NCO conversion and PIR:PUR ratio of RPUR foams catalyzed both copper and manganese complexes are summarized in Table 4.5.

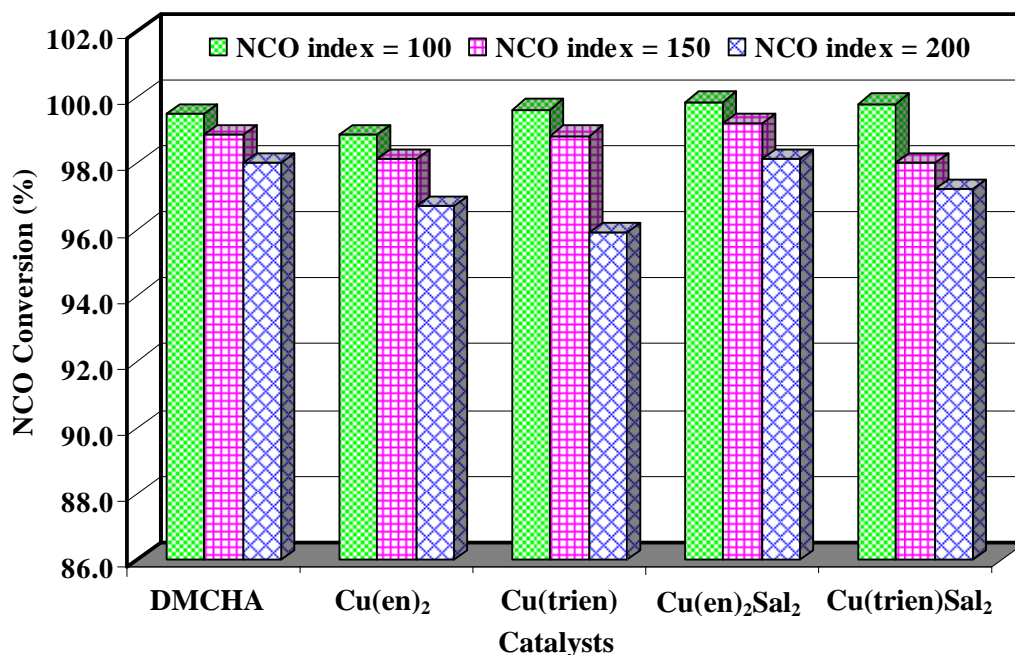


Figure 4.25 NCO conversions of RPUR foams catalyzed by different copper complexes

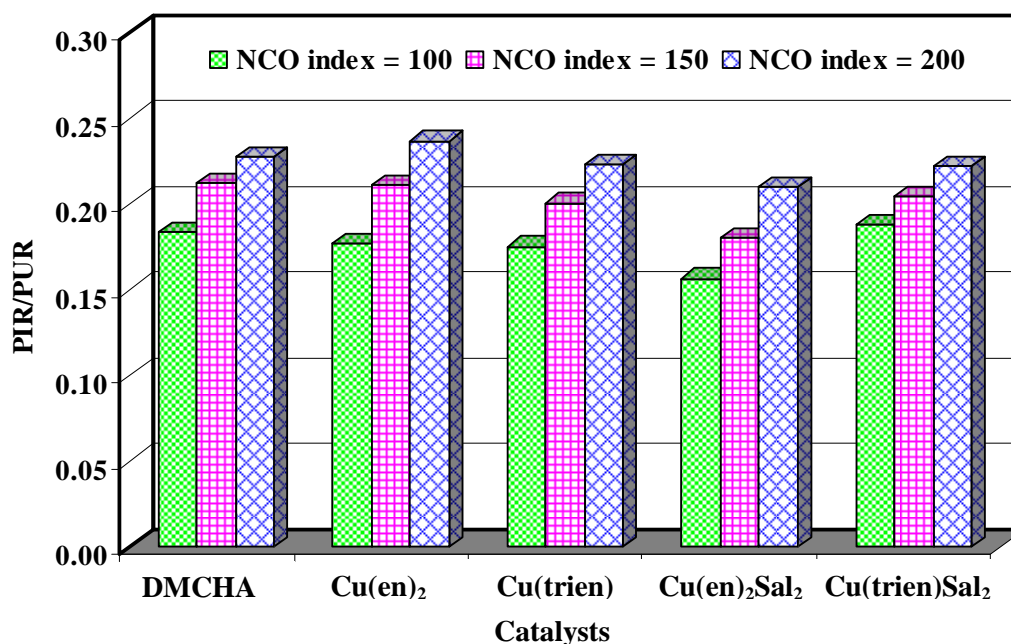


Figure 4.26 PIR:PUR of RPUR foams catalyzed by different copper complexes

Table 4.5 NCO conversions and PIR:PUR ratio of RPUR foams catalyzed copper and manganese complexes at different NCO indexes

Catalysts	NCO indexes	NCO conversion (%)	PIR/PUR
DMCHA (ref.)	100	99.5	0.184
	150	98.9	0.212
	200	98.0	0.228
Cu(en) ₂	100	98.9	0.177
	150	98.1	0.211
	200	96.7	0.237
Cu(trien)	100	99.6	0.175
	150	98.8	0.201
	200	95.9	0.224
Cu(en) ₂ Sal ₂	100	99.9	0.157
	150	99.2	0.180
	200	98.1	0.210
Mn(en) ₂	100	99.4	0.221
	130	98.9	0.237
	150	99.0	0.240
Mn(trien)	100	99.0	0.231
	130	98.8	0.236
	150	98.9	0.236
Mn(en) ₂ Sal ₂	100	99.2	0.210
	130	98.9	0.251
	150	98.9	0.229
Mn(trien)Sal ₂	100	99.2	0.232
	130	99.2	0.229
	150	98.8	0.261

4.4 Compressive properties of RPUR foams

The compression stress-strain curves of RPUR foams catalyzed by copper complexes are shown in Figure 4.27. The curves showed three stages of deformation; initial linear behavior, linear plateau region and finally, densification. The initial slope was used to calculate the compressive modulus of foam and intersection point between the initial slope and plateau slope was used to calculate the compressive strength [35]. It was observed that slope of the initial linear are the same for all RPUR foams. All RPUR foams had the same compressive modulus. The shape of plateau region depends on the morphology of cell in RPUR foam. For linear plateau, cell deformation occurs as combination of cell bending and collapse. Therefore, the foam prepared from DMCHA showed rapid cell deformation since decreasing stress was observed after yield point and its deformation showed only two stages, namely initial linear behavior and densification.

Parallel compressive strength of RPUR foams at NCO indexes of 100 and 150 is shown in Figure 4.28. It was shown that RPUR foams catalyzed by Cu(en)_2 , Cu(trien) and Cu(trien)Sal_2 showed higher compressive strength than the foam prepared from a commercial reference catalyst (DMCHA) at both NCO indexes of 100 and 150. The foams prepared at NCO index of 150 had higher compressive strength than those prepared at NCO index of 100 because of the foams prepared at NCO index of 150 had higher density than foams prepared at NCO index of 100. Since the mechanical properties of foams depend on the density [36].

Compressive strength of RPUR foams catalyzed by copper complexes in parallel and perpendicular direction of foam rising is shown in Figure 4.29. From the results, it was observed that the parallel compressive strength of foams was higher than that of perpendicular compression direction. Because of this, the foam cells were elongated in the direction of the rise [37]. All foams were anisotropic foams, the compressive properties depend on direction of measurement [38]. Generally, a high compressive strength in one direction occurred at the expense of the compressive strength in the other directions which were could be explained by the foam cell model as shown in Figure 4.30.

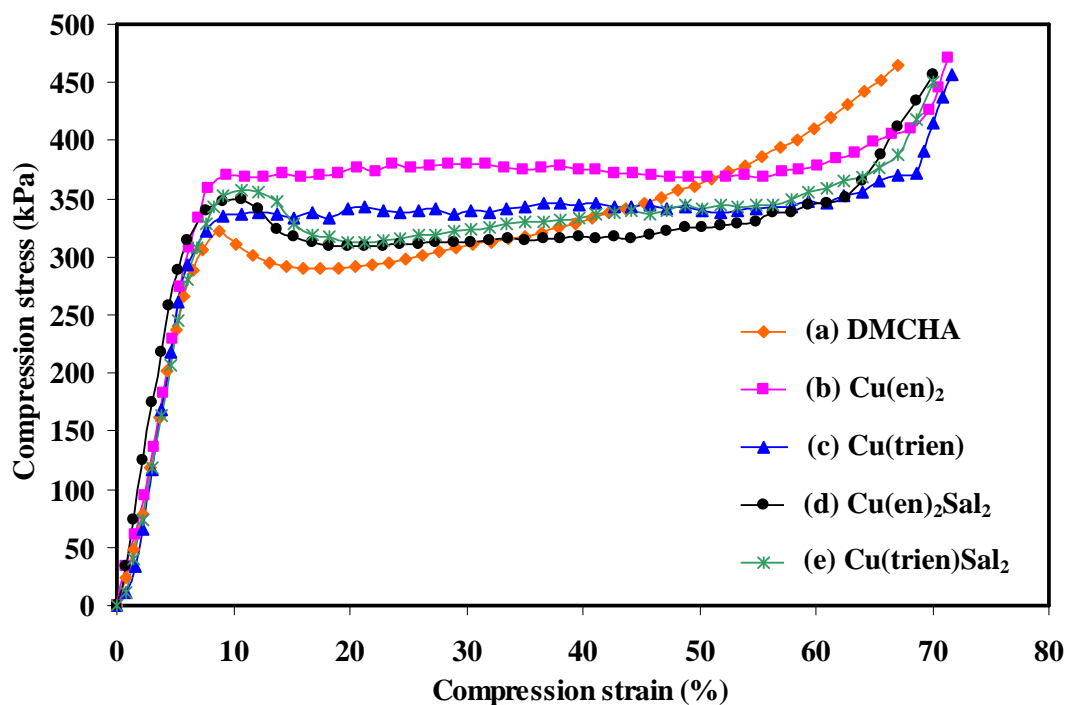


Figure 4.27 Parallel compression stress-strain curve of RPUR foams catalyzed by different catalysts at NCO index of 150 (a) DMCHA (ref.); (b) $\text{Cu}(\text{en})_2$; (c) $\text{Cu}(\text{trien})$; (d) $\text{Cu}(\text{en})_2\text{Sal}_2$; (e) $\text{Cu}(\text{trien})\text{Sal}_2$

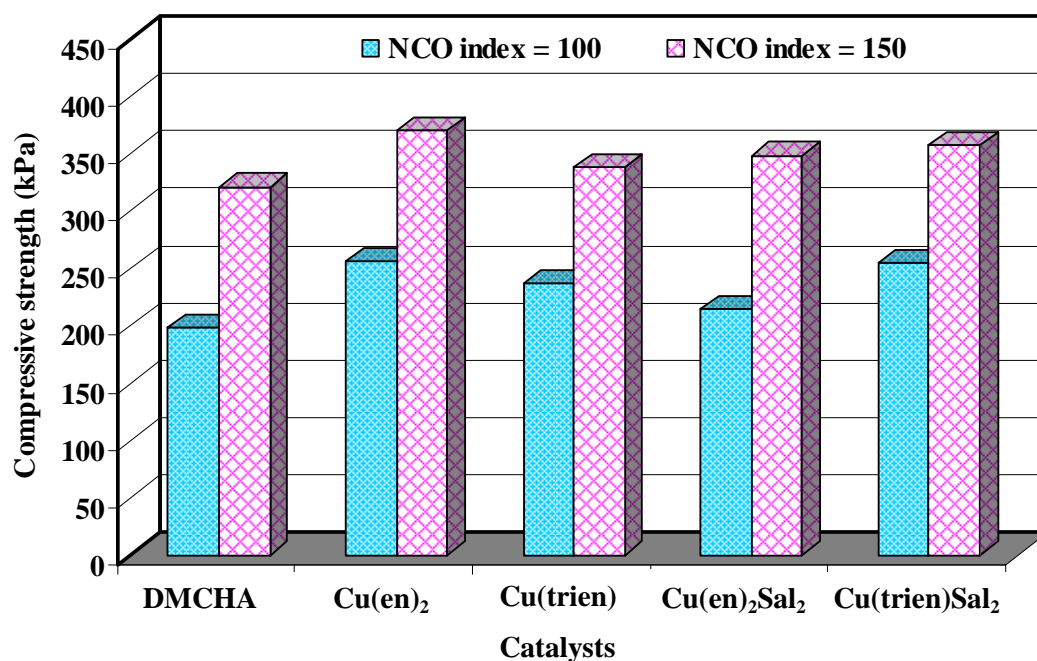


Figure 4.28 Comparison of parallel compressive strength of RPUR foams between NCO indexes of 100 and 150

Morphology of RPUR foam catalyzed by Cu(en)_2 in parallel and perpendicular direction of foam rising is of foam as shown in Figure 4.31. It was found that cell morphology showed spherical cell and elongated cell in parallel and perpendicular direction, respectively. It was demonstrated the foams were anisotropic materials which were confirmed by compressive strength and cell morphology results.

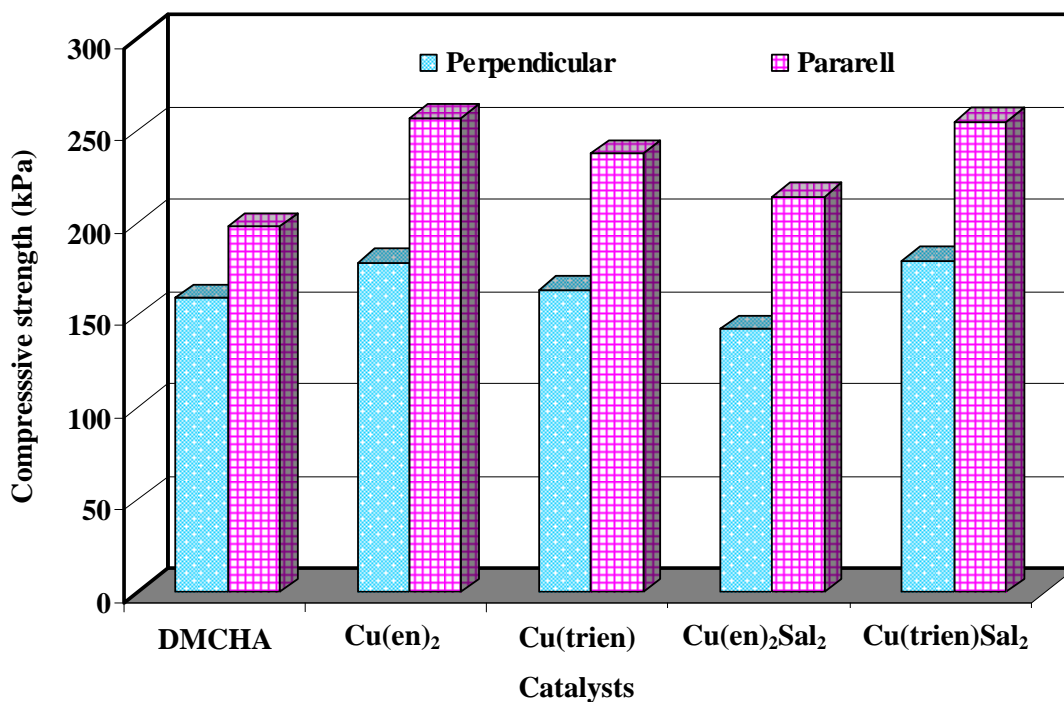


Figure 4.29 Comparison of compressive strength of RPUR foams between parallel and perpendicular direction of foam rising at NCO index of 100

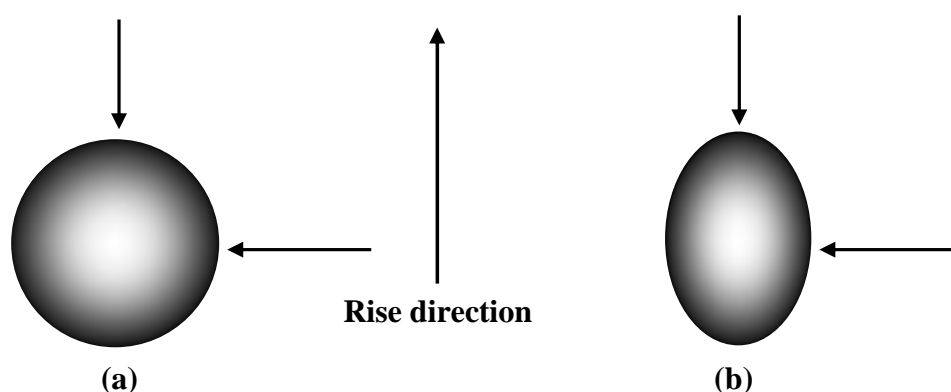


Figure 4.30 Isotropic foam (a): spherical cells, equal properties in all directions; anisotropic foam (b): ellipsoid cells, properties depend on direction [7]

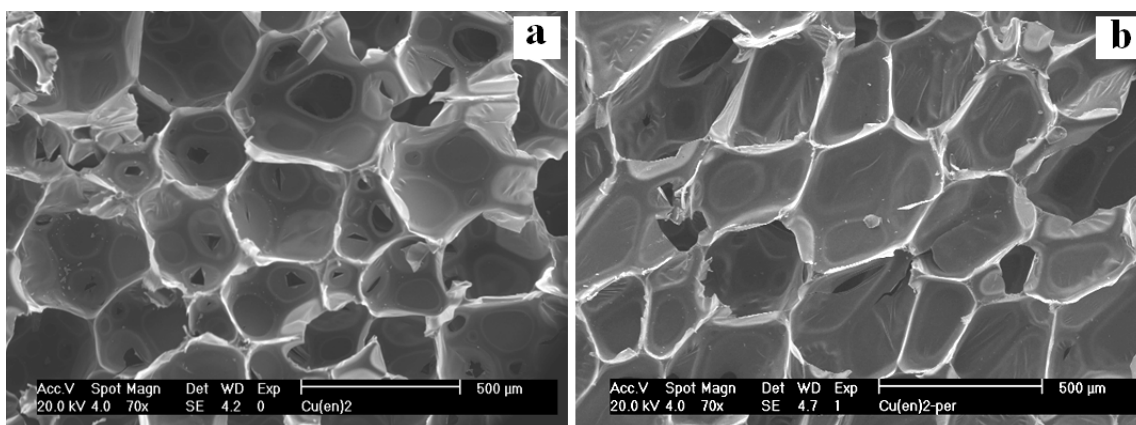


Figure 4.31 SEM of RPUR foams catalyzed by Cu(en)_2 ; (a) top view; (b) side view (70x)

SEM micrographs shown in Figure 4.32 showed that both RPUR foams prepared from DMCHA and Cu(en)_2 catalysts had closed cell, but cell size in RPUR foam catalyzed by Cu(en)_2 was smaller and more uniform than that prepared from DMCHA catalyst. This result indicated that the small cell size gave more strength to the RPUR foam [39]. Since the foam catalyzed by Cu(en)_2 had higher compressive strength than that prepared from DMCHA.

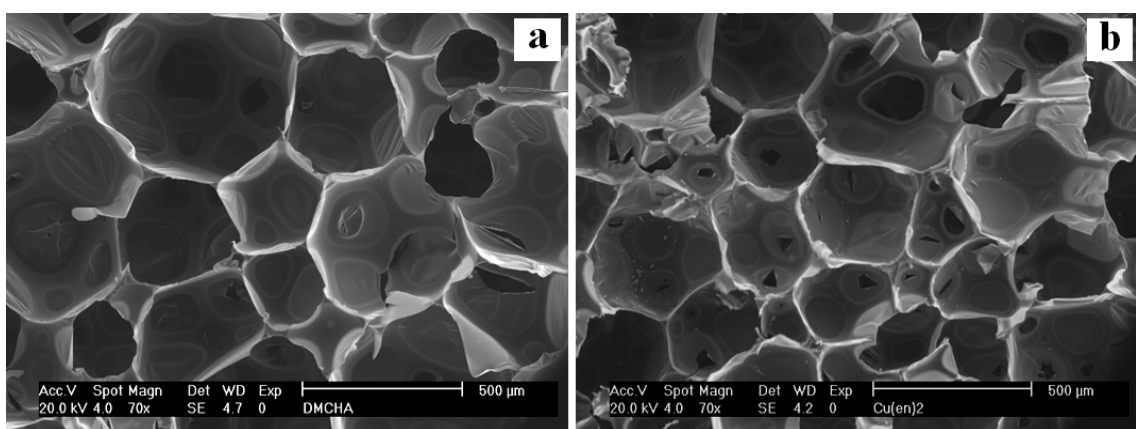


Figure 4.32 SEM of RPUR foams catalyzed by (a) DMCHA; (b) Cu(en)_2 (70x)

4.5 Thermal stability

Thermal stability of RPUR foams catalyzed by Cu(en)_2 , Cu(trien) , Cu(trien)Sal_2 and DMCHA (ref.) at NCO index of 150 were investigated by thermogravimetric analysis under nitrogen atmosphere. Their thermograms are shown in Figure 4.33 and Table 4.6. TGA thermograms of all RPUR foams showed the decomposition of foams in one step. The initial composition temperature (IDT),

which is the temperature at 5% weight loss was found in the range of 272-285 °C. The residual weights at 600 °C were in the range of 38-42%. RPUR foams catalyzed by Cu(en)₂, Cu(trien), Cu(trien)Sal₂ and DMCHA showed their maximum decomposition temperature (T_{max}) values in the range of 332-337 °C. The foams prepared from all metal complexes catalysts showed similar thermal decomposition with that prepared from DMCHA catalyst. This indicated that the metal complexes showed similar catalytic reaction with that of DMCHA.

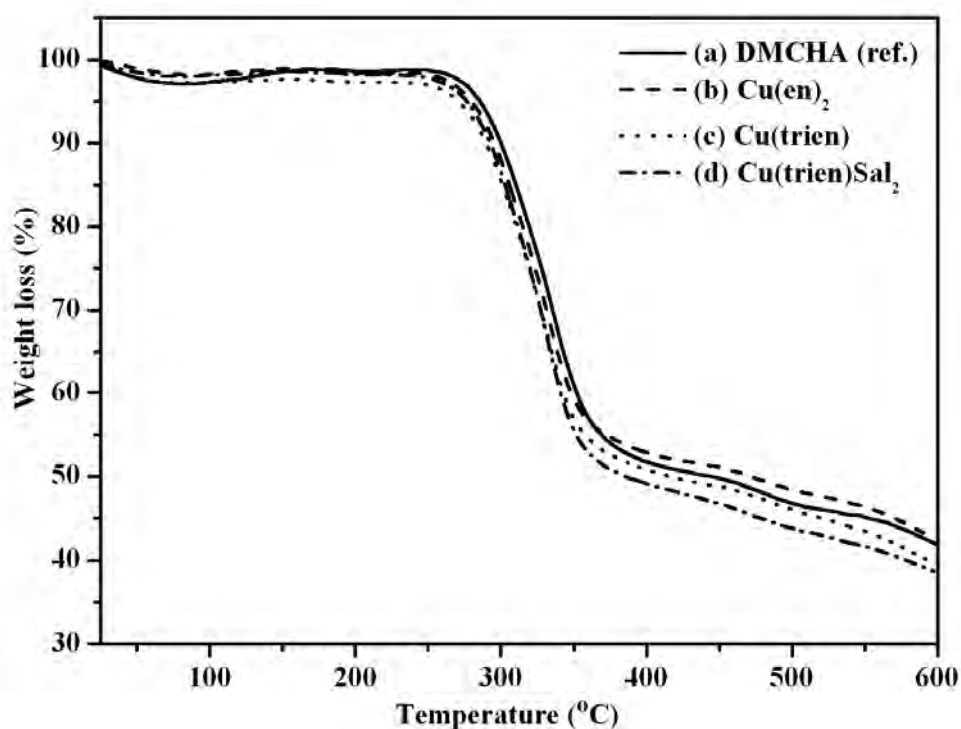


Figure 4.33 TGA thermograms of RPUR foams catalyzed by (a) DMCHA (ref.); (b) Cu(en)₂; (c) Cu(trien); (d) Cu(trien)Sal₂ at the NCO index of 150

Table 4.6 TGA data of RPUR foam catalyzed by various copper complexes catalysts at the NCO index of 150

RPUR catalyzed by various catalysts	IDT (°C)	Weight residue (%) at different temperatures (°C)					T _{max} (°C)
		200	300	400	500	600	
DMCHA (ref.)	285	99	90	52	47	42	337
Cu(en) ₂	281	98	88	53	48	43	337
Cu(trien)	272	97	86	51	46	40	332
Cu(trien)Sal ₂	279	98	88	49	44	39	336

For comparison, RPUR foams were prepared by using of metal acetates, amines and salicylic acid as catalysts. It was found that the RPUR foams with good properties could not be obtained as shown in Figures 4.34 and 4.35.



Figure 4.34 External appearance of RPUR foams catalyzed by metal acetates, amines and salicylic acid

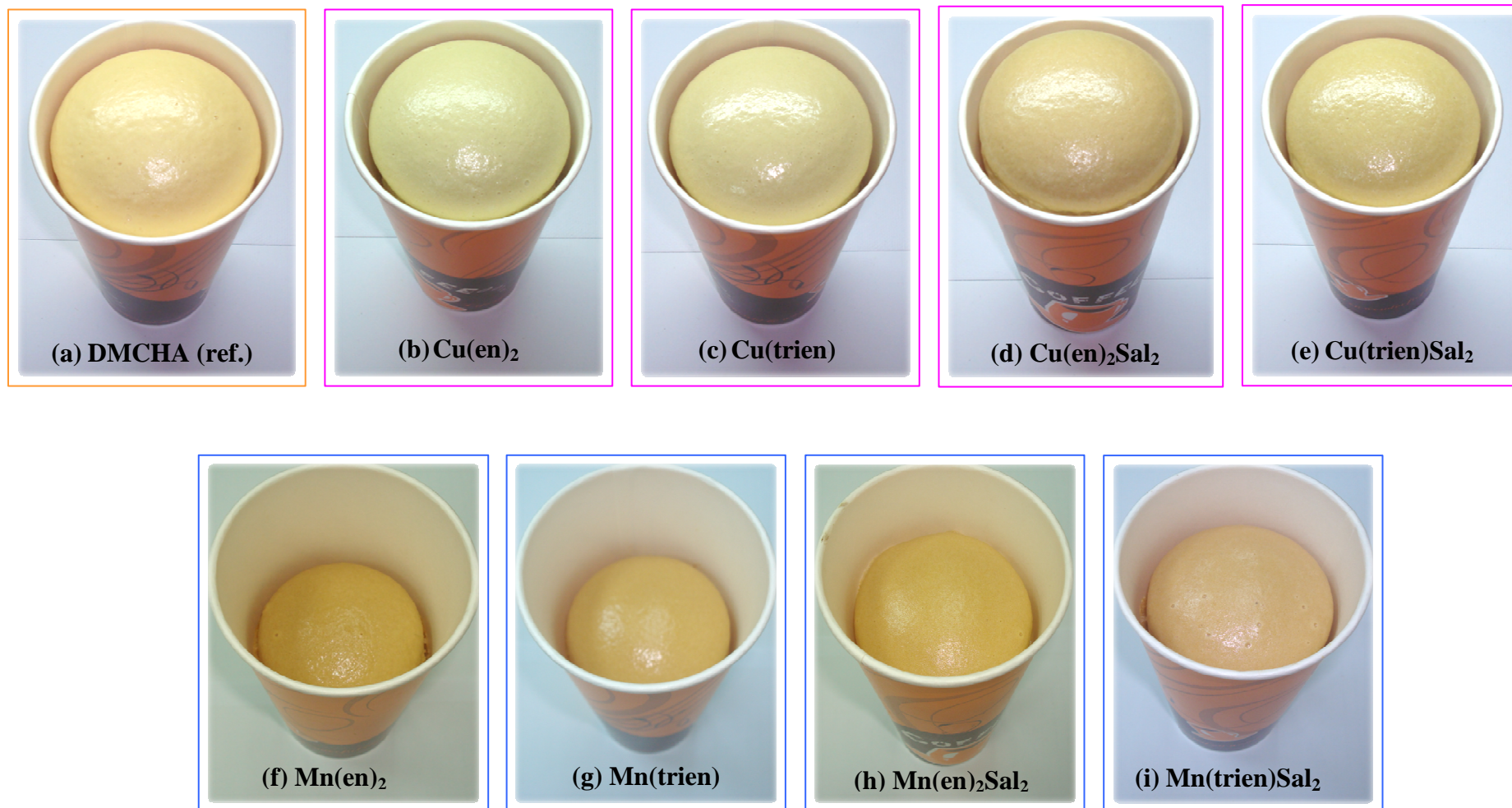


Figure 4.35 External appearance of RPUR foams catalyzed by different metal catalysts (a) DMCHA (ref.); (b) Cu(en)_2 ; (c) Cu(trien) ; (d) $\text{Cu(en)}_2\text{Sal}_2$; (e) Cu(trien)Sal_2 ; (f) Mn(en)_2 ; (g) Mn(trien) ; (h) $\text{Mn(en)}_2\text{Sal}_2$; (i) Mn(trien)Sal_2

CHAPTER V

CONCLUSION

5.1 Conclusion

Metal-amine complexes: $M(en)_2$, $M(trien)$ and metal-amine-salicylate complexes: $M(en)_2Sal_2$, $M(trien)Sal_2$ [$M = Cu$ and Mn], were synthesized and used as catalysts for rigid polyurethane foam preparation. All metal complexes were synthesized by solvent method (in acetone). They were characterized by means of IR and UV-vis spectroscopy. IR spectra of copper and manganese complexes showed that the characteristic absorption bands shifted from those of metal acetate. UV spectra also showed that the maximum wavelength of both copper and manganese complexes shifted from that of metal acetate. This indicated that the complexes between metal acetate and amines (ethylenediamine and triethylenetetramine) were obtained.

Rigid polyurethane (RPUR) foam preparations were carried out by two shot and free rise method. RPUR foams catalyzed by starting materials (Figure 4.34) showed bad appearance and brittle foam, and long time of processing time. It was indicated that starting materials were unsuitable catalytic reaction. RPUR foams catalyzed by copper complexes showed better appearance and blowing reaction than those prepared from manganese complexes, which could be observed from the foam height after the reaction was finished (Figure 4.35). The reaction times of RPUR foams catalyzed by copper complexes, especially $Cu(en)_2$ and $Cu(trien)$, showed better catalytic activity than foam catalyzed by manganese complexes and a reference commercial catalyst (DMCHA). Although $Cu(trien)Sal_2$ showed lower catalytic activity than DMCHA, it might be suitable for some foam applications which required longer gel time than DMCHA. The polymerization was exothermic reaction. The maximum core temperature of RPUR foams were in the range of 100-136°C. The maximum core temperature increased with increasing of NCO content and reached the maximum value at the NCO index of 130 and after that the maximum core temperatures decreased with increasing the NCO index.

RPUR foams catalyzed from various catalysts were characterized by FTIR spectroscopy. IR spectra of all RPUR foams showed similar characteristic absorption band. IR spectroscopy was used to determine the NCO conversion and

polyisocyanurate (PIR): polyurethane (PUR) ratio. It was found that NCO conversion of RPUR foams decreased with increasing of the NCO content. PIR:PUR ratio slightly increased with increasing of NCO content in foam formulations. Thus, it was indicated that the metal complexes could not catalyze the PIR formation.

Apparent density of RPUR foams increased with increasing of the NCO content. The foams prepared at the NCO indexes of 100 and 150 had the apparent density about of 40 and 50 kg/m³, respectively. RPUR foam catalyzed by copper complexes showed apparent density similar to the foam prepared from DMCHA catalyst, especially at the NCO indexes of 100-150. RPUR foams catalyzed by manganese complexes showed higher the apparent density than the foam foams catalyzed by DMCHA. The density of foams prepared from both copper and manganese complexes were suitable for foam applications.

The compressive properties of prepared RPUR foams catalyzed by copper complexes showed compressive modulus similar to that from DMCHA catalyst. The compressive strength of RPUR foam from Cu(en)₂, Cu(trien) and Cu(trien)Sal₂ were higher than the foam prepared from DMCHA catalyst. Their compressive strength values were 257.0, 237.7, and 255.2 kPa for NCO index of 100 and 370.6, 338.5, and 357.3 kPa for NCO index of 150, respectively. It was found that foams prepared at NCO index of 150 showed higher compressive strength than that prepared at NCO index of 100, because the NCO index at 150 gave foam with higher density than foams prepared at NCO index of 100. Compressive strength of foams in parallel direction of foam rising was higher than that in perpendicular direction which indicated that RPUR foams were anisotropic materials. All parameters of RPUR foam are concluded in Table 5.1.

5.2 Suggestion for future work

Since copper complexes showed better catalytic activity than manganese complexes catalyst, especially Cu(en)₂ and Cu(trien). These catalysts can be developed to use as catalysts in the spray polyurethane foam industry. Furthermore, copper complexes catalyst can also be catalyzed more blowing reaction than manganese complexes. The suggestion for future work is to develop catalyst mixture between copper and manganese complexes to improve the catalytic activity and

blowing reaction of manganese-based catalyst since manganese complexes are more environmental friendly than copper complexes.

Table 5.1 RPUR foams conclusion

Parameters	Conclusion				
	Cu-amine complexes				
Reaction times	Cu(en)₂	Cu(trien)	Cu(en)₂Sal₂	Cu(trien)Sal₂	DMCHA
Cream time (min)	0:36	0:42	0:54	0:55	0:32
Gel time (min)	0:44	0:54	1:31	1:54	0:37
Tack free time (min)	1:46	3:09	8:14	7:07	5:44
Rise time (min)	2:05	3:22	6:08	6:16	3:18
	Mn-amine complexes				
	Mn(en)₂	Mn(trien)	Mn(en)₂Sal₂	Mn(trien)Sal₂	DMCHA
Cream time (min)	0:48	0:45	1:01	0:57	0:32
Gel time (min)	1:45	1:04	1:36	1:50	0:37
Tack free time (min)	13:40	15:36	14:55	11:25	5:44
Rise time (min)	9:40	8:58	8:35	7:57	3:18
Catalytic activity	Cu-amine complexes > Mn-amine complexes Cu(en) ₂ and Cu(trien) > DMCHA				
Catalytic reaction	Blowing and gelling reaction				
Polymerization temperature	100-136 °C				
Density (kg/m³)	NCO index = 100		NCO index = 150		
	39.0 - 41.0		48.0 - 50.0		
Parallel Compressive strength (kPa)	Cu(en) ₂ , Cu(trien) and Cu(trien)Sal ₂ > DMCHA- RPUR foam				
	NCO index = 100		NCO index = 100		
Cu(en) ₂ -RPUR	257.0		370.6		
Cu(trien)-RPUR	237.7		338.5		
Cu(trien)Sal ₂ -RPUR	255.2		357.3		
DMCHA-RPUR	198.2		321.5		
Parallel testing > perpendicular testing	Anisotropic materials				

REFERENCES

- [1] Yin, B.; Li, Z.-M.; Quan, H.; Yang, M.-B.; Zhou, Q.-M. and Tian, Ch.-R.; Wang J.-H. Morphology and mechanical properties of nylon-10,10-filled rigid polyurethane foams. *J. Elast. Plast.* 36 (2004); 333-349.
- [2] Jackovich, D.; O'toole, B.; Hawkins, C. M. and Sapochak, L. Temperature and mold size effects on physical and mechanical properties of a polyurethane foam. *J. Cell. Plast.* 41 (2005); 153-168.
- [3] Rujira Jitwung, *Effect of parameters on high density flexible polyurethane foam mixing in batch tank*. Master's Thesis, Department of Chemical Engineering Faculty of Engineering Chulalongkorn University, 2000.
- [4] Modesti, M. and Lorenzetti, A. Improvement on fire behaviour of water blown PIR–PUR foams: use of an halogen-free flame retardant. *Eur. Polym. J.* 39 (2003): 263–268.
- [5] Wood, G. *The ICI polyurethane book*. 2nd Edition. London: John Wiley & Sons, 1990.
- [6] Pentrakoon, D. and Ellis, J.W. *An introduction to plastic foams*. Chulalongkorn University Press, 2005.
- [7] Oertel, G. *Polyurethane handbook*. New York: Hanser Publishers, 1985.
- [8] Lee, S.T. and Ramesh N.S. *Polymeric foams*. New York: CRC Press, 2004.
- [9] Modesti, M. and Lorenzetti, A. An experimental method for evaluating isocyanate conversion and trimer formation in polyisocyanurate-polyurethane foams. *Eur. Polym. J.* 37 (2001): 949-954.
- [10] Landrock, H. *Handbook of plastic foams*. USA: Noyes Publications, 1995.
- [11] Stirna, U. and Cabulis, U. Water-blown polyisocyanurate foams from vegetable oil polyols. *J. Cell. Plast.* 44 (2008): 139-159.
- [12] Naruse, A.; Nanno, H.; Kurita, M.; Inohara, H. and Fukami, T. Development of all water-blown polyisocyanurate foam system for metal-faced continuous sandwich panels. *J. Cell. Plast.* 38 (2002): 385-401.
- [13] Grimminger, J. and Muha, K. Silicone surfactants for pentane blown rigid foam. *J. Cell. Plast.* 31 (1992): 48-72.
- [14] Lim, H.; Kim, S. H. and Kim, B. K. Effects of silicone surfactant in rigid polyurethane foams. *Express. Polym. Lett.* 2 (2008): 194-200.

- [15] Modesti, M.; Lorenzetti, A.; Simioni, F. and Checchin, M. Influence of different flame retardants on fire behaviour of modified PIR/PUR polymers. *Polym. Degrad. Stabil.* 74 (2001): 475–479.
- [16] Lorenzetti, A.; Modesti, M.; Zanella, L.; Bertani, R. and Gleria, M. Thermally stable hybrid foams based on cyclophosphazenes and polyurethanes. *Polym. Degrad. Stabil.* 87 (2005): 287-292.
- [17] Murayama, S.; Fukuda, K.; Kimura, T. and Sasahara, T. Water-blown polyurethane rigid foam modified with maleate. *J. Cell. Plast.* 41 (2005): 373-378.
- [18] Modesti, M.; Lorenzetti, A.; Simioni, F. and Checchin, M. Influence of different flame retardants on fire behaviour of modified PIR/PUR polymers. *Polym. Degrad. Stabil.* 74 (2001): 475–479.
- [19] Maris, R. V.; Tamano, Y.; Yoshimura, H. and Gay, K. Polyurethane catalysis by tertiary amines. *J. Cell. Plast.* 41 (2005): 305-322.
- [20] Randall, D. and Lee, S. *The polyurethane book*. London: John Wiley & Sons, 2002.
- [21] Okuzono, S.; Tokumoto, K.; Tamano, Y. and Lowe, D. W. New Polyisocyanurate catalysts which exhibit high activity at low temperature. *J. Cell. Plast.* 37 (2001): 72-89.
- [22] Molero, C.; Lucas, A. and Rodriguez, J. F. Activities of octoate salts as novel catalysts for the transesterification of flexible polyurethane foams with diethylene glycol. *Polym. Degrad. Stabil.* 94 (2009): 533–539.
- [23] Strachota, A.; Strachotova, B. and Spirkova, M. Comparison of environmentally friendly, selective polyurethane catalysts. *Mater. Manuf. Process.* 23 (2008): 566-570.
- [24] Carroy, A. and et al. Novel latent catalysts for 2K-PUR systems. *Prog. Org. Coat.* 68 (2010): 37-41.
- [25] Inoue, Sh. I.; Nagai, Y. and Okamoto, H. Amine-manganese complexes as a efficient catalyst for polyurethane syntheses. *Polym. J.* 34 (2002): 298-301.
- [26] Kurnoskin, A. V. Metalliferous epoxy chelate polymers: 1. synthesis and properties. *Polymer.* 34 (1993): 1060-1067.
- [27] Kurnoskin, A. V. Metalliferous epoxy chelate polymers: 2. influence of structural fragments on properties. *Polymer*, 34 (1993): 1068-1076.

- [28] Braybrook, A. L.; Heywood, B. R. and Karatzas, P. An experimental investigation of crystal/solvent interactions in the copper (II) acetate monohydrate/propan-1-ol system. *J. Cryst. Growth.* 244 (2002): 327-332.
- [29] Romero, R. R.; Robert, A.; Grigsby, J. R.; Ernest, L.; Rister, J. R.; Pratt, J. K. and Ridgway, D. A study of the reaction kinetics of polyisocyanurate foam formulations using real-time FTIR. *J. Cell. Plast.* 41 (2005): 339-359.
- [30] Elwell, M. J. and Ryan, A. J. An FTIR study of reaction kinetics and structure development in model flexible polyurethane foam systems. *Polymer.* 37 (1996): 1353-1361.
- [31] Cateto, C. A.; Barreiro, M. F. and Rodrigues, A.E. Monitoring of lignin-based polyurethane synthesis by IR-ATR. *Ind. Crop. Prod.* 27 (2008): 168-174.
- [32] Jones, S. A.; Scott, K. W.; Willoughby, B. G. and Sheard, E. A. Monitoring of polyurethane foam cure. *J. Cell. Plast.* 38 (2002): 285-299.
- [33] Raffel, B. and Loevenich, C. J. High throughput screening of rigid polyisocyanurate foam formulations: quantitative characterization of isocyanurate yield via the adiabatic temperature method. *J. Cell. Plast.* 42 (2006): 17-47.
- [34] Thomson, M. A.; Melling, P. J. and Slepski, A. M. Real time monitoring of isocyanate chemistry using a fiber-optic FTIR probe. *Polymer Preprints.* 42 (2001): 310-311.
- [35] Saha, M. C.; Kabir, M. E. and Jeelani, S. Enhancement in thermal and mechanical properties of polyurethane foam infused with nanoparticles, *Mat. Sci. Eng.* 479 (2008): 213–222.
- [36] Saint-Michel, F.; Chazeau, L.; Cavaille, J.-Y. and Chabert, E. Mechanical properties of high density polyurethane foams: I. Effect of the density. *Compos. Sci. Technol.* 66 (2006): 2700–2708.
- [37] Goto, A.; Yamashita, K.; Nonomura, Ch. and Yamaguchi, K. Modeling of cell structure in polyurethane foam. *J. Cell. Plast.* 40 (2004): 481-488.
- [38] Tu, Z. H.; Shim, V P. W. and Lim, C. T. Plastic deformation modes in rigid polyurethane foam under static loading. *Int. J. Solids. Struct.* 38 (2001): 9267-9279.
- [39] Hawkins, M. C.; O'Toole, B. and Jackovich, D. Cell morphology and mechanical properties of rigid polyurethane foam. *J. Cell. Plast.* 41 (2005): 267-285.

APPENDICES

Appendix A

NCO index and NCO conversion Calculations

NCO index calculation

#Example Calculate the parts by weight (pbw) of pure PMDI (MR-200), molar mass = 365.8, functionality = 2.7 at an isocyanate indexes of 100, 130, 150, 160, 180 and 200 required to react with the following formulation:

Formulation (pbw)	Part by weight (g)
Raypol [®] 4221 (OHV = 440 mgKOH/ g, functionality = 4.3)	100.0
Catalysts	1.0
Surfactant	2.5
Blowing agent (water, M _w = 18 g/mole, functionality = 2)	3.0
PMDI (MR-200), NCO indexes of 100, 130, 150, 160, 180 and 200	?

$$\text{Equivalent weight of raypol 4221} = \frac{56.1}{440} \times 1000 = 127.5$$

$$\text{Equivalent weight of water} = \frac{18}{2} = 9.0$$

Note: Surfactants and catalysts are neglected in stoichiometric calculations because they do not react with NCO groups.

$$\text{Number of equivalent in formulation} = \frac{\text{parts by weight (pbw.)}}{\text{equivalent weight}}$$

Equivalent in the above formulation:

$$\text{Polyol (Raypol 4221)} = \frac{100}{127.5} = 0.784$$

$$\text{Water (blowing agent)} = \frac{3.0}{9.0} = 0.333$$

$$\text{Total equivalent weight} = 1.117$$

For stoichiometric equivalence, PMDI pbw is total equivalent x equivalent weight because PMDI reacts with polyol and water.

thus:

$$\text{PMDI (pbw)} = 1.117 \times \frac{\text{PMDI molar mass}}{\text{functionality}} = 1.117 \times \frac{365.8}{2.7} = 151.3$$

Note: 151.3 defines the isocyanate quantity at 100 index

where;

$$\text{Isocyanate index} = \frac{\text{actual amount of isocyanate}}{\text{theoretical amount of isocyanate}} \times 100$$

thus:

Isocyanate index = 100;

$$\text{Isocyanate actual} = \frac{151.3}{100} \times 100 = 151.3 \text{ pbw}$$

Isocyanate index = 130;

$$\text{Isocyanate actual} = \frac{151.3}{100} \times 130 = 197.0 \text{ pbw}$$

Isocyanate index = 150;

$$\text{Isocyanate actual} = \frac{151.3}{100} \times 150 = 227.0 \text{ pbw}$$

Isocyanate index = 160;

$$\text{Isocyanate actual} = \frac{151.3}{100} \times 160 = 242.0 \text{ pbw}$$

Isocyanate index = 180;

$$\text{Isocyanate actual} = \frac{151.3}{100} \times 180 = 272.0 \text{ pbw}$$

Isocyanate index = 200;

$$\text{Isocyanate actual} = \frac{151.3}{100} \times 200 = 303.0 \text{ pbw}$$

Table A1 Isocyanate quantity at different NCO indexes in the above formulations

Formulations (pbw)	NCO index					
	100	130	150	160	180	200
Polyol (Raypol [®] 4221)	100	100	100	100	100	100
Catalysts	1.0	1.0	1.0	1.0	1.0	1.0
Surfactant	2.5	2.5	2.5	2.5	2.5	2.5
Blowing agent	3.0	3.0	3.0	3.0	3.0	3.0
PMDI (MR-200)	151	197	227	242	272	303

NCO conversion calculation

The NCO conversion can be calculated by FTIR method, defined as the ratio between isocyanate peak area at time t and isocyanate peak area at time 0, following equation:

$$\text{Isocyanate conversion (\%)} = \left[1 - \frac{\text{NCO}^f}{\text{NCO}^i} \right] \times 100$$

where;

NCO^f is the area of isocyanate absorbance peak area at time t

NCOⁱ is the area of isocyanate absorbance peak area at time 0

Quantity of free NCO in RPUR foams were normalized by aromatic ring absorption band at 1595 cm⁻¹.

Table A2 Free NCO absorbance peak area in PMDI (MR-200) from ATR-IR

PMDI (MR-200) spectra	NCO Absorbance peak area Normalized @ 1.0 Ar-H peak area
1	79.378
2	81.635
3	78.262
4	79.499
5	79.491
Average (NCO ⁱ); ATR-IR	79.65
NCO ⁱ (FTIR)	98.0

Example Calculate the conversion of isocyanate (α) and PIR:PUR of rigid polyurethane foams catalyzed by $\text{Cu}(\text{en})_2$ catalyst at NCO index 150

Conversion of isocyanate (%)

Data at **Table A2**

Absorbance peak area of initial NCO = 79.65 = NCO^i

The data from **Table A4** at NCO index 150, absorbance peak area of free NCO was normalized by aromatic ring quantity:

Absorbance peak area of final NCO = 1.4768 = NCO^f

thus,

$$\begin{aligned} \text{Conversion of isocyanate (\%)} &= \left[1 - \frac{\text{NCO}^f}{\text{NCO}^i} \right] \times 100 \\ &= \left[1 - \frac{1.4768}{79.65} \right] \times 100 \end{aligned}$$

$$\% \text{ NCO conversion} = 98.1$$

PIR:PUR

Absorbance peak area of PIR (polyisocyanurate) = 10.476

Absorbance peak area of PUR (polyurethane) = 49.623

$$\text{thus, PIR:PUR} = \frac{10.476}{49.623} = 0.211$$

Table A3 NCO conversion of RPUR foam catalyzed by DMCHA at different NCO indexes

NCO indexes	Peak Area					NCO conversion (%)	PIR/PUR
	NCO 2277 cm^{-1}	Ar-H 1595 cm^{-1}	PIR 1415 cm^{-1}	PUR 1220 cm^{-1}	NCO ^f (Ar-H=1.0)		
100	8.9640	21.6310	11.6490	63.4740	0.4144	99.5	0.184
150	16.5440	18.7510	11.0780	52.3080	0.8823	98.9	0.212
200	29.1650	18.5960	11.4760	50.3580	1.5683	98.0	0.228
250	49.7270	19.7690	11.6460	45.8910	2.5154	96.8	0.254
300	56.2170	18.2640	11.0450	41.5210	3.0780	96.1	0.266

Table A4 NCO conversion of RPUR foam catalyzed by Cu(en)₂ at different NCO indexes

NCO indexes	Peak Area					NCO conversion (%)	PIR/PUR
	NCO 2277 cm ⁻¹	Ar-H 1595 cm ⁻¹	PIR 1415 cm ⁻¹	PUR 1220 cm ⁻¹	NCO ^f (Ar-H=1.0)		
100	18.2330	20.1490	10.9530	61.9250	0.9049	98.9	0.177
150	28.5940	19.3620	10.4760	49.6230	1.4768	98.1	0.211
200	51.8700	19.8490	10.8680	45.8840	2.6132	96.7	0.237
250	55.9610	19.3160	10.8160	38.4340	2.8971	96.4	0.281
300	88.6490	18.2570	10.0130	37.1940	4.8556	93.9	0.269

Table A5 NCO conversion of RPUR foam catalyzed by Cu(trien) at different NCO indexes

NCO indexes	Peak Area					NCO conversion (%)	PIR/PUR
	NCO 2277 cm ⁻¹	Ar-H 1595 cm ⁻¹	PIR 1415 cm ⁻¹	PUR 1220 cm ⁻¹	NCO ^f (Ar-H=1.0)		
100	5.6350	19.7330	10.7010	61.0630	0.2856	99.6	0.175
150	17.9890	19.4440	11.1880	55.7380	0.9252	98.8	0.201
200	64.2920	19.7870	11.0990	49.6580	3.2492	95.9	0.224
250	70.4450	18.5210	10.7550	45.9440	3.8035	95.2	0.234
300	87.8380	19.0990	11.0570	49.8640	4.5991	94.2	0.222

Table A6 NCO conversion of RPUR foam catalyzed by Cu(en)₂Sal₂ at different NCO indexes

NCO indexes	Peak Area					NCO conversion (%)	PIR/PUR
	NCO	Ar-H	PIR	PUR	NCO ^f		
	2277 cm ⁻¹	1595 cm ⁻¹	1415 cm ⁻¹	1220 cm ⁻¹	(Ar-H=1.0)		
100	1.9880	19.9300	10.5360	67.2200	0.0997	99.9	0.157
150	8.9420	14.3350	11.8520	65.8240	0.6238	99.2	0.180
200	29.8860	20.1990	11.0290	52.5640	1.4796	98.1	0.210
250	71.3660	20.2410	11.5230	57.0240	3.5258	95.6	0.202
300	87.5130	20.0650	11.0170	52.1680	4.3615	94.5	0.211

Table A7 NCO conversion of RPUR foam catalyzed by Cu(trien)Sal₂ at different NCO indexes

NCO indexes	Peak Area					NCO conversion (%)	PIR/PUR
	NCO	Ar-H	PIR	PUR	NCO ^f		
	2277 cm ⁻¹	1595cm ⁻¹	1415cm ⁻¹	1220cm ⁻¹	(Ar-H=1.0)		
100	3.2330	20.8670	6.3660	33.8820	0.1549	99.8	0.188
150	31.6980	19.9710	11.6810	57.1780	1.5872	98.0	0.204
200	45.6000	20.5500	11.8360	53.3030	2.2190	97.2	0.222
250	46.5030	19.8490	11.4950	56.3150	2.3428	97.1	0.204
300	93.6740	20.4610	10.8560	52.8550	4.5782	94.3	0.205

Table A8 NCO conversion of RPUR foam catalyzed by Mn(en)₂ at different NCO indexes

NCO indexes	Peak Area					NCO conversion (%)	PIR/PUR
	NCO	Ar-H	PIR	PUR	NCO ^f		
	2277 cm ⁻¹	1595 cm ⁻¹	1415 cm ⁻¹	1220 cm ⁻¹	(Ar-H=1.0)		
100	0.2312	0.4219	0.1296	0.5859	0.5480	99.4	0.221
130	1.5910	1.4990	0.4900	2.0710	1.0614	98.9	0.237
150	2.6010	2.7070	0.9750	4.0650	0.9608	99.0	0.240

Table A9 NCO conversion of RPUR foam catalyzed by Mn(trien) at different NCO indexes

NCO indexes	Peak Area					NCO conversion (%)	PIR/PUR
	NCO	Ar-H	PIR	PUR	NCO ^f		
	2277 cm ⁻¹	1595 cm ⁻¹	1415 cm ⁻¹	1220 cm ⁻¹	(Ar-H=1.0)		
100	1.6120	1.6520	0.5270	2.2840	0.9758	99.0	0.231
130	1.8180	1.6060	0.5590	2.3700	1.1320	98.8	0.236
150	1.8470	1.6740	0.7990	3.3900	1.1033	98.9	0.236

Table A10 NCO conversion of RPUR foam catalyzed by Mn(en)₂Sal₂ at different NCO indexes

NCO indexes	Peak Area					NCO conversion (%)	PIR/PUR
	NCO	Ar-H	PIR	PUR	NCO ^f		
	2277 cm ⁻¹	1595 cm ⁻¹	1415 cm ⁻¹	1220 cm ⁻¹	(Ar-H=1.0)		
100	2.2350	2.9530	0.9810	4.6700	0.7569	99.2	0.210
130	1.5820	1.4100	0.5100	2.0300	1.1220	98.9	0.251
150	2.8080	2.6680	1.1220	4.9080	1.0525	98.9	0.229

Table A11 NCO conversion of RPUR foam catalyzed by Mn(trien)Sal₂ at different NCO indexes

NCO indexes	Peak Area					NCO conversion (%)	PIR/PUR
	NCO	Ar-H	PIR	PUR	NCO ^f		
	2277 cm ⁻¹	1595cm ⁻¹	1415cm ⁻¹	1220cm ⁻¹	(Ar-H=1.0)		
100	0.9090	1.1010	0.3120	1.3450	0.8256	99.2	0.232
130	2.3400	2.8420	1.0630	4.6370	0.8234	99.2	0.229
150	1.3230	1.0860	0.4140	1.5890	1.2182	98.8	0.261

Appendix B

Compression Curves and Data

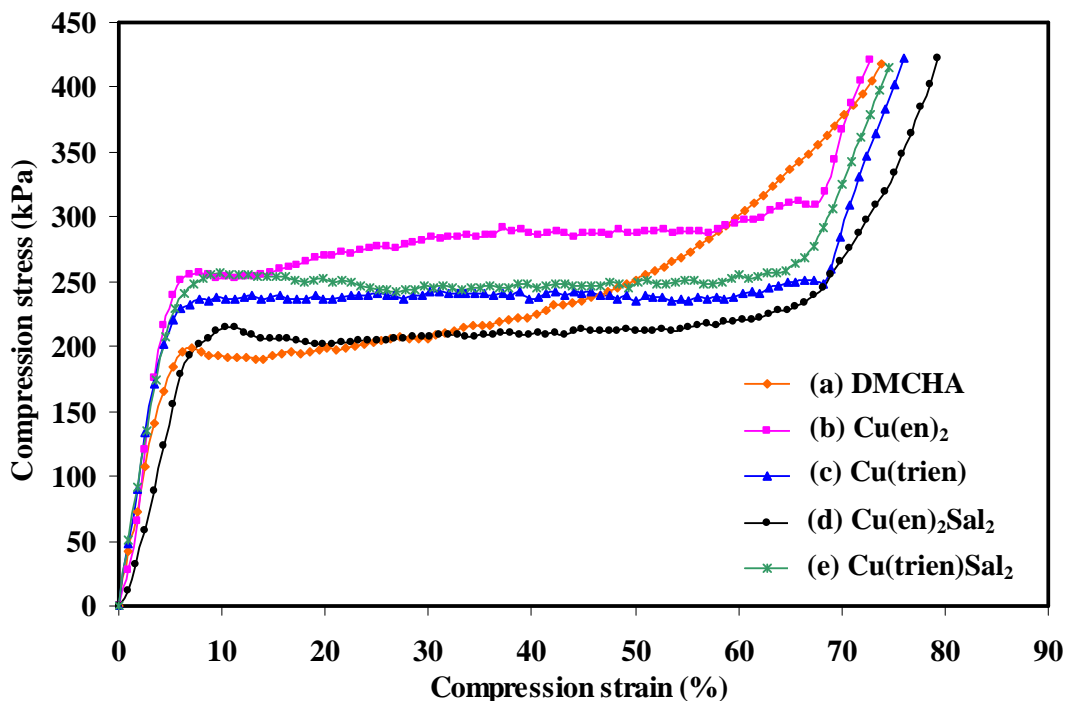


Figure B1 Parallel compression stress-strain curve of RPUR foams catalyzed by different catalysts at NCO index of 100

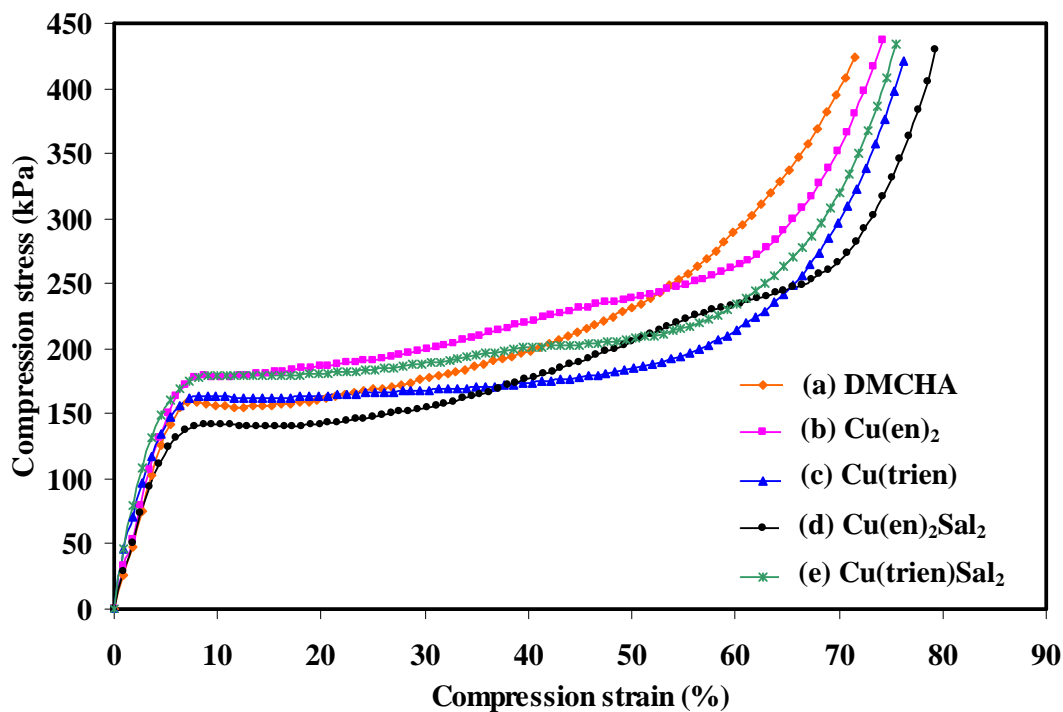


Figure B2 Perpendicular compression stress-strain curve of RPUR foams catalyzed by different catalysts at NCO index of 100

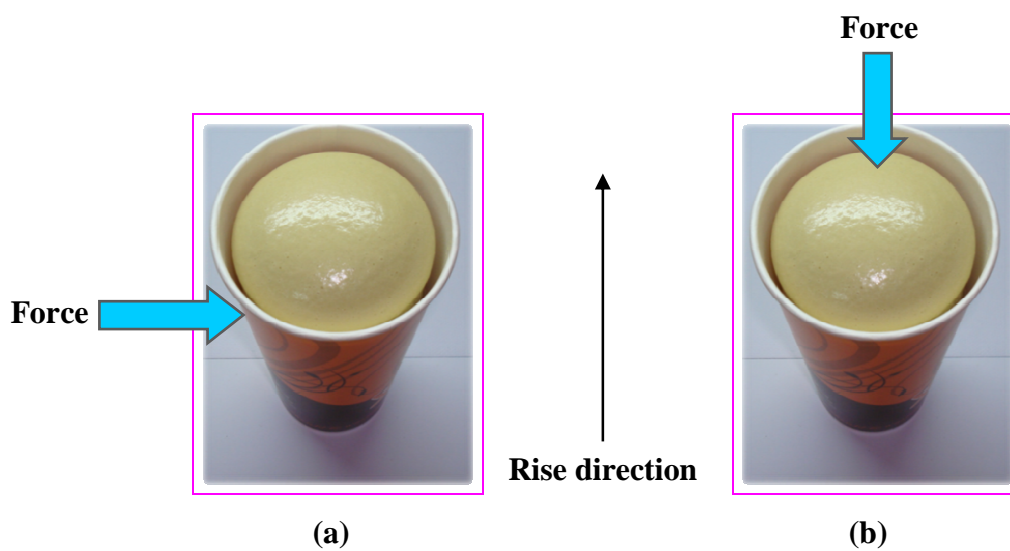


Figure B3 Compression direction of RPUR foams (a) perpendicular direction;
(b) parallel direction

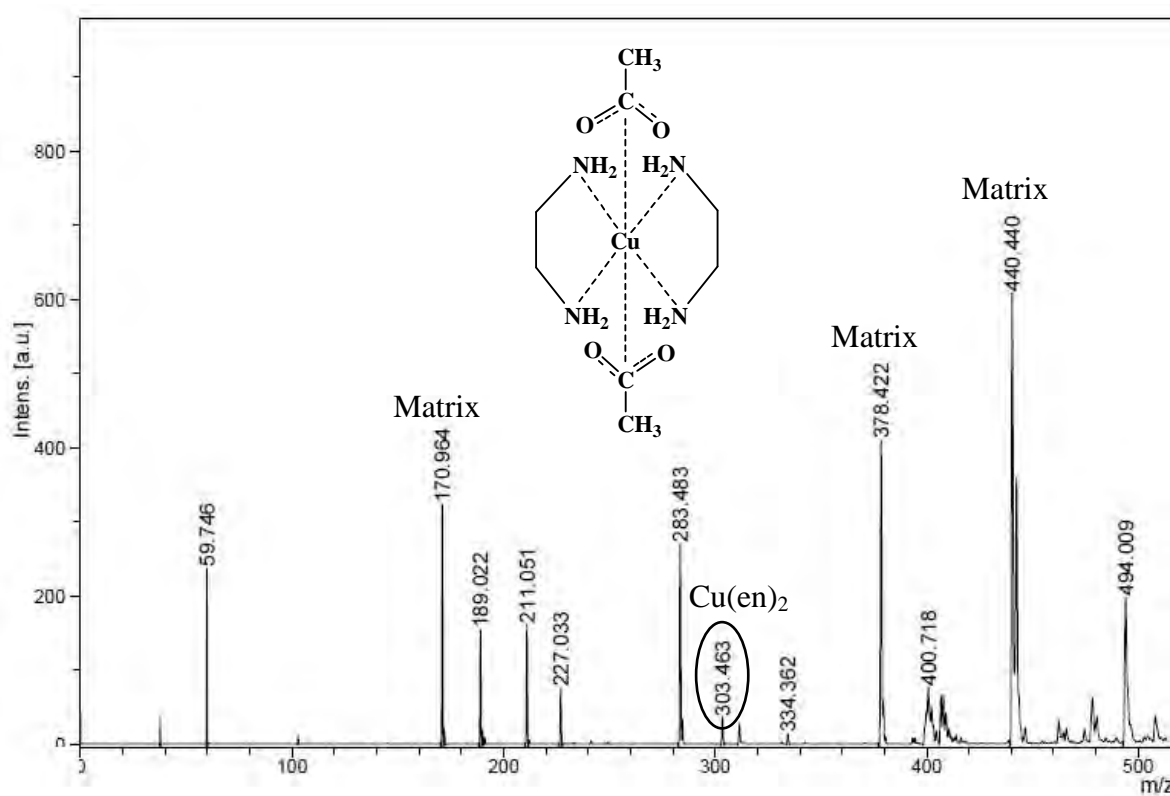


Figure B4 Mass spectrum of Cu(en)_2 complex (MALDI-TOF MS)

Table B1 Formulations, reaction times, physical and mechanical properties of RPUR foams catalyzed by copper complexes

Formulations (pbw)	Catalysts at different NCO indexes															
	DMCHA (Ref.)			Cu(en) ₂			Cu(trien)			Cu(en) ₂ Sal ₂			Cu(trien)Sal ₂			
	100	130	150	100	130	150	100	130	150	100	130	150	100	130	150	
Raypol [®] 4221	100	100	100	100	100	100	100	100	100	100	100	100	100	100	100	
Catalysts	1.0	1.0	1.0	1.0	1.0	1.0	1.0	1.0	1.0	1.0	1.0	1.0	1.0	1.0	1.0	
B8460	2.5	2.5	2.5	2.5	2.5	2.5	2.5	2.5	2.5	2.5	2.5	2.5	2.5	2.5	2.5	
H ₂ O	3.0	3.0	3.0	3.0	3.0	3.0	3.0	3.0	3.0	3.0	3.0	3.0	3.0	3.0	3.0	
MR-200	151	197	227	151	197	227	151	197	227	151	197	227	151	197	227	
Reaction times																
Cream time (min.)	0:30	0:32	0:35	0:35	0:36	0:40	0:38	0:42	0:44	0:52	0:54	0:59	0:52	0:55	0:58	
Gel time (min.)	0:35	0:37	0:39	0:41	0:44	0:48	0:51	0:54	0:59	1:27	1:31	1:37	1:27	1:54	1:54	
Tack free time (min.)	4:45	5:44	5:49	1:35	1:46	1:54	2:48	3:09	3:22	7:56	8:14	8:44	6:46	7:07	7:35	
Rise time (min.)	3:04	3:18	3:25	2:02	2:05	2:15	3:06	3:22	3:44	5:33	6:08	7:23	6:08	6:16	6:27	
Max. rise rate (cm/s)	0.15	0.15	0.14	0.33	0.30	0.27	0.26	0.23	0.21	0.06	0.06	0.05	0.14	0.13	0.11	
Density (kg/m³)	39.6	46.1	50.3	40.2	46.1	49.8	39.4	46.7	48.8	40.8	47.3	50.5	41.8	48.2	50.6	
Mechanical properties																
// Compressive strength (kPa)	198.2	-	321.5	257.0	-	370.6	237.7	-	338.5	214.3	-	348.8	255.2	-	357.3	
⊥ Compressive strength (kPa)	159.6	-	-	178.9	-	-	163.8	-	-	142.4	-	-	179.8	-	-	
// Compressive modulus (MPa)	3.54	-	4.92	5.18	-	5.38	4.34	-	5.98	3.36	-	5.44	4.32	-	5.12	

Table B2 Formulations, reaction times, physical and mechanical properties of RPUR foams catalyzed by manganese complexes

Formulations (pbw)	Catalysts at different NCO indexes														
	DMCHA (Ref.)			Mn(en) ₂			Mn(trien)			Mn(en) ₂ Sal ₂			Mn(trien)Sal ₂		
	100	130	150	100	130	150	100	130	150	100	130	150	100	130	150
Raypol [®] 4221	100	100	100	100	100	100	100	100	100	100	100	100	100	100	100
Catalysts	1.0	1.0	1.0	1.0	1.0	1.0	1.0	1.0	1.0	1.0	1.0	1.0	1.0	1.0	1.0
B8460	2.5	2.5	2.5	2.5	2.5	2.5	2.5	2.5	2.5	2.5	2.5	2.5	2.5	2.5	2.5
H ₂ O	3.0	3.0	3.0	3.0	3.0	3.0	3.0	3.0	3.0	3.0	3.0	3.0	3.0	3.0	3.0
MR-200	151	197	227	151	197	227	151	197	227	151	197	227	151	197	227
Reaction times															
Cream time (min.)	0:30	0:32	0:35	0:48	0:48	0:52	0:42	0:45	0:47	0:56	1:01	1:04	0:51	0:57	0:58
Gel time (min.)	0:35	0:37	0:39	1:42	1:45	1:55	0:58	1:04	1:05	1:30	1:36	1:39	1:45	1:50	1:52
Tack free time (min.)	4:45	5:44	5:49	13:36	13:40	13:45	15:32	15:36	16:02	14:48	14:55	15:42	11:12	11:25	14:32
Rise time (min.)	3:04	3:18	3:25	9:50	9:40	9:55	8:54	8:58	9:04	8:30	8:35	8:44	7:55	7:57	8:04
Max. rise rate (cm/s)	0.15	0.15	0.14	0.02	0.03	0.02	0.05	0.05	0.04	0.04	0.06	0.03	0.04	0.05	0.04
Density (kg/m³)	39.6	46.1	50.3	51.4	51.7	54.9	48.3	51.2	55.0	42.4	46.0	47.5	43.7	44.0	48.4
Mechanical properties															
// Compressive strength (kPa)	198.2	-	321.5	-	-	-	-	-	-	-	-	-	-	-	-
⊥ Compressive strength (kPa)	159.6	-	-	-	-	-	-	-	-	-	-	-	-	-	-
// Compressive modulus (MPa)	3.54	-	4.92	-	-	-	-	-	-	-	-	-	-	-	-

Table B3 Formulations, reaction times, physical properties of RPUR foams catalyzed by metal acetates, amines and salicylic acid

Formulations (pbw)	Starting materials at NCO index of 130					
	Cu(OAc)₂	Mn(OAc)₂	en	trien	Salicylic acid (sal)	Non-catalyst
Raypol [®] 4221	100	100	100	100	100	100
Catalysts (starting materials)	1.0	1.0	1.0	1.0	1.0	1.0
B8460	2.5	2.5	2.5	2.5	2.5	2.5
H ₂ O	3.0	3.0	3.0	3.0	3.0	3.0
MR-200	197	197	197	197	197	197
<i>Reaction times</i>						
Cream time (min.)	1:21	1:10	0:54	0:48	0:45	1:36
Gel time (min.)	2:35	2:44	1:49	2:36	2:05	2:27
Tack free time (min.)	20:40	22:25	19:54	19:58	21:28	24:29
Rise time (min.)	14:16	15:10	7:454	13:03	12:20	12:15
<i>Density (kg/m³)</i>	57.1	57.9	-	-	55.1	-
<i>External appearance</i>	Cu(OAc) ₂	Low blowing	Brittle foam	Brittle foam	Low blowing	Brittle foam

VITAE

Name : Mr Wittaya Pengjam
Date of birth : November 20, 1985
Nationality : Thai
Address : 47/1 Wangyarw, Danchang, Suphunburi, 72180
University Education : Bachelor's Degree from Department of Materials
Science and Engineering, Program in Petrochemicals
and Polymeric Materials, Faculty of Engineering and
Industrial Technology, Silpakorn University, 2004-2008

Master's Degree from Program in Petrochemistry
and Polymer Science, Faculty of Science,
Chulalongkorn University, 2008-2010

Conference attendance: Poster presentation "Preparation of rigid polyurethane
foam catalyzed by copper-amine complexes" at The 3rd
Silpakorn University Research Fair on Creative
Economy Conference in Nakhon Pathom, Thailand